BRUNET, M. 2021. *Novel nanoparticle drug delivery systems: application in the in vitro study of Bisnaphthalimidopropyl derivatives against human colorectal cancer cell lines*. Robert Gordon University, MRes thesis. Hosted on OpenAIR [online]. Available from: https://doi.org/10.48526/rgu-wt-1446968

Novel nanoparticle drug delivery systems: application in the in vitro study of Bisnaphthalimidopropyl derivatives against human colorectal cancer cell lines.

BRUNET, M.

2021

The author of this thesis retains the right to be identified as such on any occasion in which content from this thesis is referenced or re-used. The licence under which this thesis is distributed applies to the text and any original images only – re-use of any third-party content must still be cleared with the original copyright holder.

OpenAIR @RGU

This document was downloaded from https://openair.rgu.ac.uk

CC BY NC

Novel nanoparticle drug delivery systems: application in the *in vitro* study of Bisnaphthalimidopropyl derivatives against human colorectal cancer cell lines.

Mathieu Brunet

MRes **2021**

Novel nanoparticle drug delivery systems: application in the *in vitro* study of Bisnaphthalimidopropyl derivatives against human colorectal cancer cell lines.

Mathieu Brunet

A thesis submitted in partial fulfilment of the

requirements of the

Robert Gordon University

for the degree of Master of Research

April 2021

Declaration

This thesis has been produced by myself, any external support or resources have been documented, referenced and acknowledged. This work is original and has never been submitted before to obtain a degree at any other academic institution.

Mathieu Brunet

Acknowledgments

Throughout this project, I have received great support from my supervisory team which help me to develop myself both personally and professionally. I would first like to sincerely thank my principal supervisor Dr. Marie Goua who gave me the opportunity to join this project. It has been a long way since my arrival as a 2nd year intern and you have supported me ever since to become a better person and a better scientist. Merci pour tout!

I would also like to thank Dr. Colin Thompson and Prof. Paul Kong Thoo Lin for their valuable guidance, kindness and understanding. I really enjoyed working with you both during these last three years.

I would like to acknowledge the support of the wider staff community of the Robert Gordon University. I would like to thank Prof. Susan Duthie for her mentorship and technical support with the DNA damage study; Chris Fletcher for his day-to-day management of the laboratories and great spirit, Dr. Gemma Barron for her support, Dr. Laurie Smith and Slawomir Rybczynski for their help in the pharmaceutical laboratory; Emily Hunter, Dr. Jenny Macaskill, Joanne Robertson, Stephen Williamson and Lauren Wilson for their technical support in the laboratories; Dorothy McDonald, Andrea McMillian and Nick Anderson for their engagement with the student community and administrative support.

Further thanks go to Jackie, Lise and Margaux which contributed to my experimental progress during their internship.

I am also very grateful for the research financial support provided by the Robert Gordon University and the local charity Friends of ANCHOR.

A special thanks go to David and Laura who have been supporting me throughout this journey despite the distance.

Thank you to my Greek family for their constant support! Maria (the twin), Zoi and Dimitris, ευχαριστώ πολύ !

Of course, I would like to thank my Aberdonian friends! Teodora, Viviana, Mhairi, Hazel, Sam and Martin, you made these years memorable.

Thank you to all my colleagues and friends including Matteo, Franziska, Moomin, Josh, Calum, Tesnime, Chrys, Abdullah, Tom and all the others, I was lucky to meet you all!

Finally, thank you to my family for their trust in my choices and abilities and for their constant support.

Abstract - Novel nanoparticle drug delivery systems: application in the *in vitro* study of Bisnaphthalimidopropyl derivatives against human colorectal cancer cell lines. – submitted for the obtention of the degree of Master of Research by Mathieu Brunet.

Colorectal cancer is one of the most severe causes of mortality worldwide accounting for 10% of total cancer cases. Although recent advances in early diagnosis have reduced the mortality rate associated with CRC, patients suffering from the later metastatic stage of the disease have a 5-year survival rate of only 14%. To enhance the current treatment options, bisnaphthalimides (BNIPs) were developed as a new group of chemotherapeutic agents. Presenting promising results *in vitro* against colon cancer cell lines, these anti-cancer drugs are limited by a poor aqueous solubility and a dose-limiting toxicity. In recent years, nanoparticle drug delivery systems have been developed to enhance the solubility and the clinical response of encapsulated anti-cancer agents. In this study, the latest generation of BNIP derivatives including bisnaphthalimidopropyl-piperidylpropane (BNIPPiProp), bisnaphthalimidopropyl-ethylenedipiperidine (BNIPPiEth) and bisnaphthalimidopropyl diaminodicyclohexylmethane (BNIPDaCHM) have been studied against SW480 and SW620 colorectal cancer cell lines. First, BNIPPiProp has been successfully encapsulated within solid lipid nanoparticles and a comparative cytotoxicity study was performed using MTT assay. After a 24-hour treatment, the 3 compounds alone demonstrated a strong cytotoxicity with IC_{50} values ranging from 1.3 to 2.6 µM in both SW620 and SW480. However, the drug-free nanoparticle formulation was found to cause a high toxicity level. BNIP-treatments also led to a significant increase of ROS levels after a 24-hour treatment associated with an increase of DNA damage with the significant creation of DNA strand breaks against both cell lines (both at IC_{50}). According to proteome profiler array, BNIPPiProp, BNIPPiEth and BNIPDaCHM were found to up-regulate and downregulate apoptosis-related proteins in a cell line and drug dependant manner. However, no increase in caspase-3 levels was detected after 24 hours against both cell lines using the 3 compounds studied. Together, these findings demonstrate the relevance of BNIP derivatives in the treatment of colorectal cancer and offer a first-stepping stone in the design of a BNIP-drug delivery system.

Keywords: Bisnaphthalimidopropyl, solid lipid nanoparticles, colorectal cancer

Contents

List of figures

List of tables

List of abbreviations

5-FU	5-Fluorouracil
APAF1	Apoptotic Protease Activating Factor 1
APC	Adenomatous Polyposis Coli
Bcl-2	B-cell lymphoma 2
BNIP	Bisnaphthalimidopropyl
BNIPDaCHM	Bisnaphthalimidopropyl diaminodicyclohexylmethane
BNIPDaoct	Bisnaphthalimidopropyldiaaminooctane
BNIPOPut	Bisnaphthalimidopropyl oxaputrescine
BNIPPiEth	Bisnaphthalimidopropylethylenedipiperidine dihydrobromide
BNIPPiProp	Bisnaphthalimidopropyl-piperidylpropane
BNIPPut	Bisnaphthalimidopropyl putrescine
BNIPSpd	Bisnaphthalimidopropyl spermidine
BNIPSpm	Bisnaphthalimidopropyl spermine
BSA	Bovine Serum Albumin
CRC	Colorectal Cancer
DISC	Death-inducing signalling complex
DLS	Dynamic light scattering
DMSO	Dimethyl sulfoxide
DSB	Double strand break
EPR	Enhanced permeation and retention
FBS	Fœtal bovine serum
FDA	U.S. Food and Drug Administration
GRAS	Generally Recognized as Safe
HNPCC	Hereditary nonpolyposis Colorectal Cancer
HPLC	High performance liquid chromatography
IC	Half maximal inhibitory concentration
LDH	Lactate dehydrogenase
LMP	Low melting point

MPS	Mononuclear phagocyte system
MRI	Magnetic resonance imaging
MTT	3-(4,5-Dimethylthiazol-2-yl)-2,5-Diphenyltetrazolium Bromide
NLC	Nanostructured lipid carriers
PBS	Phosphate buffer saline
PDI	Polydispersity index
PEG	Polyethylene glycol
PGA	Poly-I-glutamic acid
PGLA	Polylactic-co-glycolic acid
PI	Propidium iodide
PLA	Polylactic acid
PS	Phosphatidyl serine
RGU	Robert Gordon University
ROS	Reactive oxygen species
SCGE	Single gel electrophoresis
SLN	Solid lipid nanoparticles
SSB	Single strand break
TEM	Transmission electron microscopy
TNM	Tumour / Node / Metastatis
WHO	World Health Organization
XTT	2,3-bis-(2-methoxy-4-nitro-5-sulfophenyl)-2H-tetrazolium-5-carboxanilide

Chapter 1

Introduction

1.1. Colon Cancer

1.1.1. Overview of Colon Cancer

The World Health Organization (WHO) has declared in their 2014 report that cancer represents one of the deadliest diseases worldwide estimating 14 million new cases in 2012. WHO has also projected that this disease caused 9.6 million deaths in 2018. After cardiovascular diseases, cancer is considered the leading cause of death worldwide (World cancer report, 2014).

Cancer can be described as a heterogenous disease causing abnormal cell proliferation which can result in the formation of tumours. When this condition develops at the level of the colon or the rectum, it is then described as colon cancer or colorectal cancer (CRC). This subtype of cancer is one of the most diagnosed worldwide with more than 2 million cases reported every year (Stewart and Kleihues, 2003). More than 50% of the total number of cases are found in developed western countries, however, it has spread in numerous developing countries in recent years making it a major global challenge (Brody, 2015). A number of risk factors increase the likelihood of developing CRC, with age, diet, physical activity and the presence of additional bowel-related conditions being the most prevalent factors (John and Houlston, 2001; Haggar and Boushey, 2009).

CRC mortality has been reduced with the use of early diagnosis and with the development of screening programs which have offered a greater survival rate to patients responding more positively to the available treatments (Moiel, 2011). Moreover, the number of treatment options has increased in the recent years with the development of innovative strategies and the improvement of existing therapies. Nevertheless, only 1 in 10 patients survive the metastatic form of CRC making it a major health issue (Ries *et al.*, 2008).

1.1.2. Pathophysiology of colon cancer

CRC precursors are benign neoplasms or serrated polyps which correspond to the development of small cell clumps on the external surface of the colon epithelium (Ionov *et al.*, 1993). Over many years, local inflammatory changes or endogenous genetic modifications can cause the polyp to slowly become cancerous. Epigenetic and genetic mutations account for 70% of CRC cases. The loss of genomic stability represents a central event, initiating the development of CRC (Grady and Carethers, 2008). The sequential progression of CRC from benign polyp to metastatic cancer has been divided into 5 stages. These stages have many subtypes based on criteria of the TNM (Tumour / Node / Metastasis) staging system which indicate the progress of the disease in the tissue or in the entire body (figure 1) (Cunningham *et al*., 2010). Figure 1 presents the different stages of CRC with stage 0 being the benign presence of a polyp to stage 4 when the disease spread into different parts of the body also known as the metastatic stage.

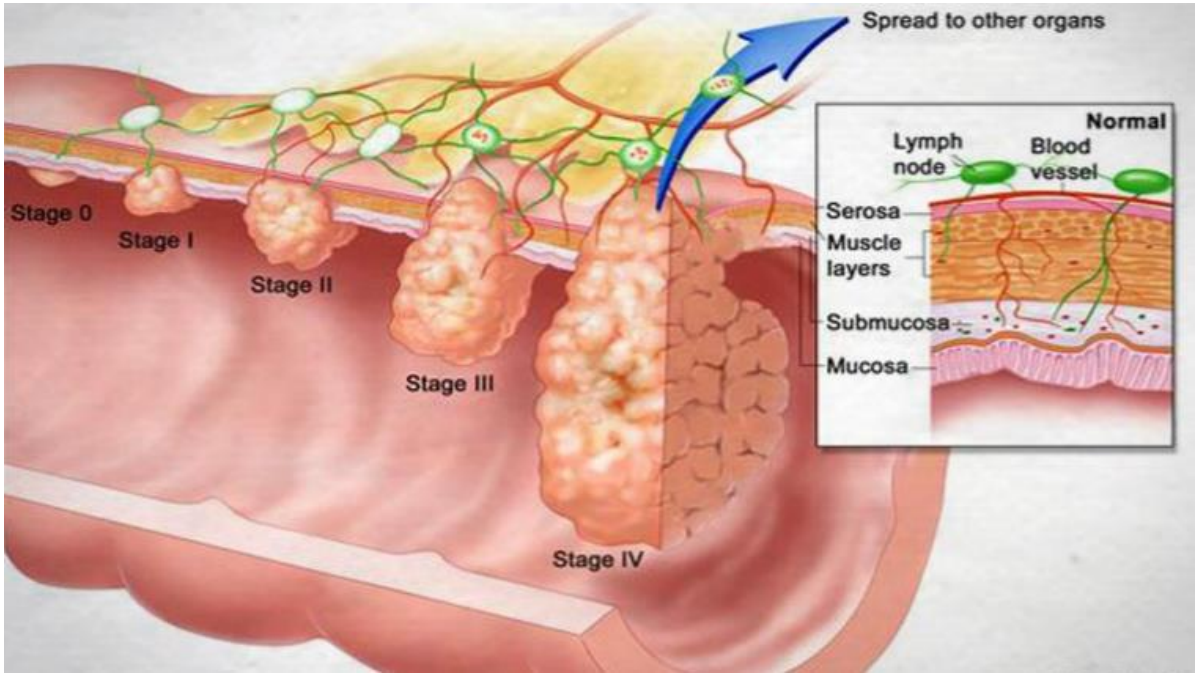

Figure 1. Representation of the staging evolution of CRC (Terese Winslow, National Cancer Institute, 2011).

The pathogenesis of CRC originates with the generation of genetic mutations, which can be inherited and shared in the family, or acquired. The resulting genetic or epigenetic alterations disrupt the genomic stability creating malignant cells (Pino and Chung, 2010). In the case of inherited mutations, genes such as *LH1*, *APC*, *MSH2* and *PMS2* can be altered but account for only 5% of CRC cases (Kinzler and Vogelstein, 1996). Acquired mutations generally generate a cascade of genetic alterations leading to a chromosomal instability. The apparition of the cancerous phenotype is mostly due to the alteration of the *APC*, *KRAS* or *p53* genes (Simon, 2016). *APC* is linked to the cell division processes and code for a transcription factor involved in the regulation of oncogenes. *KRAS* is an oncogene involved in cell growth and differentiation whereas *p53* is related to apoptosis initiation. Therefore, the alteration of these genes can create the conditions of tumour growth. Other tumour suppressor genes such as *PTEN*, *TP53* or *MLH1*, *MSH2* and *MSH6* also take part in the pathophysiology of colon cancer when inactivated (Markowitz and Betagnolli, 2009). Alternatively, aberrant DNA methylation or DNA repair defects can also be responsible for the genomic instability (Ashktorab and Brim, 2014). Moreover, if they are not directly involved with CRC pathogenesis, several genes have been found to be involved in the disease development *via* the disruption of key cellular pathways including WNT or TGF-β.

Nowadays, a 90%-survival rate is reported when patients are diagnosed with CRC stages I and II. However, if the cancer is not diagnosed before reaching the metastatic late-stage, a survival rate of 13% is then reported (KMA Cancer Committee, 2005). The continuous improvement of the understanding of CRC pathophysiology at the molecular level has allowed advances in the design of diagnostic tools and therapy. Nevertheless, the advanced stages on CRC remain difficult to treat and require the development of innovative therapeutic approaches.

1.1.3. Current therapeutic approaches

Treatment options are available for patients suffering from CRC and the therapeutic approach is decided upon various factors including CRC stage, the age and health status of the patient, and the analysis of the tumour characteristics (size and location). The correct staging of CRC involves the use of colonoscopy combined with a biopsy to obtain a precise diagnosis when possible, however, imaging techniques such as computerised tomography scans and magnetic resonance imaging are also employed (Barret *et al*., 2013).

One of the main treatment options offered remains surgery with the removal of the primary tumour using the complete mesocolic excision procedure or polypectomy (Hohenberger *et al*., 2009). Surgery is often the chosen procedure at stage I/II of CRC. Alternatively, for high risk stage II CRC, radiotherapy can also be employed as an adjuvant to eliminate cancerous cells using high energy X-ray (Castaneda and Strasser, 2017). Moreover, adjuvant chemotherapy can also be used to reduce the tumour mass and control cancer progression and avoid recurrence.

From stage III, chemotherapy is the treatment of choice and it is based on the use of cytotoxic compounds eliminating malignant cells (Aydinlik *et al.*, 2016). For CRC, effective chemotherapy began with the development of 5-fluorouracil (5-FU) in the late 1950s (Heildelberger *et al.*, 1957). This compound inhibits tumour growth by inhibiting cancer cell proliferation (inhibitor of thymidylate synthase). Alternative compounds such as oxaliplatin (DNA replication inhibitor) or irinotecan (topoisomerase I inhibitor) can act synergistically with 5-FU resulting in more positive outcomes for patients (Yildiz *et al*., 2018). However, these anti-cancer drugs have presented serious side effects such as organ toxicities as their action is not specific to malignant cells. Moreover, after exposure to chemotherapy, cancer cells can develop a resistance to the mechanism of action of the drug used also known as chemoresistance (Yeldag *et al.*, 2018). To mitigate these limitations, clinicians have to lower the dosage, thus, reducing the efficacy of the treatment and decreasing the survival rate in patients (Laura *et al.*, 2015). For late metastatic CRC, the low 5-year survival rate demonstrates the need for new therapeutic options.

For the last twenty years, researchers and clinicians have been trying to enhance current available chemotherapy and to identify new molecular targets for the treatment of CRC. Nowadays, the backbone of CRC treatment remains the combination of fluorouracil with a second anti-cancer drug with for example irinotecan (FOLFIRI) or oxaliplatin (FOLFOX) (Díaz-Rubio *et al*., 2007; Guo *et al*., 2016). Among the most innovative strategies, the use of monoclonal antibodies has been explored. These antibodies such as cetuximab and panitumumab target endothelial growth factor (EGF) and the associated EGF receptor (R) (Jonker *et al.*, 2007; Amado *et al.* 2008). EGFR is a CRC prognostic factor and its expression is linked to initiate events such *KRAS* mutation. These antibodies can either bind to EGFR (panitumumab) and provoke the receptor's internalisation or act as a competitive ligand preventing other molecules to activate EGF signalling pathways (de Mello *et al*., 2013). Alternative targets have also been studied, for example the use of bevacizumab to inhibit angiogenesis. Moreover, the addition of these antibodies to the pre-existing combination chemotherapy has demonstrated better tolerated toxicities and increase survival outcome in patients.

However, even combination therapy including the monoclonal antibodies leads to adverse effects such as skin rash, hypomagnesemia and nausea (Monti *et al.*, 2007). As 25% of patients diagnosed already experience advance CRC (stage 4), the development of new drugs and potentially new targets is necessary to achieve the clinical translation of augmented therapies, to overcome the current treatment limitations and the increase of chemoresistance (Huang and Sadee, 2006).

In this project, a promising family of chemotherapeutic agents developed at the Robert Gordon University has been studied as potential new treatment for CRC.

1.2. The BNIP derivatives, a promising family of chemotherapeutic agents

1.2.1. The history of the BNIPs

The history of naphthalimide compounds started in the 1970s when they were reported to be initially synthesised (Chen *et al.*, 1993). Naphthalimide (figure 2) is comprised of three six-membered rings and has demonstrated its potential as a chemotherapy agent presenting a strong anti-cancer activity (Brana *et al.*, 2001; Ralton *et al.*, 2007). Interestingly, naphthalimide compounds have intense UV and fluorescent properties which led to their use in a range of other applications such as fluoride ion sensors or fluorescent tracers (Xu *et al.*, 2005; Stewart, 1978).

Structurally, naphthalimides have a flat aromatic structure which have been linked to their ability to bind with DNA by intercalation. Moreover, the presence of a basic terminal group on its side chain is essential to its anti-cancer properties as a decrease of basicity in this group was shown to lower the drug cytotoxicity (Kamal *et al.*, 2013).

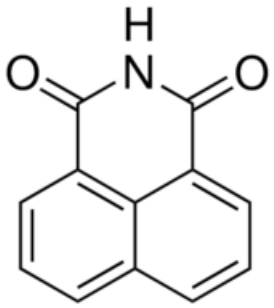

Figure 2. Representation of the chemical structure of naphthalimide.

The design of this compound is comprised of shared structural similarities with other chemotherapy agents such as cycloheximide or CG-630 (Brana *et al.*, 2001). After the synthesis of the naphthalimide monomer, Brana and Ramos (2001) attempted variations of the side chain and of the aromatic ring to enhance its activity. Interestingly, oxygen and sulphur atoms were found to decrease the molecule's activity.

Among all the derivatives developed by Brana *et al.* (2001), mitonafide and amonafide were screened and selected by the National Cancer Institute (USA) as the more potent compounds. After an extensive *in vitro* study against leukaemia and cervical cancer, the inhibition of topoisomerase II was presented as their anti-cancer mechanism of action. Moreover, based on their strong anti-cancer activity, these two drugs reached Phase I and II clinical trials (Leaf *et al*., 1997; Cassado *et al.*, 1996). Unfortunately, central nervous system toxicity leading to dementia was reported with the use of mitonafide whereas important myelosuppression was reported with the use of amonafide (Alami *et al.*, 2007). These early clinical trials showed the potential of naphthalimide as chemotherapeutic agents. Nevertheless, the existence of a dose-limiting toxicity was still a critical limiting factor (Brana *et al.*, 2001).

To augment the therapeutic efficacy of the naphthalimide, Brana *et al.* (2003) developed an innovative symmetrical compound associating two naphthalimide groups together and were named bisnaphthalimides. The union of the two naphthalimido rings was performed using a polyamine-type linker chain. The *in vitro* study of bisnaphthalimides against colon HT-29 cells showed an increased cytotoxicity compared to the previous generation of BNIPs. Additionally, it was observed that the length of the chain and its alterations were linked to the resulting cytotoxicity of the compound.

Bisnafide and Elinafide reached clinical trial Phases I and II, however side effects such as neuromuscular toxicity remained. Subsequent formulation improvements focused on the design of the linker chain to overcome the current limitations of this family of compounds including a poor aqueous solubility and a dose-limiting toxicity.

The use of polyamines has proven to be a key discovery in the formulation of BNIPs improving both their *in vivo* and *in vitro* activities. Kong Thoo Lin and Pavlov (2000) created a new generation of BNIPs involving the use of natural polyamines with a variation in the length of the chain and the number of heteroatoms. Bis-naphthalimidopropyl putrescine (BNIPPut), spermidine (BNIPSpd), spermine (BNIPSpm) and oxaputrescine (BNIPOPut) were synthesised and studied *in vitro* (Kong Thoo Lin and Pavlov, 2000). Their study concluded that the presence of heteroatoms in the linker chain improved the

drugs' aqueous solubility whereas the increased length of the linker chain decreased the drugs' cytotoxicity level. Interestingly, Brana *et al*. (2005) also demonstrated that the symmetrical structure of the linker chain was associated with the resulting cytotoxicity (Brana *et al.*, 2005).

The development of BNIPs with the optimisation of their linker chain was continued by Barron *et al.* (2010) which reported that the addition of cyclohexane rings or nitrogen atoms in the linker chain augments the cytotoxic activity of the compound. From this work, bisnaphthalimidopropyl diaminodicyclohexylmethane (BNIPDaCHM) was studied *in vitro* against breast cancer cells (human breast epithelial MDA-MB-231) and exhibited a stronger cytotoxic activity (IC_{50} < 5 µM after 24 h treatment) than the anti-cancer agent doxorubicin. Further investigations revealed that BNIPDaCHM induces DNA double strand breaks and an inhibition of DNA repair against human breast adenocarcinoma cell line (MDA-MB-231). This new information led to a better understanding of their mechanism of action (Barron *et al.*, 2010). However, many questions remained unanswered regarding further improvement of the formulation and the mechanism of action of this family of compounds depending on the type of cancer targeted.

1.2.2. The last generation of BNIP derivatives

Based on the promising results obtained with BNIPDaCHM, Kopsida *et al.* (2016) synthesised the most recent generation of BNIPs using the latter as a parental compound to investigate if the ring position and the length of linker chain could augment the cytotoxic and DNA-binding properties of BNIPs. Therefore, bisnaphthalimidopropyl-piperidylpropane (BNIPPiProp) and bisnaphthalimidopropylethylenedipiperidine dihydrobromide (BNIPPiEth) were created (figure 3).

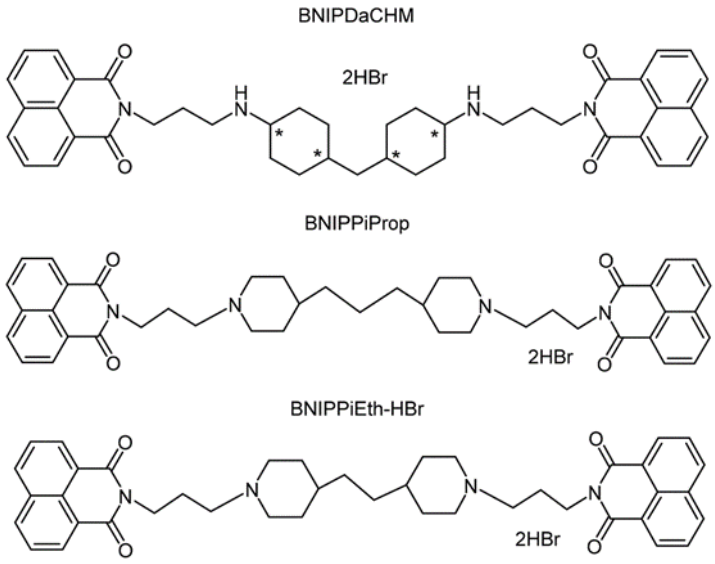

Figure 3. Representation of BNIPPiProp, BNIPPiEth and BNIPDaCHM chemical structures (adapted from Kopsida *et al.*, 2016).

BNIPPiProp is a structural isomer of BNIPDaCHM whereas BNIPPiEth is an isoform of BNIPPiProp having one less carbon at the centre of the linker chain. The resulting 3 compounds were studied *in vitro* in human breast cancer cells. BNIPPiEth was reported as the most cytotoxic compound against MDA-MB-231 and SKBR-3 cells (IC_{50} values ranging 0.2-3.3 μM) suggesting that the shorter linker chain enhanced its cytotoxicity (Kopsida *et al.*, 2016).

The main barriers between the BNIPs and their use as a chemotherapeutic agent are their poor aqueous solubility and achieving a targeted delivery. To overcome these limitations, this project will study the use of nanoparticles as a delivery system for the BNIPs to enhance their efficacy against CRC.

1.3. Nanoparticles as delivery systems for anti-cancer agents

The term nanoparticle was coined during the 1960s with the first formulation of lipid-based nanoparticles reported by Shlunk and Lombardi in 1969. Nanoparticles correspond to objects having a size ranging from 1 to 1,000 nm (Shlunk and Lombardi, 1969). A wide range of nanoparticle formulations exist and can be used in different fields, however, most of them are designed to treat or diagnose different diseases. Several medical applications are currently used: in bioimaging, with novel nanoparticle-based contrast product for MRI, or in biosensing with the detection of cancer biomarkers (Wilczewska *et al.*, 2012). However, the main use of nanoparticles is as drug carriers with the encapsulation of therapeutic molecules such as anti-cancer agents.

1.3.1. The benefits of nanoparticles in a drug delivery system

Using nanoparticles as a drug carrier is beneficial on two levels. First, the use of a drug carrier has a protective function for the encapsulated drug permitting its transport as well as limiting its premature degradation *in vivo* (Sagar *et al*., 2011). The drug can be protected from being damaged by its environment including biological barriers such as the mononuclear phagocyte system (MPS) (Blanco *et al*., 2016). The encapsulation within a nanoparticle drug delivery system can also improve the drug's intrinsic physicochemical properties with for example the sustained and controlled release of the drug and the reduction of its systemic toxicity (Aleksandrowicz *et al*., 2017).

Being administered in the human body mostly *via* the intravenous administration route, the aqueous solubility of the drug is often a challenge. Arriving in the blood stream, sequential obstacles are presented to the anti-cancer agents limiting their action (Ferrari, 2010). Resident macrophages from the MPS can uptake the circulating drug and the non-specificity of free drug can result in the potential accumulation of the drug in healthy organs such as the spleen or the liver. Even when the drug has reached the tumour site, the tumour microenvironment can be challenging and the cellular internalisation can be uncertain due to the endosomal escape (Li *et al*., 2020).

One of the most interesting aspects of the use of nanoparticles as drug carriers is the possibility of actively or passively targeting a specific organ, tissue or cell type and thus overcoming the issues associated with non-specific delivery. The active targeting corresponds to the addition of molecules such as antibodies, aptamers or peptides at the surface of the drug carrier allowing the nanoparticles to bind to a specific target such as a malignant cell (Acharya and Sahoo, 2011). With active targeting, treatment efficiency can be increased, and side effects can be prevented as the ligands improve the binding of drug carriers to the targeted cells, and therefore, enhance their cellular uptake in targeted cancer cells and not in healthy cells (Yoo *et al*., 2019). However active targeting presents important limitations as this approach does not represent a guiding system for the nanoparticle but an enhancer to its specific cell-binding properties which does not improve large-scale distribution in the body (Choi *et al*., 2009). Moreover, the cost of the development of such a system needs to be considered as high specificity ligands can be very expensive and can be a limiting-factor in the design of large-scale production (Cheng *et al*., 2012).

Importantly, nanoparticles can also undertake passive targeting which is particularly interesting in cancer therapy. Once a tumour has reached a diameter of a few millimetres, it will need to build a nutrient supply network *via* angiogenesis (Baban and Seymour, 1998) which is triggered by the tumour itself. The lack of O_2 triggers the production of growth factors which, in turn, induce the formation of blood capillaries. These capillaries can link to the original blood system; however, they present irregularities in their structure such as weak inter-cellular epithelial junctions and high levels of membrane channels (Pope Harman *et al.*, 2007). The nanoparticles take advantage of these cancer specificities and passively accumulate in the tumour due to their nano-size (> 200 nm) which allow them to cross the epithelial junctions. This phenomenon is also called the EPR (Enhanced Permeation and Retention) effect as presented in figure 4 (Maeda *et al.*, 2000).

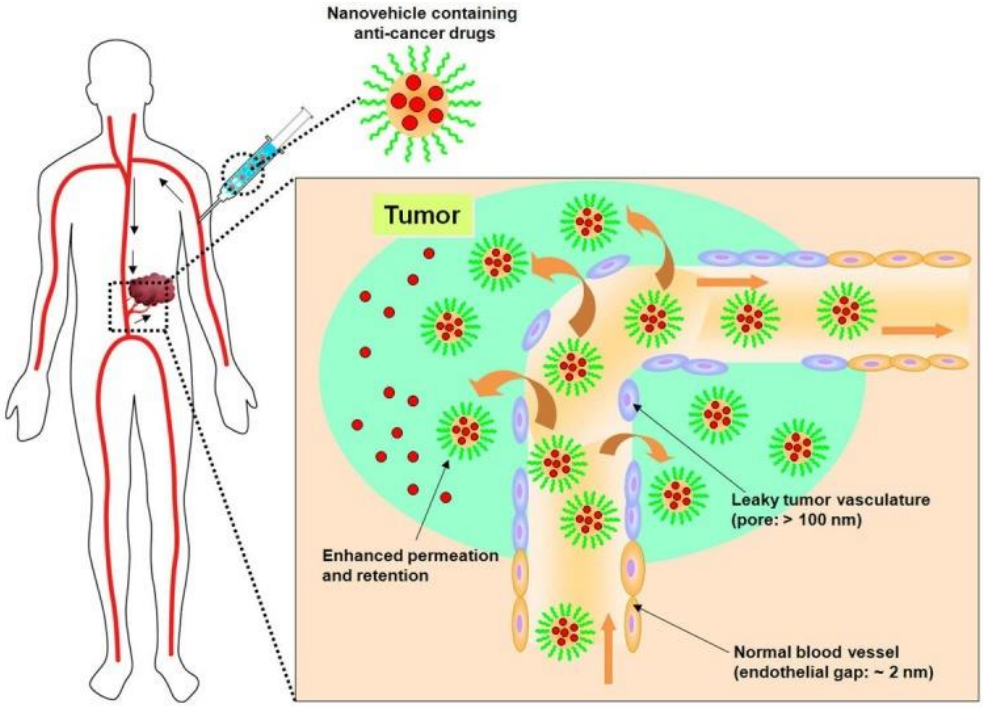

Figure 4. Representation of the enhanced permeability and retention (EPR) effect associated with the use of anti-cancer drug delivery systems (Bae *et al*., 2011).

The EPR effect is responsible for the passive targeting of the nanoparticles and it is based on the small size of the delivery system making the treatment cancer specific. However, it is critical to reflect on the EPR-based cancer therapy design as the understanding of EPR effect has evolved since its first description in 1986 by Matsumura and Maeda (Matsumura and Maeda, 1986). During the last 10 years, several studies showed that the EPR effect was heterogenous depending on the stage of the tumour development and on the tumour type which can lead to bias in pre-clinical studies for the development of nanomedicines (Tanaka *et al*., 2017; Golombek *et al*., 2018).

Therefore, the use of nanoparticles as a drug delivery system presents numerous advantages for the facilitated delivery of anti-cancer drugs while reducing the associated drug side effects. Although these benefits are shared by all nano-drug delivery systems, each type of nanoparticle has specific properties which need to be evaluated before the design of a formulation.

1.3.2. Types of nanoparticles

Despite its youth, the nanomedicine field has expanded rapidly in recent years with the development of a large variety of nanotechnological platforms (figure 5). Nanoparticles can be split into two categories: the organic nanoparticles, including the polymeric and lipid nanoparticles, and the inorganic nanoparticles. The latter are metal-based formulations (mostly iron- and gold-based) with interesting optical and magnetic properties. These particles have been widely investigated as drug carriers allowing a high drug loading capacity and an ease to functionalise their external surface. Among successful examples, mesoporous silica, gold, iron and copper-derived nanoparticles can be mentioned (Hu *et al.*, 2013; Bobo *et al.*, 2016). Moreover, this class of nanoparticles is used for specific bioimaging techniques such as iron oxide nanoparticles in MRI (Chertok *et al.*, 2008). Interestingly, the combination of diagnostic and therapeutic approaches is called the theranostic strategy when the drug delivery system can simultaneously be used as an imaging agent (Yang *et al.*, 2011). Nevertheless, these inorganic nanoparticles are limited by safety issues associated with their low biocompatibility and the lack of knowledge regarding their long-term cytotoxicity (Laurent *et al.*, 2008).

To obtain greater biocompatibility, organic nanoparticles have been designed as drug carriers. The encapsulated molecule of interest can be DNA, proteins or drugs (Jong and Borm, 2008). Within the organic class of nanoparticles, the polymeric and lipid-based formulations are distinguished by the nature of their composition and structural differences.

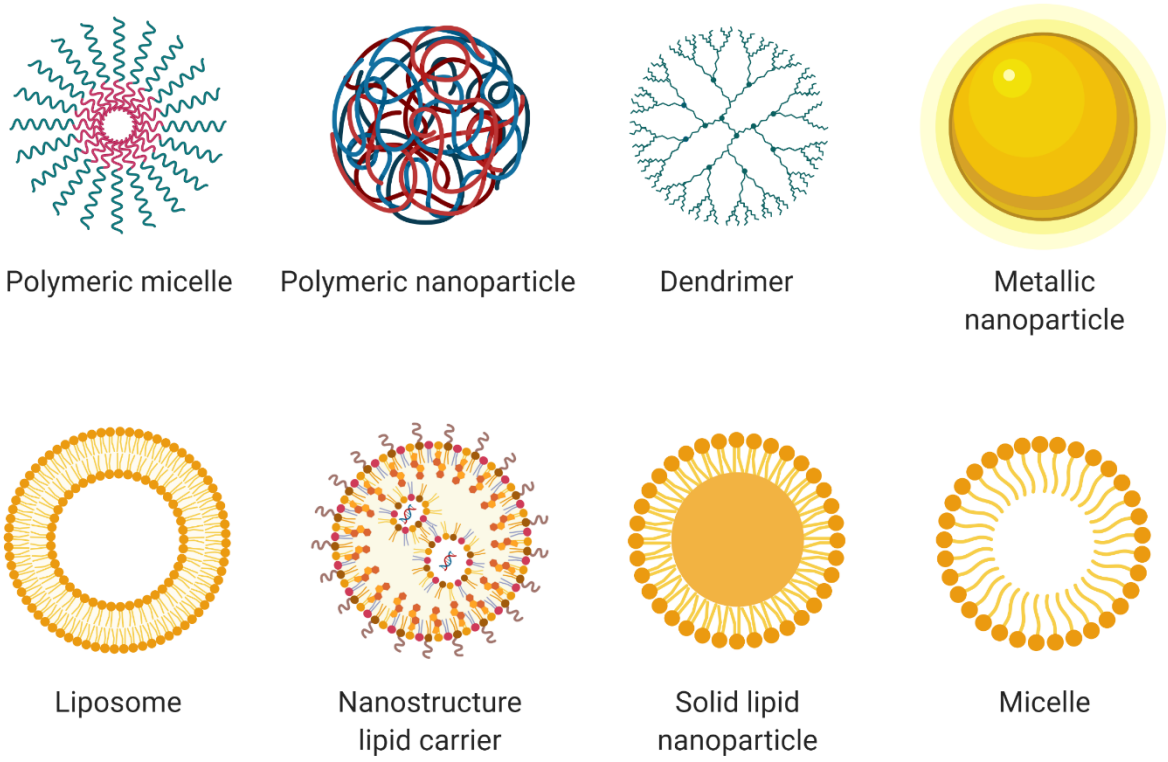

Figure 5. Schematic representation of the structure of the most common types of nanoparticle drug delivery systems (created using BioRender™).

Regarding polymeric nanoparticles, they are made of repeated subunits and chains of polymers and can be used to entrap or be conjugated to a drug of interest. Polymers such as chitosan, albumin or heparin have been extensively used for the delivery of nucleic acids, proteins or drugs. For example, the abraxane formulation has been developed to encapsulate the anti-cancer drug paclitaxel within polymeric nanoparticles composed of albumin. Since, it has been used clinically for the treatment of metastatic cancer (William *et al.*, 2005). Moreover, the use of biodegradable polymers such as polyethylene glycol (PEG) or poly-l-glutamic acid (PGA) have also been employed to enhance the anti-cancer efficacy of a multitude of drugs including camptothecin (Sabbatini *et al.*, 2004; Bhatt *et al.*, 2003). Alternatively, the development of polymeric micelles (also called amphiphilic block copolymers) and dendrimers have been reported as promising resources. Polymeric micelles are composed of a hydrophobic core containing the therapeutic agent of interest with a hydrophilic polymeric shell

whereas dendrimers are nanoparticles exhibiting branches of monomers around a central core (Cho *et al.*, 2008). Both technologies have shown promising results with, for example, the conjugation of cisplatin with dendrimer (Malik *et al.*, 1999) or (PEG-poly(D,L-lactide)-paclitaxel which is a polymeric micelle formulation of paclitaxel that reached clinical trial phase I (Kim *et al.*, 2004). The main advantage of using polymeric nano-formulations is that they can be designed as tailored-nanomedicines with reproducible and predictable properties. However, all polymeric nanoparticles are not biocompatible and their production can require the use of organic solvents which are toxic for patients (Chan *et al.*, 2010).

To overcome these limitations, lipid-based formulation of nanoparticles has been designed. They do not require the utilisation of hazardous organic solvents in their production and the use of lipids offer a great biocompatibility and degradation capacity *in vivo*. The first lipid-based formulation created was the liposome in 1965 and is still the most extensively studied and used lipid-based drug delivery system today (Bangham, 1993). With more than 10 liposomal products clinically approved, these self-assembling nanoparticles harbouring a lipid-bilayer membrane are formidable carriers of hydrophilic agents (Torchilin, 2005).

To deliver lipophilic compounds such as BNIPs, other lipid-based systems named solid lipid nanoparticles (SLN) and nanostructured lipid carriers (NLC) have become very popular due to their versatility (figure 6) (Talegaonkar and Bhattacharyya, 2019). The formulation of SLNs was first introduced by Müller in 1993 whereas NLCs appeared a decade after (Müller *et al.*, 1993). Both formulations are nanoparticles formed by a lipid core, however SLNs have a solid lipid core instead of the liquid lipid core found in NLCs. The creation of SLNs revealed that these nanoparticles presented several advantages including the protection of the encapsulated molecule against environment degradation, the increase bioavailability of hydrophobic molecules, the low cost and ease of production and the absence of organic solvent in their preparation (Das and Chaudhury, 2011).

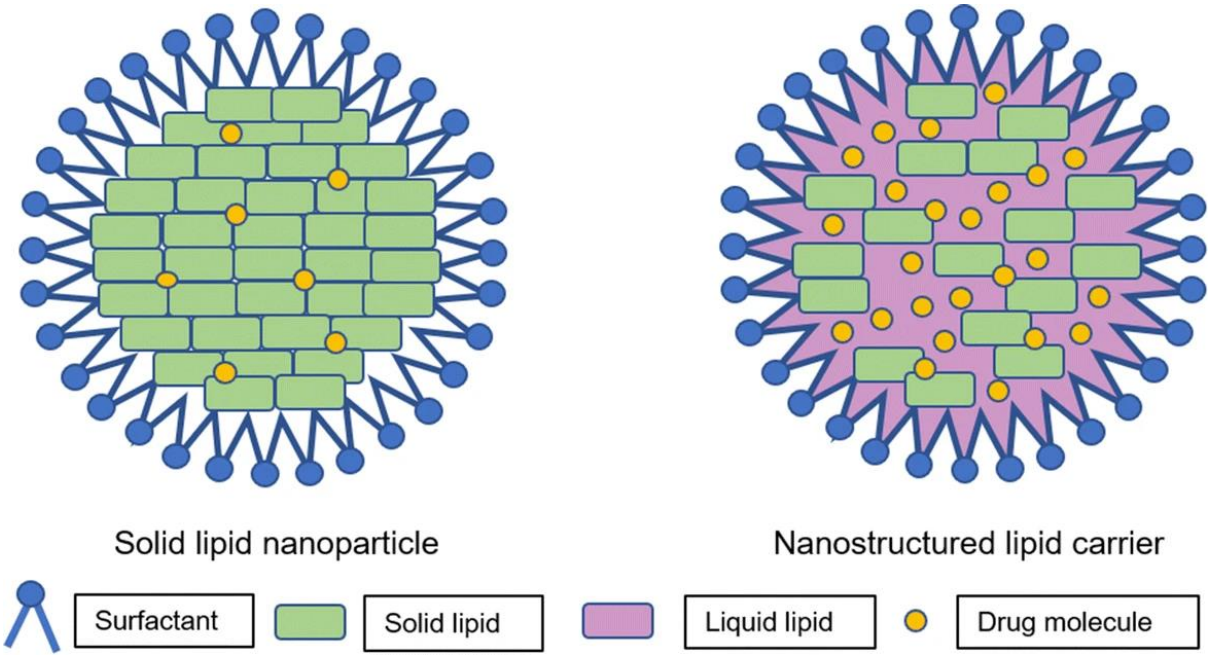

Figure 6. Schematic representation of SLNs and NLCs (Subramaniam *et al.*, 2020).

SLNs are mainly composed of lipids and surfactants, and the choice of each is critical for the resulting nanoparticles' properties. All components chosen are preferably of GRAS (Generally Recognized As Safe) or approved by the U.S. Food and Drug Administration (FDA). The lipid is the major component of the nanoparticle matrix, making the type of lipid chosen very important. Most of the lipids used are fatty acids such as stearic acid (Severino *et al.*, 2011), triglycerides such as tricaprin (Lim and Kim, 2002) or waxes such as cetyl palmitate (Farboud *et al.*, 2011). Stearic acid is a natural lipid found ubiquitously which is safe and biodegradable (Gonzalez-Mira *et al*., 2010). Stearic acid has also demonstrated the specific ability to accumulate in the cytoplasm of cancer cells making it ideal to transport BNIP compounds (Severino *et al*., 2011). Other derivatives such as palmitic or oleic acids can be chosen alternatively or in combination, as the crystallinity of the lipid core can enhance the drug loading capacity (Bavani *et al.*, 2020).

The surfactant is the second major SLN component and it is used as a stabilising agent, essential to obtain a good dispersion of the nanoparticles when the lipid and aqueous phases are mixed. It is also responsible for the stability of the nano-

structure during storage, and for maintaining the shape and the dispersion of the SLNs *in vivo* (Mehnert and Mäder, 2001). A surfactant can be cationic, anionic, non-ionic or amphoteric depending on the design of the nanoparticles to maintain a good hydrophile-lipophile balance. Tween 80 and Poloxamer 188 appear to be the most widely used stabilising agents and a combination of surfactants is usually chosen (Leonardi *et al.*, 2014). In this project, Tween 80 and Span 20 were the two non-anionic surfactants used as stabilisers chosen for their known biocompatibility and extensive use in the formulation of SLNs. The phospholipid egg lecithin was also present due to its emulsifying capacity as amphoteric surfactant.

Regarding their production method, SLNs are mostly produced through the hot homogenisation method which consists of the dispersion of the melted lipid phase in an aqueous phase containing surfactant (Schwarz *et al.*, 1994). Subsequently, the mix is homogenised at high speed, maintaining the emulsion at a temperature greater than the lipids' melting points. The resulting nanoparticles in suspension are then cooled down to form solid matrices. An alternative technique, the cold homogenisation, can also be used when lipophobic or thermosensitive drugs are employed. Nevertheless, this method has demonstrated the creation of more polydispersed and larger particles (Mehnert and Mäder, 2001).

Determining the ideal formulation of a nanoparticle will depend on the encapsulated molecule but also on the chemical property requirements such as release rate, storage time and hydrophobicity. For example, the lipase enzymes can degrade lipids by splitting their ester linkage and it has been shown *in vitro* that the velocity of this degradation depends on the lipid matrix and surfactant composition which can be critical for the targeted biodistribution of SLNs (Yang *et al.*, 1999).

Although thousands of formulations have been reported, only a few have been approved by the FDA. This is partly due to the fact that for most compounds, the nanoencapsulation demonstrated a small potency increase, which is not sufficient for pharmaceutical companies to develop a reformulated product (Venditto and Szoka, 2014).

Many solid lipid nanoparticle delivery systems have been reported to encapsulate anti-cancer drugs successfully such as paclitaxel (Lee *et al.*, 2007), camptothecin (Yang and Zhu, 2002) or doxorubicin (Wong *et al.*, 2006). In these cases, the use of nanoparticles as a delivery system has increased the anti-cancer activity of the SLN-encapsulated drug compared to the free drug showing promising results for the SLN-encapsulation of BNIP derivatives.

To obtain similar results with an increased anti-cancer activity from the BNIPs, their poor aqueous solubility must be addressed. Tetrandrine and Emodin, two anti-cancer agents, shared the same limitation. However, both drugs have been successfully encapsulated into lipid nanoparticles, making the use of SLNs a promising approach to address the hydrophobicity of BNIPs (Wang *et al.*, 2012; Li *et al.*, 2011). Adapting nanotechnology to the BNIPs is an idea that researchers have already explored: BNIPs has been encapsulated into Poly Lactic Acid (PLA) and Poly Lactic-co-Glycolic Acid (PGLA) polymeric nanoparticles against *Leishmania infantum* (Costa Lima *et al.*, 2012). However, BNIPs encapsulation into lipid nanoparticles to treat colon cancer has not been studied yet.

In addition to the development of a drug delivery system, understanding the mechanism of action of an anti-cancer drug and its cellular fate is key in developing tailored nanomaterials and this can be studied in a synergistic way to achieve faster clinical translation.

1.4. The evaluation of the impact of the BNIPs on their efficacy as anti-cancer agents

1.4.1. SW480 and SW620 as *in vitro* model for colon cancer

For this project SW480 and SW620 were the two cell lines used to study CRC *in vitro*. Used worldwide, these two colon carcinoma cell lines offer a unique platform for CRC research as they were derived from the same patient, at two different stages of his CRC. Therefore, they offer an interesting alternative to non-metastatic CRC cell lines such as CaCo-2 or HT-29 which are employed most of the time.

SW480 cells were derived from a 50-year old patient at an early stage from primary tumours whereas SW620 cells were derived 6-month later when mesenteric lymph node metastases were discovered (Rober *et al.*, 2000). Deriving from the same individual, these two cell lines shares the same genetic background allowing a more precise *in vitro* analysis of the phenotypic differences between the early and late stage of CRC as confirmed by the study of their chromosomal markers (Melcher *et al.*, 1995).

Although this *in vitro* model has already been used to study SLNs-encapsulated anti-cancer drugs, the study of BNIPs have not been explored (Yassin *et al*., 2010).

1.4.2. Apoptosis

Apoptosis is a naturally-occurring cellular mechanism also known as programmed cell death. In healthy humans, apoptosis is a critical process involved in tissue development and cellular homeostasis *via* the regulation of the balance between cell death and cell proliferation (Claire *et al.*, 2018). Opposed to apoptosis, necrosis can be described as accidental cell death due to tissue damage provoking the lysis of the cells in the surrounding environment leading to inflammation. On the other hand, apoptosis is a highly regulated and sophisticated mechanism involving the fragmentation of the cellular content within membrane vesicles to be phagocytosed, therefore preventing an inflammatory reaction (Elmore, 2007).

For programmed cell death to be activated, specific conditions including DNA damage or abnormal cell growth must trigger one of the two cellular apoptotic pathways (Lopez and Tait, 2015). They are known as the intrinsic and extrinsic pathways or, respectively, mitochondrial and death receptor pathways. These two different routes are separated upon on the nature of the triggering signal. Both pathways converge at a common end-point being the activation of the caspases (cysteine aspartyl-specific proteases) cascade (figure 7) (Julien and Wells, 2017).

First, with the intrinsic pathway, internal stimuli such as DNA damage, biochemical stress, the lack of growth factors, oxidants or microtubule targeting drugs will induce the activation of mitochondrial proteins such as Bcl-2 or Bax, which are pro-apoptotic proteins bound to the mitochondria membrane (Zaman *et al*., 2014). The resulting disruptions of the mitochondrial membrane then lead to the release of the cytochrome c in the cytoplasm. It will then form a complex with the protein APAF1 called the apoptosome, which activates the initiator caspase-9 leading to the activation of the caspase cascade.

On the other hand, the extrinsic pathway relies on specific extracellular signalling to be activated also known as cell death ligands (Goldar *et al.*, 2015). Once attached to death receptors such as Fas (CD95), TNF (TNFR1) or TRAIL, the activation of the formed complex then initiates the recruitment of adaptor proteins such as Fas-associated death domain (FADD) and TNF receptor-associated death domain (TRADD) (Goldar *et al.*, 2015). Subsequently, the death-inducing signalling complex (DISC) is then created *via* the association of initiator procaspase 8 and 10 to the adaptors. Once formed, DISC can then activate the caspase cascade through the activation of procaspase 8 and 10 (Karp, 2008).

The activation of caspase 9 (intrinsic pathway) or caspase 8 (extrinsic pathway) results in the activation of caspase 3. From that event, the last stage of apoptosis initiation begins and is known as the execution pathway (D'Arcy, 2019). Caspases are the key mediators of apoptosis as they are responsible for the dismantlement of the cell through the cleavage of a large number of proteins (Lopez and Tait, 2015). Within this family of proteins, caspases 2, 8, 9 and 10 are known as initiator caspases whereas caspases 3, 6 and 7 are the executioner caspases. In both pathways, when an initiator caspase is activated, it then leads to the activation of effector caspases by proteolytic cleavage. The execution pathway results in the activation of endonucleases and proteases for the degradation of the cell cytoskeleton and chromosomes. Cells then organise their compartmentalisation with the creation of apoptotic bodies which can be eliminated through phagocytosis protecting the cellular environment from collateral damage (Poon *et al*., 2014).

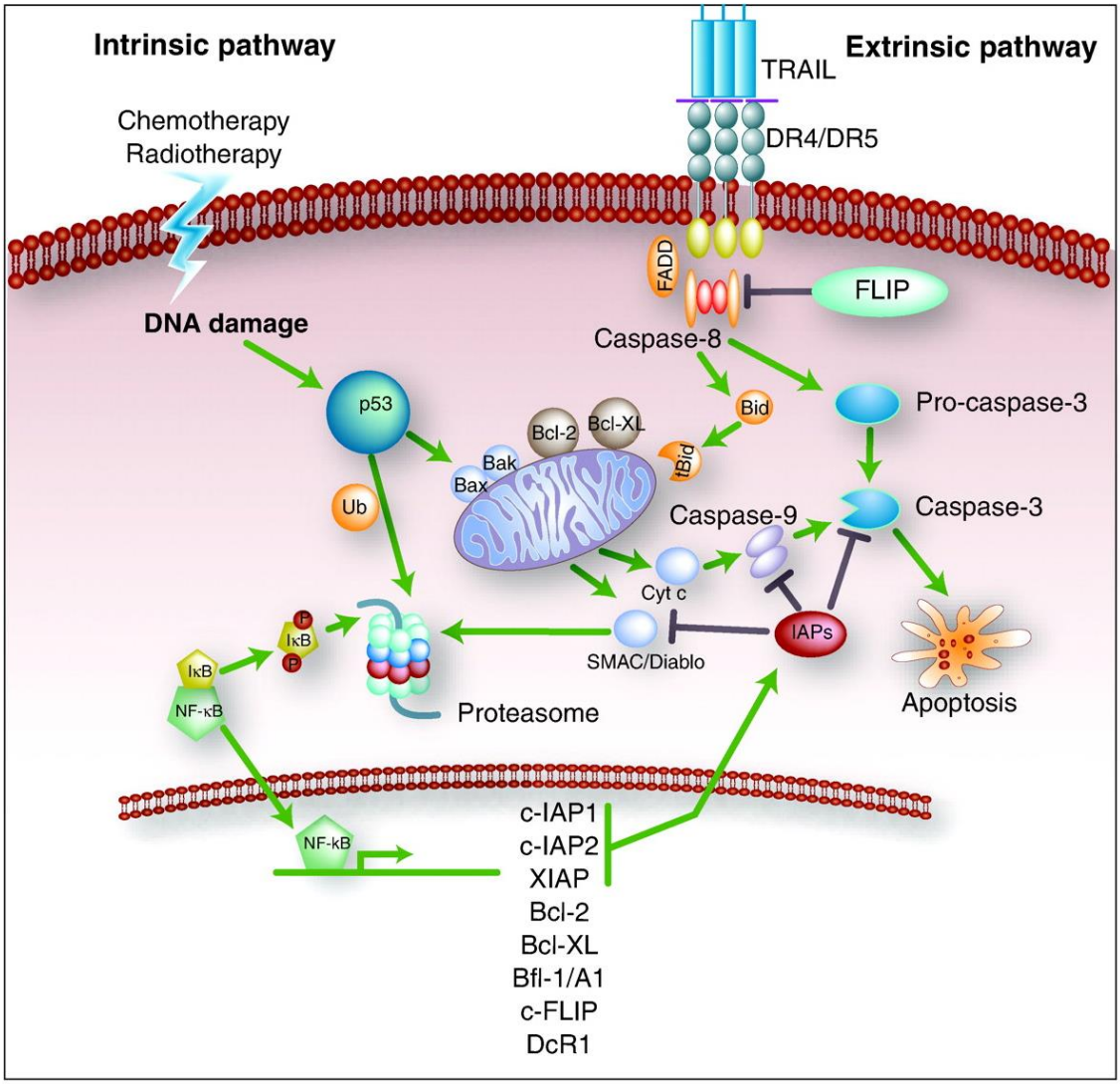

Figure 7. Representation of the intrinsic and extrinsic pathway of programmed cell death (Elisabeth *et al.*, 2006). Green arrow = activation / Black arrow = inhibition

Discovered by Kerr *et al.* (1972), the apoptotic mode of cell death has been studied extensively targeting its induction for treating diseases. Drugs, such as navitoclax which inhibits apoptotic inhibitors (Bcl-2 family) leads to an increased programmed cell death (Olsterdorf *et al.*, 2005). These strategies are used in the fight against cancer making the enhancement of apoptosis levels a therapeutic target. The induction of cell death *via* apoptosis using chemotherapy is not limited to molecular targets involved in programmed cell death pathways but can also be triggered by stress response to oxidative or DNA damage (Tannock and Lee, 2001). Consequently, it is judicious to study the cell death mechanism of action that BNIP derivatives can induce against SW480 and SW620 CRC cell lines

starting with the study of apoptosis. Subsequently, underlying the cellular events leading to cell death is also important to design better drug delivery systems helping the drug to be more effective.

1.4.3. Reactive oxygen species

Reactive oxygen species (ROS) are radicals, ions or molecules which own an unpaired electron in the furthest shell of electrons such as superoxide (O_2^-), hydroxyl radical (•OH), hydrogen peroxide (H_2O_2) or nitric oxide (NO•) (Liou *et al.*, 2010). They can be found in healthy cells as a natural by-product of the normal metabolism of oxygen during the mitochondrial respiration. ROS are also involved in several cellular signalling pathways including NFκB or MAPK (Zhang *et al.*, 2016), or in immunity support with oxidative bursts during phagocytosis (Dahlgren and Karlsson, 1999). Although ROS are essential for the cellular activity, the ROS level needs to be regulated to maintain homeostasis. Low levels of ROS can be responsible for cardiomyopathy with the generation of reductive stress (Liou *et al.*, 2010) whereas too high levels can provoke oxidative stress (Liemburg-Apers *et al.*, 2015). Oxidative stress is particularly dangerous for the cells as it can damage cellular structures and reacts with a range of biomolecules such as nucleic acids or proteins. Therefore, oxidative stress can be perceived as a mediator of genomic instability which can lead to cell death (Cooke *et al.*, 2003). Consequently, there is a necessity for cells to use efficient mechanisms for ROS detoxification through the action of antioxidant enzymes such as superoxide dismutases or non-enzymatic molecules such as glutathione, flavonoids and vitamins A, C and E (Bardaweel *et al.*, 2018).

In cancer, the disruption of the ROS balance has been highlighted as an important cause of development and spread of cancer with most cancer cells exhibiting important ROS levels (Saikolappan *et al.*, 2019). The interferences in cells' signalling pathways such as NF-κB can produce an inflammatory environment stopping programmed cell death (Puar *et al.*, 2018). Nevertheless, ROS can also be used to defeat cancer as part of the therapeutic strategy with the development of anti-cancer therapies focused on the generation of ROS to create oxidative stress (Wang and Yi, 2008). This paradoxical manipulation of ROS level relies on

the higher basal ROS level observed in cancer cells. Due to their abnormal proliferation rate, cancer cells adapt to increased ROS concentration. However, a chemotherapy-induced ROS generation is capable of being cytotoxic for cancer cells. Due to their higher ROS-survival threshold, malignant cells can then be selectively affected by the treatment making it more specific with less side effects (Kim *et al.*, 2019). Accordingly, oxidative stress has been identified as a cancer therapy target and drug development has been focused on targets such as ROS inducing pathways or pro- and anti-oxidant regulatory proteins, notably with Paclitaxel (Alexandre *et al.*, 2006) or Etoposide (Bragado *et al.*, 2007). Hence, investigating the capacity of BNIPs to generate ROS levels in CRC cells could be an important indication of their mechanism of action which could be linked to DNA damage and cell death.

1.4.4. DNA damage

Most of the cells in the human body experience DNA lesions on multiple occasions every day (Lindhal and Barnes, 2000). These genetic alterations can be induced by chemical or physical events such as UV or chemicals exposure, thus, being referred to as DNA damage (Curtin, 2012). The range of DNA damage lesions includes single and double strand breaks but also base insertions, deletions or alkylation and can be responsible for disrupting DNA transcription and replication.

In the treatment of cancer, many compounds have been identified as DNA-damaging drugs including cisplatin, oxaliplatin doxorubicin or daunorubicin (Cheung-Ong *et al.*, 2013). The first two examples are DNA crosslinkers, with a platinum core capable of binding guanine residues after cellular uptake forming DNA crosslinks. On the other hand, the last two examples, doxorubicin and daunorubicin, are drugs that cause single or double DNA strand breaks by creating a complex with topoisomerase I or II enzymes. These two enzymes are key participants of DNA replication and transcription for its winding, thus, making them effective targets.

A complex cellular machinery is in place to repair the DNA damage caused called the DNA damage response which exists to maintain the genomic integrity. Minor changes due to base alterations can be restored by excision repair whereas more

serious lesions such as DNA strand breaks can be repaired by nucleotide excision repair (Hoeijmakers, 2009). Although different forms of DNA damage exist such as base alteration or single strand breaks, DNA double strand breaks (DSBs) are the most dangerous DNA lesions for a cell for being mutagenic and they can be caused by radiation of alkylating anti-cancer drugs (Rastogi *et al.*, 2010). DNA repair mechanisms' efficiencies can be limited if the level of damage is too high for the repair capacity of the cell. In this case, the DNA lesions can lead to apoptosis stopping cancer progression (Bernstein *et al.*, 2013). On that note, DNA repair mechanisms have also been studied as emerging cancer therapies with for example the overexpression of DNA repair factors (Sato and Itamochi, 2015).

From the study of approved anti-cancer drugs such as doxorubicin, links between the generation of ROS, oxidative stress and DNA damage have been made (Coussens and Werb, 2002). The resulting induction of apoptosis *via* this mechanism of action has inspired the formulation of a new generation of chemotherapy. Based on the current knowledge of BNIPs with their high cytotoxicity, DNA binding properties and indication of apoptotic cell death induction, this project has explored the mechanism of action of these drugs in CRC to enhance their future therapeutic use.

1.5. Aims

The aims of this project were to enhance the potency of BNIP derivatives as chemotherapeutic drugs in the treatment of colorectal cancer by the development of a solid lipid nanoparticle drug delivery system and to study the mechanism of action of the drugs.

In the first instance, the formulation of solid lipid nanoparticles encapsulating BNIPPiProp have been reported and the drug delivery system was subsequently characterised. Based on these results, the cytotoxicity of the BNIPs were evaluated *in vitro* in the colorectal cancer cell lines SW480 and SW620. After comparison with the use of the solid lipid nanoparticle (SLN) drug delivery system, the mode of cell death induced by BNIPs and its associated cellular mechanism were also studied.

Chapter 2

Development of solid lipid nanoparticles encapsulating BNIP derivatives

2.1. Background

Encapsulating BNIP derivatives has been the chosen path to overcome the current limitations of this family of drugs, including their poorly solubility in water. Previous studies have initiated the development of a drug delivery system for BNIP derivatives with the encapsulation of BNIPDaoct inside CH_5-poly(allylamine) biopolymeric self-assemblies. The associated *in vitro* and *in vivo* studies revealed an increased aqueous solubility associated with a tumour reduction efficacy at a similar level to gemcitabine against pancreatic cancer (Hoskins *et al.*, 2010). This study was the stepping stone into the enhancement of BNIPs efficacy as a cancer treatment using a nanoparticle drug delivery system.

To develop a novel drug delivery carrier for BNIPs, it must be biocompatible and biodegradable but also non-toxic to human tissues. Solid lipid nanoparticles have been the carrier of choice for the BNIP derivatives as they constitute an emerging class of nanoparticles exhibiting several benefits compared to liposomes or polymeric nanoparticles, such as a greater ability to carry lipophilic drugs and an affordable and safe option for pre-clinical assessment (Muller *et al.*, 2002). This class of particle is composed of a hydrophobic solid matrix made of solid lipids which can entrap efficiently hydrophobic drugs such as BNIPs. In this chapter, the formulation of solid lipid nanoparticles encapsulating BNIPPiProp have been performed and the resulting formulation has been characterised using dynamic light scattering for the determination of the size, PDI and zeta-potential. Moreover, TEM observations have been made and HPLC-UV were used to determine the percentage of drug loading within the formulated SLNs.

2.2. Experimental

2.2.1. Materials

Chemicals	Supplier
Tween 80	Acros Organics
Stearic Acid	Sigma Aldrich
Trehalose	Sigma Aldrich
Span 20	Sigma Aldrich
Acetonitrile	Sigma Aldrich
Octan sulfonic acid	Sigma Aldrich
Ethanol	Fisher Scientific
Dimethyl sulfoxide	Fisher Scientific
Acetic acid	Fisher Scientific
Sodium acetate	Fisher Scientific
PEG stearate	Fisher Scientific
Lecithin (72% egg)	Fisher Scientific
BNIPPiProp	Synthesized in RGU

Instrumentation	Supplier
Homogeniser	Bennett Scientific ltd. Germany
Freeze Dryer - Advatage 2.0 XL	VirTis
Zetasizer - nano series	Malvern
HPLC - UVD	Agilent Technologies

2.2.2. Manufacture of the solid lipid nanoparticles

The manufacture method used to develop the BNIP drug delivery system has been adapted from the work of Aditya *et al*. (2014). The nanoparticles were produced using the hot homogenisation method requiring the preparation of a lipid phase and an aqueous phase (figure 8). The aqueous phase was prepared by adding 4 g of Tween 80 to 90 mL of distilled water whereas the lipid phase was composed of 0.5 g of Span 20, 0.5 g of egg lecithin and 4 g of stearic acid.

Table 1. Summary of the composition of solid lipid nanoparticle formulations produced.

	Drug added	Aqueous phase		Lipid phase			
Batch ID	BNIPPiProp	Tween 80	PEG stearate	Span 20	Egg Lecithin	Stearic acid	PEG stearate
Ab	X	4 g	X	0.5 g	0.5 g	5 g	X
Ae	50 mg	4 g	X	0.5 g	0.5 g	5 g	X
B	X	X	4 g	0.5 g	0.5 g	5 g	X
C	X	4 g	X	X	X	5 g	1 g
D	X	X	4 g	X	X	5 g	1 g
E	50 mg	X	4 g	X	X	5 g	1 g

From this original formulation, alternatives have been produced using PEG stearate (table 1). Both phases were then heated separately to 75°C using a hot plate stirrer. When both phases reached the desired temperature and the lipids phase was completely melted, the aqueous phase was poured into the lipid phase and kept on heat. Instantly, both phases were homogenised at 27,000 rpm for 10 min. Once the mixing step was complete, the mixture was cooled at room temperature for 45 min and 1 g of Trehalose, used as cryoprotectant, was added to the cooled nanoparticle suspension. The preparation was then transferred into petri dishes and finally freeze-dried.

The previous protocol described the manufacture of the empty nanoparticles. For the encapsulation of BNIP derivatives, the same procedure was followed except for the addition of the drug to the lipid phase prior to homogenisation. The drug was added at a 100:1 ratio to stearic acid, thus, 50 mg of drug were added to the lipid phase. Once freeze dried, every batch of nanoparticles was characterised.

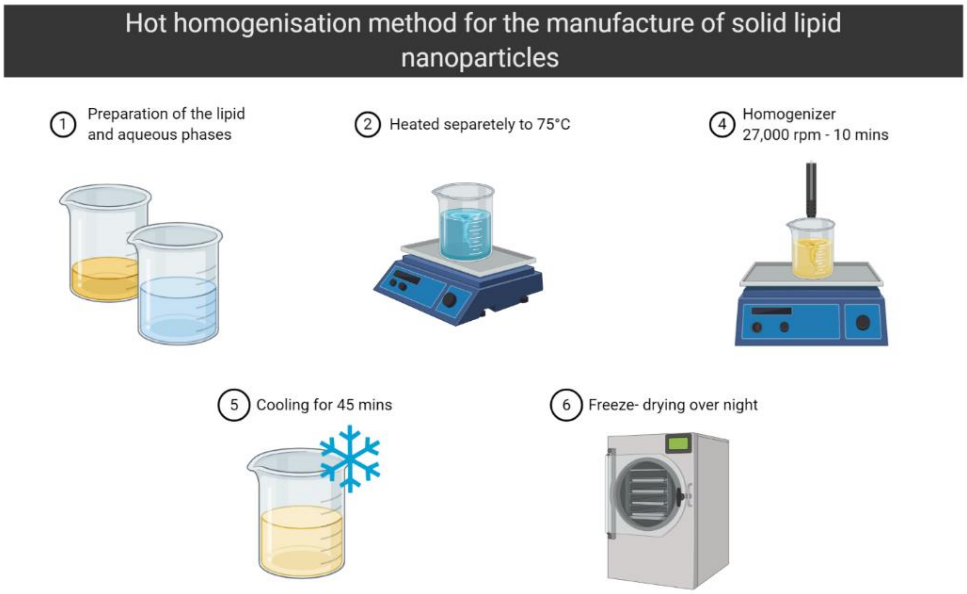

Figure 8. Schematic representation of the protocol for SLN preparation (created using BioRender™).

2.2.3. Dynamic Light Scattering (DLS): particle size, polydispersity index and zeta potential determination

All the following analysis was performed using a Zetasizer (Malvern) with a nanoparticle suspension at a concentration of 1 mg of freeze-dried nanoparticles /mL of distilled water at 25°C. The suspension was prepared by adding 10 mg of nanoparticles into 10 mL of distilled water. The suspension was shaken by hand for 20 seconds and filtered using a 0.22 µm syringe filter. For each batch, the analysis was performed in triplicate with the preparation of three independent suspensions. For the size and PDI determination, 1 mL of the filtered suspension was placed into a low volume plastic cuvette. For the determination of the zeta potential, folded capillary cells were used. These specialised containers have electrodes on their sides allowing an electric current to pass through the suspension to measure the zeta potential. Each folded capillary cell was washed with ethanol and water prior use and the zeta potential analysis was performed once for each batch of nanoparticles. Particle size and PDI analysis were performed in triplicate from 3 different suspensions. Zeta-potential was determined in triplicate from a single suspension.

2.2.4. High Performance Liquid Chromatography (HPLC) to evaluate the drug loading

Exploiting the fluorescent properties of the BNIP derivatives, Segundo *et al*. (2016) developed a validated analytical method to detect and quantify these compounds by using HPLC coupled with fluorometric detector. This method was adapted to quantify the amount of BNIP derivatives inside the nanoparticles allowing the use of low sample volumes with a high sample throughput.

The HPLC system was composed of a C-18 reversed-phase monolithic column (Chromolith RP-18e, 100 mm × 4.6 mm i.d., Merck) coupled with a fluorometric detector (338 nm). The separation was performed with an injection volume of 10 µL. An aqueous buffer (acetic acid/acetate 0.10 M, pH 4.5, 0.010 M octane sulfonic acid) was prepared by adding 16.64 g of sodium acetate and 3.89 g of 1-octane sulfonic acid into 1.95 L of distilled water to be dissolved. The pH was

then adjusted and stabilised at 4.5 by adding acetic acid dropwise to the solution before the final volume of the solution were adjusted up to 2 L. The mobile phase used was composed of the prepared aqueous buffer and acetonitrile in a 60:40 ratio (v/v) and was passed through the system at a flow rate of 1.5 mL/ min using the isocratic mode.

To allow the quantification of BNIPPiProp using this method, calibration standards were prepared with the non-encapsulated drug. The standards were prepared using BNIPPiProp stock solution (1 mg of BNIPPiProp/ mL of DMSO) which was diluted in acetonitrile to obtain 6 calibration standards with a concentration ranging from 25 to 150 µg/ mL.

For the nanoparticle analysis, 250 mg of freeze-dried nanoparticles was completely dissolved in 10 mL of acetonitrile. After optimisation, this nanoparticle concentration was chosen so the results were within the calibration curve. From the HPLC analysis, the total mass of drug detected was calculated using the calibration curve giving the concentration of drug.

From the determination of the mass of drug in the analysed sample the percentage of drug loading was obtained as follow:

$$\%\ Drug\ Loading\ = \frac{Mass\ of\ drug\ determined\ (mg)}{Total\ mass\ of\ the\ sample\ (250mg)} \times 100$$

2.2.5. Transmission electron microscopy

The transmission electron microscopy (TEM) were performed externally using the Electron Microscopy Research Services of the University of Newcastle.

The negative staining procedure were first performed using solid nanoparticles samples at a 1 mg/mL of PBS buffer (pH 7.4) concentration. A droplet (10 µL) was applied to support film on 300- or 400- mesh grids held in forceps. In the same way, a 10 µL droplet of 2% aqueous uranyl acetate was then applied to the grid. After allowing the grid to dry, the grids were examined on a Hitachi HT7800 transmission electron microscope using an Emsis Xarosa camera with Radius software. Two images per sample were obtained (50,000 and 100,000 magnifications).

2.3. Results and Discussion

2.3.1. Manufacture of BNIPPiProp-encapsulated solid lipid nanoparticles

First, different batches of solid lipid nanoparticles have been produced with differences in composition as described in table 1 (section 2.2). All the batches were produced in triplicate and no batch-to-batch variabilities have been observed during the manufacturing process with no visible changes perceived.

SLNs are composed of solid lipid, water (or organic solvent in some cases) and emulsifier. The lipid choice is the main factor as it influences the drug loading capacity as well as the drug release property and the stability of the drug in the nanoparticle. Here, stearic acid was chosen due to its complexity as a fatty acid leading to more imperfections in the lipid core structure allowing more drug to be encapsulated in the space created by the imperfections (Naseri *et al*., 2015). It has also been reported that this lipid in SLNs enhances the bioavailability of its cargo (Begum *et al.*, 2008).

Regarding the surfactants, they have been chosen based on their hydrophilic/lipophilic balance allowing the reduction of the interfacial tension between the lipid and the aqueous phases preventing particle agglomeration (Ma *et al.*, 2009). This aggregation inhibition can also be explained by the steric hindrance stabilisation provided by the brush barrier formed by surfactant chains at the level of the nanoparticle corona (Napper, 1983; Guo and Hui, 1997).

Surfactants consist of molecules harbouring long chains such as polyols or sugar derivatives allowing stearic stability (Landfester, 2001). Here, the combination of two non-ionic surfactants, Span 20 and Tween 80, has been used to prevent particle aggregation and to stabilise the nanoparticles. The phospholipid lecithin was also used as a co-emulsifier. Non-ionic surfactants were chosen for their greater hydrophobicity allowing them to solubilise poorly soluble drugs such as the BNIPs. Importantly, non-ionic surfactants are less toxic than cationic surfactants and could enhance bioavailability of the BNIPs (Wempe *et al*., 2009). The additional use of egg lecithin as a co-emulsifier was decided as this

amphoteric surfactant helps the preparation of a more stable colloidal system exhibiting both positively and negatively charged groups.

The use of PEG stearate was also explored as a substitute for other surfactants. This was investigated because PEG is commonly used in the formulation of drug delivery systems to stabilise the nanoparticles. It has been extensively used in liposome formulations such as Doxil® (Barenholz, 2012). The presence of PEG in the formulation limits the adsorption of the immunoproteins which prevents the creation of a protein corona around the nanoparticles, therefore, reducing the digestion of nanoparticles by macrophages which cannot recognise them. This strategy increases the circulation time of the treatment (Müller *et al.*, 1997). Additionally, Muller *et al.* (1997) manufactured SLNs using glyceryl palmitostearate which showed an impressive stability over 3 years.

From this first manufacturing steps, all the formulations produced were characterized to determine their size, polydispersity index, zeta potential and percentage of drug loading.

2.3.2. Dynamic Light Scattering (DLS): particle size, polydispersity index and zeta potential determination

The characterisation of the manufactured nanoparticles was an essential step as it allowed the validation of the nanoparticle quality compared to the optimised original method which led to the choice of the optimal formulation to perform the *in vitro* study. The determination of the particle size, the polydispersity index (PDI) and the zeta potential are key to understanding the physicochemical properties of the nanosized objects produced.

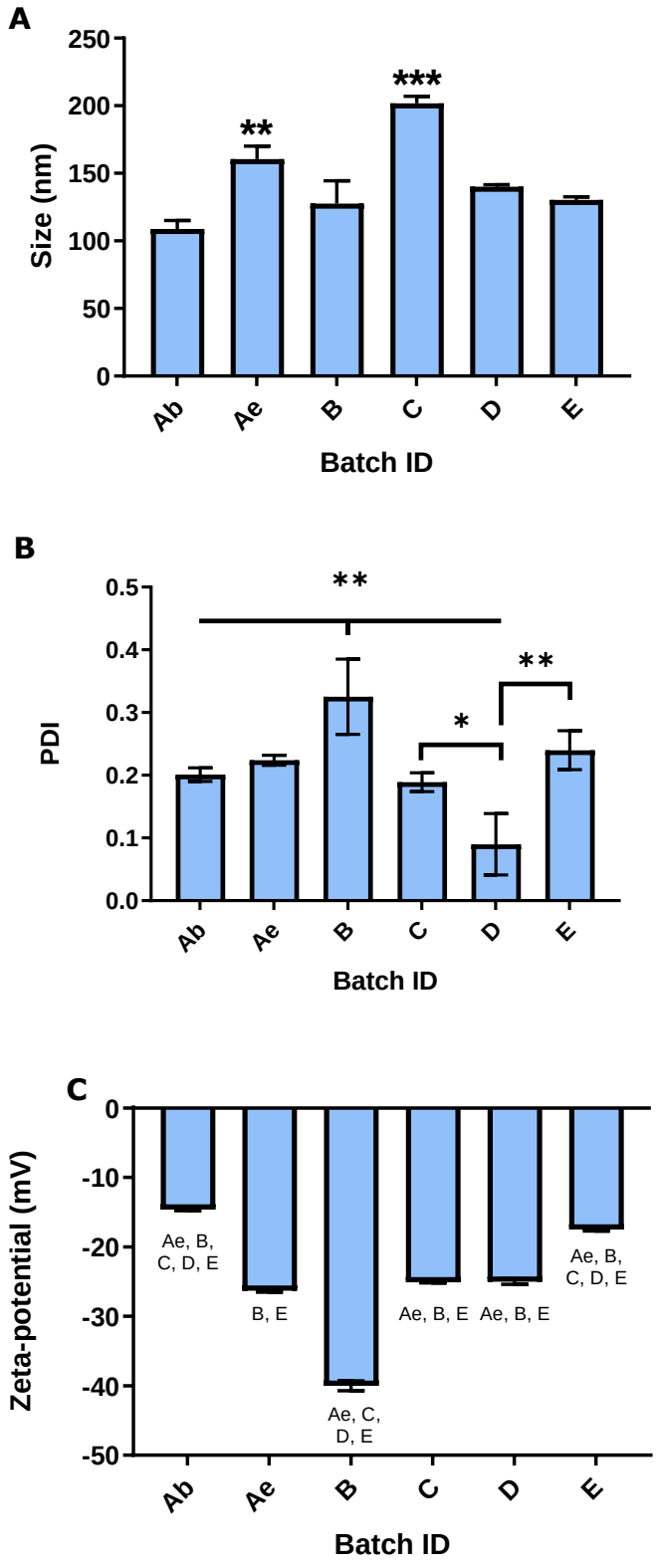

Figure 9. Physicochemical characterisation of SLNs using DLS. (A) Size (nm); data presented as mean ± SD, n=3 with statistical significance determined using a multiple comparison shown with *p<0.05, **p<0.01, ***p<0.001. and **(B)** PDI; data presented as mean ± SD, n=3 with statistical significance

determined using a multiple comparison shown with *p<0.05, **p<0.01, ***p<0.001. **(C)** Zeta-potential (mV), data presented as mean ± SD, n=3 with a p-value of <0.05 was considered statistically significant and it is represented by different letters corresponding to the paired batch ID showing a significant comparison.

The results presented in figure 9 (A) showed that all the formulations had a diameter between 100 and 200 nm. Only batches Ae and C were significantly larger with measurements above 150 nm compared to the other batches. Ae was notably larger than Ab showing that the addition of the drug potentially led to a size increase. However, this was not observed between batch D and E.

With the size of the gap junctions at the level of tumour cells or endothelial cells being 200 nm, it has been accepted that a nanoparticle delivery system should exhibit an average diameter of 100 nm to be able to pass through these cellular structures with ease (Yuan *et al.*, 1995). Currently, clinically approved nanomedicine have sizes ranging from 100 to 200 nm such as DOXIL® or CAELYX® (Uster *et al.*, 1998). Recently, studies showed that the miniaturisation of nanomedicines improved *in vivo* performance of the nanoparticles *via* a greater cellular uptake, and tumour inhibition when a smaller size of 50 nm or below was reached (Cabral *et al*., 2011; Tang *et al*., 2012). However, in the context of drug delivery, it is important to take other factors into consideration such as the faster diffusion of smaller systems out of the tumour and the renal clearance or lymphatic fenestration size threshold for nanoparticles smaller than 20 nm (Moghimi *et al*., 2005). Importantly for drug delivery systems, the size between 100 and 200 nm increases the circulation time of the nanoparticles in the body as macrophages could capture larger particles and it can also allow enough core volume to encapsulate the anti-cancer agents.

Regarding the PDI values on figure 9 (B), most batches showed PDI values below 0.200 except for batches Ae, B and E. Significantly, batch B had a higher PDI (0.325) compared to all batches except batch E. The polydispersity index is scaled between 0 and 1. Values above 0.7 indicates a very broad size distribution whereas a PDI value under 0.2 indicates a monodisperse suspension (Danaei *et al.*, 2018). In the case of the produced formulations, all the batches demonstrated a good dispersity except batch B presenting a higher value. The

increased polydispersity of batch B suggested that PEG stearate produced more polydisperse particles than with use of Tween 80 as a surfactant. However, the opposite effect was observed between batch C and D showing that the presence of PEG stearate in both phases might be responsible for the reduction of PDI observed in batch D. The combination of PEG stearate with Span 20 or lecithin might also have had undesirable interactions. The significant increase of PDI for batch E compared to batch D indicated that the drug encapsulation resulted in a more polydispersed sample.

The zeta-potential results in figure 9 (C) showed negative values for all the batches. Batches Ab and E showed the highest potential with values above -20 mV. All three batches Ae, C and D showed similar values between -20 and -25 mV which was significantly lower than Ab and E ($p<0.001$). Finally, batch B presented the lowest zeta-potential approaching -40 mV. Zeta-potential is an important characterisation method as it indicates the strength of the repulsive force between the particles in suspension (Kathe *et al.*, 2014). Here, all the batches exhibited negatives values below -10 mV which showed a good stability of the colloidal system. Based on their zeta-potential, the batches can be separated into three groups Ab, E (0 to -20 mV) > Ae, C, D (-20 to -30) > B (<-30). Interestingly, batch B with the higher PDI exhibited the lowest zeta potential. Due to the greater repulsion, it could be expected that the PDI would be smaller, yet contrasting results were obtained. Moreover, the use of PEG stearate could have reduced the surface charge by acting as a shield for the nanoparticle corona, but this which was not observed either. Additionally, PEG stearate in the water phase seemed to induce a less monodisperse suspension with a lowest zeta-potential.

2.3.3. Determination of the percentage of drug loading *via* HPLC

The chromatograph in figure 10 showed a unique peak allowing quantification of BNIPPiProp. Using BNIPPiProp standards of known concentrations, the area under the curve obtained with the samples allowed to determine the amount of BNIPPiProp present in the samples (figure 11). The standard curve presented a linear correlation between BNIPPiProp concentration and area under the HPLC peak.

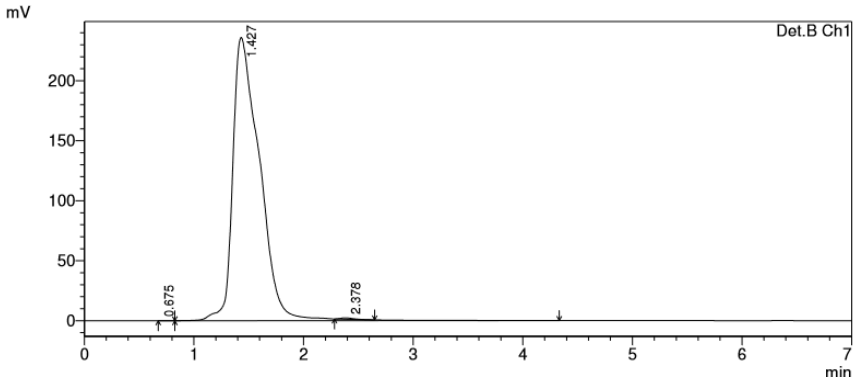

Figure 10. Example of BNIPPiProp-detection chromatogram. (obtained using the adapted method from Segundo *et al.* (2016) for the analysis of batch Ae)

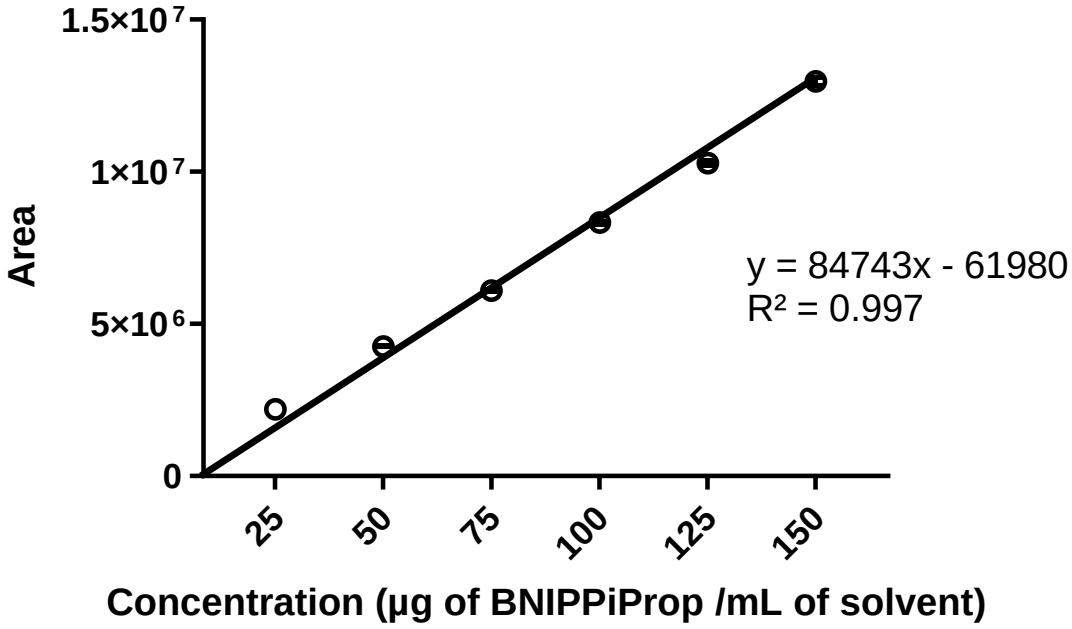

Figure 11. BNIPPiProp standard curve. Area under the curve (A.U.) in function of the concentration of BNIPPiProp [0-150 µg/mL]. Data presented as mean (±SD), n=3.

The calculations, presented below, were used to determine the mass of BNIPPiProp in the nanoparticles and the associated percentage of drug loading.

All of the HPLC tests were carried out in triplicate and the combined results of the different series of batches are shown in the table 2 below.

To determine the drug concentration within the analysed sample, the calibration standard equation was used: $y = 84743x - 61980$ to perform the following calculations:

$$\text{Concentration of BNIPPiProp in µg/mL} = \frac{Area\ (A.U.) + 61980}{84743}$$

$$\text{Concentration of BNIPPiProp in µg/mL} = \frac{13854599 + 61980}{84743} = 164.22\ \text{µg/mL}$$

$$Mass\ of\ drug = Determined\ concentration\ of\ drug\ in\ sample\ \times sample\ volume\ (mL)$$

$$Mass\ of\ drug = 164.22\ \times 10 =\ 1642.21\ \mu g$$

Once the total mass of drug was determined, the percentage of drug loading can be calculated as follow:

$$\%\ drug\ loading = \frac{Mass\ of\ drug\ determined}{Total\ mass\ of\ the\ batch\ (200\ mg)} \times 100$$

$$\%\ drug\ loading = \frac{1642.21\ \times 0.001}{250}\ \times 100 = 0.66\ \%$$

The results obtained for the batches encapsulating BNIPPiProp can be found in the table 2 below.

Table 2. Determination of BNIPPiProp percentage of drug loading using HPLC-UVD. Results were calculated from the average of 3 analysis.

Batch	Area	BNIPPiProp (µg/mL)	% of loading
Ae	13,854,598	164.2	0.66
E	5,975,546	71.2	0.28

Using the equation of the standard curve, the percentages of drug loading have been determined for the two batches encapsulating BNIPPiProp with 0.66% obtained for batch Ae and 0.28% obtained for batch E. There is a 2-fold increase in the drug loading capacity of batch Ae compared to batch E. For solid lipid nanoparticles, the drug loading capacity is based on the core structure of the

nanoparticle. With the choice of a single lipid, a more homogenous structure at the particle core could be observed with fewer imperfections (Mukherjee *et al*., 2009). Therefore, in this homogenous matrix model, the drug can be found in the state of amorphous clusters (Mishra *et al.*, 2018). This could explain the low percentage of drug loading obtained as a large quantity of BNIPPiProp could not solubilise in the lipid melt. Using an increased amount of drug (superior to the current 50 mg) would increase the drug:lipid ratio and potentially increase the drug loading.

This observation showed that the use of a combination of lipids instead of a singular molecular species could yield more imperfections at the core of the nanoparticle. Here, the formulation with multiple lipids used only stearate lipids which might have led to the production of a more compact and crystalline core resulting in a lower drug loading.

A first study from Fang *et al.* (2012) used PEG stearate onto solid lipid nanoparticles to encapsulate a novel chemotherapeutic agent PK-L4. The study showed a 99% encapsulation efficiency for their compound, and the presence of PEG stearate or stearic acid did not impact the loading of the drug but PEGylated SLNs were found to be more stable over a month (Fang *et al.*, 2012).

Stearic acid-based SLNs have previously been formulated for the delivery of Paclitaxel reporting a drug loading of 3.85%. This study evaluated different core lipids, thus, stearic acid demonstrated the best properties (Yuan *et al.*, 2008). Drug loading values below 5% are common due to the structure of SLNs. Having a low percentage of drug loading, it is then necessary to use a greater mass of nanoparticles to reach the quantity of drug required for the treatment.

The change in the ratio of drug/lipid could be explored to determine whether more drug could be loaded if the starting quantity of drug was higher. This difference of loading can be explained by the presence of PEG stearate instead of stearic acid. The drug concentration which was used did not show a disruption in the stability of the nanoparticles based on the values obtained using DLS.

2.3.4. TEM observations

TEM observations of all of the batches were obtained with the help of the Electron Microscopy Research Services of the University of Newcastle.

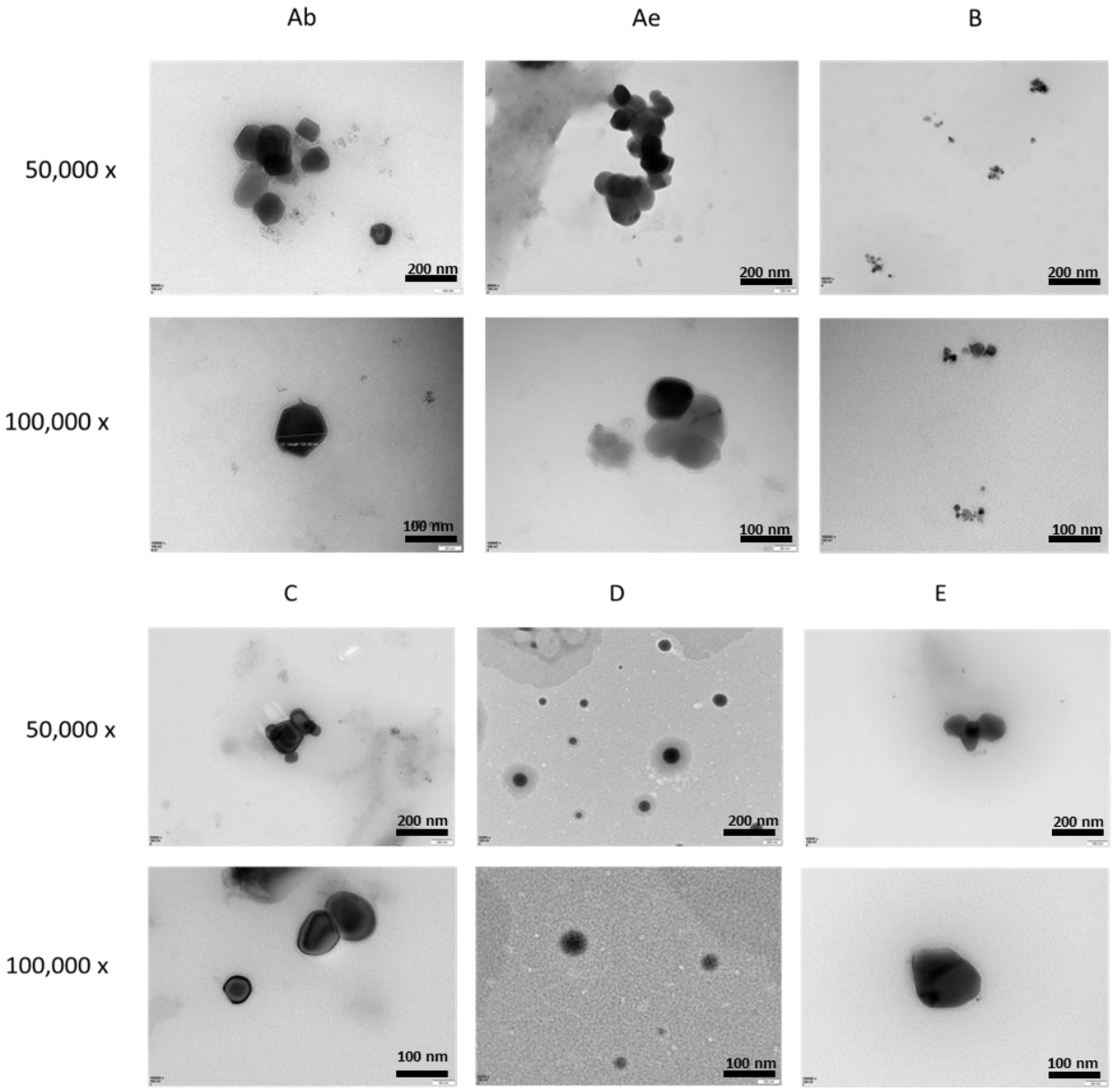

Figure 12. TEM observations of all SLNs batches. Each batch was imaged using negative staining and two images (50,000 x and 100,000 x) were obtained for each sample.

The TEM pictures (figure 12) enabled the visualisation of the spherical shapes of SLNs for all the batches. It is important to notice that the particle sizes obtained using TEM are smaller than the DLS measurements. This can be explained by the differences of methodology as DLS measures hydrodynamic sizes, whereas the TEM requires the samples to be dried on the grid leading to a reduction in the particle size due to the loss of water content. This phenomenon can also be observed with the use of EvoView™ systems which determine the size of exosomes after the drying of the natural nanoparticles on a chip. To obtain more robust data, nanoparticle tracking analysis could be performed to have a third method of validating the size of the different batches (Mourdikoudis *et al*., 2018).

Between batches Ab and Ae, respectively blank and loaded SLNs, no changes of shape were observed. The particles observed for batch C appeared to have more regular edges than the other batches such as A. Interestingly, particles of batch D exhibited a halo representing twice the size of the core of the particle. This halo could be due to the presence of PEG stearate and visible only in D due to the quality of the samples exhibiting the lowest PDI value. Finally, batch E showed a similar appearance to batch A, indicating that the presence of BNIPPiProp appeared to have no consequence on the structures observed by TEM.

Staining contrast differences observed for batches C-E compared to batches A and B showed that structural differences might exist between these batches with the deep and regular staining for batches A and B potentially indicating the presence of SLN due to their dense solid core. For batches C-E, the presence of PEG stearate could be producing a bilayer structure around the nanoparticle, a structure that can be found similarly in liposomes or extracellular vesicles. The use of PEG stearate in batches C-E also shows less aggregated nanoparticles.

2.4. Conclusion

In this chapter, the successful formulation of solid lipid nanoparticles encapsulating BNIPPiProp has been reported. Although all the formulations presented viable physicochemical properties to continue into the *in vitro* study, batch Ae were chosen as it presented the highest percentage of BNIPPiProp loading with 0.66%. Moreover, the physicochemical properties were consistent between the empty and loaded SLNs. Further optimization of this formulation strategy has also been discussed in chapter 4.

Chapter 3

In vitro study: exploring the cytotoxicity and the mechanism of action of BNIP derivatives.

3.1. Introduction

To study the potential of BNIPPiProp, BNIPDaCHM and BNIPPiEth as anti-cancer drugs for the treatment of colorectal cancer, the cell lines SW480 and SW620 were selected as previously discussed in section 1.4.1.

From the results obtained in the formulation section where a solid lipid drug delivery system was made for BNIPs, batch Ae was chosen for further studies against colon cancer cell lines SW480 and SW620. Any improvement in the anti-cancer activity of BNIP as a result of applying SLN delivery system will be analysed and discussed. Cytotoxicity studies using the native BNIPs drugs and the encapsulated BNIPPiProp were performed using the MTT assay. From those results, the possible mechanism of action of the BNIPs derivatives was studied in those colorectal cancer cell lines after evaluating the ROS levels, the DNA damage and the mode of cell death.

3.2. Materials

3.2.1. Materials

Chemicals	Supplier
Dimethyl Sulfoxide	Aldrich, UK
Reactive Oxygen Species (ROS) Detection Assay Kit	Biovision, USA
Caspase-3 Colorimetric Assay Kit	BioVision, USA
CaspGLOW™ Fluorescein Active Caspase-3/7 Staining Kit	Biovision, USA
Bio-Rad Protein Assay Kit	Bio-Rad, UK
Leibovitz's media	Gibco, UK
Penicillin/Streptomycin	Invitrogen, UK
Hydrogen Peroxide	Fisherbrand, UK
Sodium Hydroxide	Fisherbrand, UK
Tris Base	Fisherbrand, UK
Sodium Chloride	Fisherbrand, UK
AnnexinV/ PI kit	Nexcelom Bioscience, UK
Human Apoptosis Array kit	R&D systems, USA
Proteome Profiler Array	R&D systems, USA
Ethylenediaminetetraacetic acid	Sigma-Aldrich, UK
Phosphate buffered saline	Sigma-Aldrich, UK
Methylthiazolyldiphenyl-tetrazolium bromide	Sigma-Aldrich, UK
Agarose (1% w/v)	Sigma-Aldrich, UK
Low Melting Point Agarose	Sigma-Aldrich, UK
Agarose	Sigma-Aldrich, UK
Triton X-100	Sigma-Aldrich, UK
Trypsin-EDTA	Sigma-Aldrich, UK
Fetal Bovine Serum	Sigma-Aldrich, UK

3.2.2. Instruments

Instrumentation	Supplier
96-well plate reader	Synergy/HT, BIOTEK, USA
ALC Multispeed Refrigerated Centrifuge	Thomson Scientific, UK
Electrophoresis Tank	Bio-Rad, UK
CL-XPosure X-ray film	Thermoscientific, UK
BIO-1D™ imaging software	PeqLab, UK
FUSION-FX7	Vilber, Germany
HERACell incubator	Heraeus, Germany
Haemocytometer	Neubauer, Germany
Leica DMIL light microscope	Leica Microsystems, UK
HERASafe Class II Safety Cabinet	Thermo Electron Corporation, Germany
Cellometer	Nexcelom Bioscience, UK
SD-100 Image cytometry slides	Nexcelom Bioscience, UK

3.3. Methods

3.3.1. Cell maintenance and culture

Both SW620 and SW480 (from American Type Culture Collection) cell lines were grown in an incubator at 37°C with 5% CO_2 in a humidified atmosphere. The cell culture medium was Leibovitz's L-15 which was supplemented with 10% Foetal bovine serum (FBS) and 1% Penicillin/ Streptomycin (named 10% Leibovitz's thereafter). The media was stored at 4°C and warmed up to 37°C prior each use.

Originally stored in liquid nitrogen, cells were recovered by slowly defrosting the vials. Fifteen millilitres of 10% Leibovitz's medium was added to a 75 cm^2 flask in which 1 mL of cell suspension was transferred. The cells were incubated at 37°C under 5% CO_2 for 24 hours. The next day, the medium was discarded, the

cells washed with PBS to remove any dead cells and traces of DMSO (=cryoprotectant) before the addition of 15 mL 10% Leibovitz's.

The cells grew in optimal conditions when the medium was changed every three days. When the cells reached around 70-80% confluence, the medium was removed, and the cells were washed twice with 5 mL PBS. One mL Trypsin/EDTA was then added to the cells for 5 mins at 37°C. Once the cells detached, 5 mL 10% Leibovitz's was added to inhibit the effects of the trypsin. The cell suspension was then centrifuged for 5 mins at 500 *xg* (ALC centrifuge). The supernatant was discarded, and the cell pellet resuspended in 10 mL 10% Leibovitz's.

The cells were enumerated using a haemocytometer. Fifteen µL of cell suspension was inserted inside one of the counting chambers. Cells were counted using a light microscope. The cells in the sections A, B, C and D (figure 13) of the chamber were then counted.

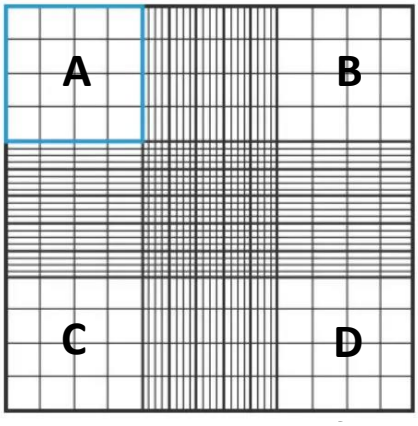

Figure 13. Haemocytometer gridlines (adapted from Abcam.com).

Then, the cell concentration was determined by the following equation:

$[(A+B+C+D)]/4] \times 10^4 \times$Dilution Factor = number of cells/mL

The required cell concentrations were then calculated and cells were seeded accordingly in 10% Leibovitz's.

3.3.2. *In vitro* treatment with BNIP derivatives

The BNIP derivatives were synthesised by Prof Kong at the Robert Gordon University, Aberdeen, in the School of Pharmacy and Life Sciences. For each BNIP derivative, a 10 mM stock solution were prepared in DMSO/ water (50/50; v/v) and stored at 4°C until use.

Prior to cell treatment, the stock solutions were warmed up using a heat gun to ensure complete dissolution of the drugs in DMSO/water. They were then diluted in 10% Leibovitz's.

3.3.3. MTT assay

To assess the cytotoxicity of the BNIPs on SW480 and SW620 cells, MTT (3-(4,5-dimethylthiazol-2-yl)-2,5-diphenyltetrazolium bromide) assays were performed. The cells were seeded at $2.5x10^4$ cells/well/100 µL in 96-well plates. After 24 hours, BNIPPiProp, BNIPDaCHM and BNIPPiEth treatment solutions were prepared at concentrations ranging from 0 to 5 µM and they were added to the cells for 24 hours.

Once the BNIP treatment was completed, the solution was removed and 100 µL MTT solution (1 mg/ml MTT in 10% Leibovitz's, prepared in the dark and filtered with a 0.2 µM filter) was added to each well. The plate was then incubated for a further 3 hours, in the dark at 37 °C. The wells were then emptied and 200 µL DMSO was added to dissolve the formazan crystals formed for 15 mins under agitation. The absorbance was then read at 560 nm on the plate reader. The data was acquired with the Gen5 software and IC_{50} determined.

3.3.4. Annexin V/ PI detection using image cytometry

To understand the mode of cell death in SW480 and SW620 cells triggered by BNIPs, image cytometry was used. Annexin V/PI detection was performed to determine if BNIPs were triggering cell death *via* apoptosis. In 6-well plates, 742,500 cells were seeded in each well and were incubated for 2 hours at 37°C.

The existing medium was then removed, and the cells were treated with the BNIPPiProp at its IC_{50} value, for 2 hrs. In each assay, a negative control (untreated cells) was included. After incubation, the cells were collected as previously described and the cell pellet was resuspended in 0.3 mL PBS. The cell concentration was determined using the counting mode of the image cytometer and the sample concentrations were adjusted to 2 $x10^6$ - 3 $x10^6$ cells/mL. Fifty microliters of the cell suspension were added, centrifuged at 500 *xg* for 5 mins and the supernatant discarded. The cell pellet was resuspended in 40 µL Annexin V binding buffer and 5 µL Annexin V-FITC and 5 µL PI solutions were then added (respectively Nexcelom Part# CS1-0114 and 0116). The samples were then incubated for 15 mins in the dark at room temperature. Two hundred and fifty microliters of PBS were then added, and the cells were centrifuged as before. The supernatant was discarded, and the cells resuspended in 40 µL Annexin V Binding Buffer. Using a microscope slide from the kit, 20 µL of cell suspension was added to each chamber and analysed using the Annexin V/PI detection mode of the Nexcelom Vision software. The data was analysed using the FCS Express 4 software.

3.3.5. COMET assay

To study the effects of BNIPs on DNA damage, SW480 and SW620 cells were seeded on 6-well plates at 742,500 cells/well with 3 mL 10% Leibovitz's and incubated for 24 hours. The BNIP treatment at its IC_{25} value was then prepared and added to the wells, then the plates were placed in the incubator for 24 hours. Once the treatment was completed, each well was emptied and washed twice with PBS. Five hundred microliters of Trypsin/EDTA were then added and the cells were collected in 1.5 mL centrifuge tubes. The cell suspensions were centrifuged at 400 *xg* for 5 mins at 4°C. During the centrifugation, 85 µL agarose was poured on frosted microscopy slides covered with 18x18 mm cover slips. The slides were placed for 10 mins at 4°C to solidify. After centrifugation, the supernatant was discarded, and the cell pellet was resuspended quickly into 85 µL LMP agarose solution and the mix was poured onto the pre-coated microscope slides (existing cover slip removed prior to addition of the second layer*)*. The

final two-layer gel was covered with a 18x18 mm cover slip and the slides were kept at 4°C for 10 mins.

The slides were then placed into a black staining jar containing 200 mL lysis buffer (2.5 M NaCl, 0.1 M EDTA, 10 mM Tris Base, 1% (v/v) Triton-X-100, NaOH pH=10) for 60 mins at 4°C. An electrophoresis tank was set up at 4°C (cold room) and was filled with electrophoresis buffer (0.3 M NaOH, 1 mM EDTA, pH 13). The slides were placed horizontally in the electrophoresis tank and left to equilibrate for 40 mins. The electrophoresis was subsequently carried out at 25 V (999 mA) for 30 mins at 4°C. The slides were then washed 3 times for 5 mins with cold neutralising buffer (0.4M Tris, pH 7.5) and stained with 20 µL 1 µg/mL DAPI and covered with a 22x22 mm cover slip. The comets were analysed with a fluorescent microscope (Leica DMRB fluorescence microscope with D filter (ex: 355 – 425 nm – em: 470 nm). Comets were discriminated into 5 different classes, each representing a different level of DNA damage. One hundred comets were counted per gel giving a score from 0 (no damage) to 400 (high damage) (arbitrary unit).

3.3.6. Reactive oxygen species level detection

ROS level was detected using the ROS detection kit from BioVision. ROS detection was performed to evaluate the level of ROS present after BNIP treatment as an increased level could explain the triggered apoptosis and DNA damage revealing another aspect of BNIPs' mechanism of action.

For each cell line, 2.5 x 10^4 cells (200 µL) were seeded per well in a 96-well plate and were incubated for 24 hrs. The medium was removed after 24 hrs and 100 µL ROS assay buffer was added to wash the cells. Then, 100 µL of the ROS labelling solution (H_2DCFDA) was added and the plate was incubated for 45 mins at 37°C in the dark. After incubation, the dye solution was removed, and the cells were washed as before. The BNIP treatment (BNIPDaCHM, BNIPPiProp and BNIPPiEth at their IC_{25} and IC_{50} values) solutions were then added to the wells (100 µL) for 24 hrs. At the end of the treatment, the fluorescence was measured at Ex/Em = 495/529 nm in end point mode using a plate reader and the data was acquired with the Gen5 software.

3.3.7. Protein assay

In this project, the protein assay was used to quantify the total protein content in the cell lysate for the caspase 3 assay and the human protein array (described in sections 3.10 and 3.11). A concentration range (0 to 1.25 mg/mL) of Bovine Serum Albumin (BSA) standard solution, containing 1% Triton-X, was prepared. The protein lysates were diluted 1:2 and 5 µL of sample (in duplicate) or standard (4 replicates) were added to the wells of a 96-well plate. From the BioRad Protein Assay Kit, 25 µL solution A was added followed by 200 µL of solution B according to the manufacturer's instructions. The plate was incubated at room temperature for 15 mins and then read at 650 nm on the plate reader using the Gen5 software to acquire the data. The total protein concentration (in mg/mL) was determined using the equation of the BSA standard curve.

3.3.8. Caspase-3 colorimetric assay

Caspase-3 is a well-known marker of apoptosis, so its activity was assessed to further understand the mechanism of cell death triggered by BNIPs in both cell lines (Elmore, 2007). This assay was performed using the BioVision Caspase-3/CPP32 Colorimetric Assay Kit. Cells were seeded at 1.5 x 10^6/T25 flask/ 5 mL 10% Leibovitz's in duplicate and BNIPDaCHM, BNIPPiProp and BNIPPiEth were used at their respective IC_{25} concentration. After 24 hours, the medium was removed, and the cells collected as before. The cell pellet was resuspended with 50 µL cold cell lysis buffer and the cell suspension was incubated on ice for 10 mins. The suspension was centrifuged for 1 min at 10,000 *xg*. The supernatant containing the cytosolic extract was transferred to a new tube and stored at -20°C until further use.

The protein concentrations were determined as described in section 3.3.7 and each sample was then prepared to have 150 µg total protein in a 50 µL final volume with cell lysis buffer. The samples were added to a 96-well plate and 50 µL 2X reaction buffer (containing 10mM DTT) and 5 µL of the 4mM DEVD-pna substrate (200 µM final concentration) were added. The plate was incubated at 37 °C for 2 hrs before being read at 405 nm on the plate reader. The data was

acquired as stated before and the results for each sample were standardised to the control (untreated) for each experiment.

3.3.9. Human apoptosis protein array

The Human Apoptosis Array Kit was used to determine the expression profile of apoptosis related proteins in SW620 and SW480 cells after treatment for 24 hrs with IC_{25} BNIPs. The array allows for the detection of 35 apoptosis-related proteins, each spotted in duplicate on the membrane,

After treatment, following the manufacturer's instructions (www.rndsystems.com), the medium was removed and 2 mL lysis buffer was added to the cells and incubated for 30 mins. The solution was collected and centrifuged at 14,000 *xg* for 5 minutes. The protein concentration was determined as described in section 3.3.7. For each array membrane, 200 µg protein was used and was made up to 250 µL final volume with PBS. The membranes were blocked with the Array Buffer for an hour. Fifteen µL of the detection antibody cocktail were added to the protein samples and the mixture was added to the membrane for 1 hr at 4°C with continuous shaking. The protein solution was discarded and each membrane was washed 3 times (10-minute wash) before being incubated with 2 mL Streptavidin-HRP solution for 30 mins. The solution was discarded and the membrane washed as before. Chemiluminescence detection reagents (1/1; v/v) were then added on top of the membrane and incubated for 1 minute in the dark. In the dark room, the membrane was then exposed to an X-Ray film for 10 minutes. The film was developed by soaking it in developer for 1 min, then washed briefly in tap water and finally fixed in fixing solution for 1 min. The film was rinsed and left to dry prior analysis.

A picture of the film was taken on the FUSION FX7 imaging system and the pixel density of each spot was then analysed using the FUSION FX7 imaging software.

Quality control spots are present on each membrane with positive spots needing to be pixel dense and negative spots with no colour change. Monitored on each membrane, these spots validate the good execution of the protocol. The average signal i.e. the pixel density was determined for each spot and an average of each

duplicate was calculated. The data was then analysed by removing the average pixel density of the negative control (PBS) to determine the relative changes in the expression of the protein of interests. For each set of four membranes, the treatments were the following: BNIPPiProp (24 hrs IC_{25}), BNIPPiEth (24 hrs IC_{25}), BNIPDaCHM (24 hrs IC_{25}) and control without BNIP treatment. The data was analysed as a ratio treatment/control to evaluate the relative protein expression levels.

3.3.10. Statistical analysis

Unless otherwise stated, each experiment was performed at least 3 times independently. The data was expressed in relation to the relevant controls and presented accordingly. Statistical analysis was performed using GraphPad Prism 8.0 software (GraphPad Software, San Diego, CA, USA).

Statistical significance was assessed with:

- the Student's t-test with *p<0.05, **p<0.01, ***p<0.001.
- The one-way ANOVA test followed by a Tukey's post-test with *p<0.05, **p<0.01, ***p<0.001.

3.4. Results and discussion

3.4.1. The effects of BNIPs and SLN-loaded BNIPPiProp on cellular cytotoxicity on colorectal cancer cells

The use of formazan dyes is one of the most common methods to determine cytotoxicity. The formazan dyes are chromogenic compounds produced by tetrazolium salts' reduction (3-(4,5-dimethylthiazol-2-yl)-2,5-diphenyltetrazolium bromide (MTT) or 2,3-bis-(2-methoxy-4-nitro-5-sulfophenyl)-2H-tetrazolium-5-carboxanilide (XTT)) by dehydrogenases (lactate dehydrogenase) and reductases, and they are released during cell death (Fathin *et al.,* 2017). The principle of these assays relies on the fact that dying cells often present serious structural damages allowing the release of intracellular content and the admission of fluorescent dyes inside the cells. Importantly, the MTT assay relies on the enzymatic reduction of the MTT compound to the purple crystal formazan which is obtained once MTT has been catalysed by mitochondrial succinate dehydrogenase.

In this study, the cytotoxicity of both the naked BNIPs and the encapsulated drugs in the lipid nanoparticles has been assessed against SW620 and SW480 cell lines.

3.4.1.1. The effects of BNIPs on cell cytotoxicity on colorectal cancer cells

The results presented in figure 14 show the effect of BNIPDaCHM, BNIPPiProp and BNIPPiEth on colorectal cancer cells after a 24-hour treatment. The percentage of cell viability decreased with the increase of BNIP concentrations up to 5 µM. This cytotoxic effect has been observed against both cell lines using these 3 compounds.

From the MTT assay results, the IC_{50}, i.e. the concentration for which 50% of cells are dead compared to the solvent control cells, was determined and summarised in table 3; IC_{25} values were also determined. The half maximal inhibitory concentration was very useful as it allows the direct comparison of the cytotoxic potency of the drugs between cell lines or between themselves.

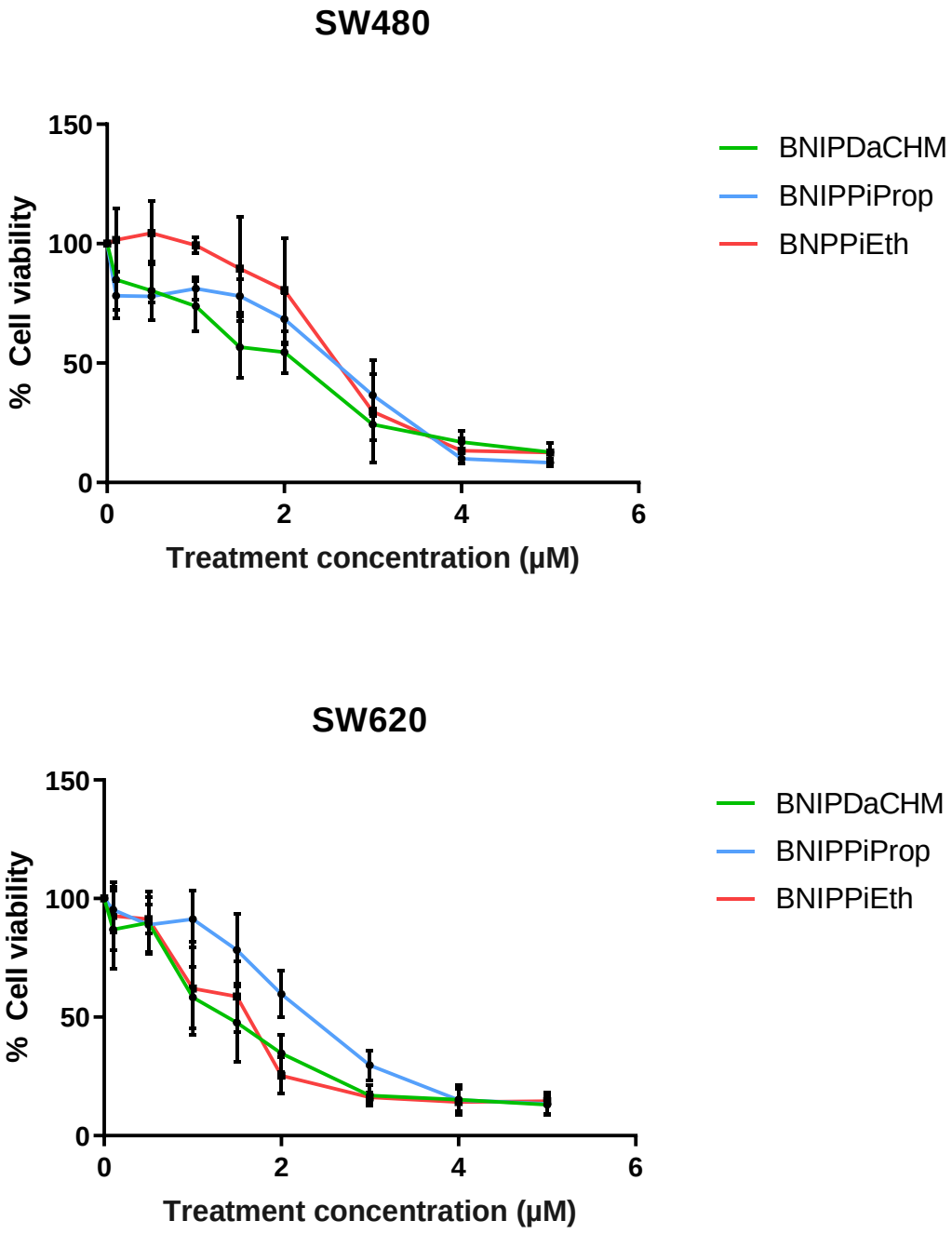

Figure 14. MTT Assay: the effects of BNIPDaCHM, BNIPPiProp and BNIPPiEth against SW620 (A) and SW480 (B) cells after a 24 hr-treatment. The data are expressed as percentage of the solvent control (DMSO/H_2O) and are presented as mean ± SEM of 3 in dependent experiments (n=3)

Table 3. IC_{50} and IC_{25} determined from the MTT assay after the 24-hr treatment with BNIPPiProp, BNIPDaCHM and BNIPPiEth against SW620 and SW480 cell lines.

Conc. (μM)	BNIPDaCHM IC_{50}	BNIPPiProp IC_{50}	BNIPPiEth IC_{50}	BNIPDaCHM IC_{25}	BNIPPiProp IC_{25}	BNIPPiEth IC_{25}
SW480	2.2	2.6	2.6	1	1.7	0.8
SW620	1.3	2.3	1.6	0.75	1.6	2.1

In SW480 cells, the three drugs had similar IC_{50} values between 2.2 and 2.6 μM. However, for SW620 cells, BNIPDaCHM and BNIPPiEth were more toxic with respective IC_{50} values of 1.3 and 1.6 μM. Moreover, in both cell lines, the 3 BNIP derivatives have exhibited a similar cytotoxic profile showing that the metastatic characteristics of SW620 are not leading to a resistance to BNIP cytotoxic effects, as no significant difference has been observed between the two cell lines.

Thus, three drug candidates were tested for the first time against SW480 and SW620 cell lines, however, BNIPs cytotoxic effects have already been studied against several other cell lines. The three drugs presented IC_{50} values ranging from 1.8 to 3.3 μM against MDA-MB-231 and from 0.3 to 0.7 μM against SKBR-3 making them strong candidates as anti-cancer drugs by exhibiting such potent cytotoxic effects (Kopsida *et al*, 2018). Kopsida *et al.* (2018) also showed that BNIPPiEth was the most cytotoxic drug in both MDA-MB-231 (1.8 μM) and SKBR-3 (0.3 μM) breast cancer cell lines compared to BNIPDaCHM and BNIPPiProp. These cytotoxicity studies on different *in vitro* models have shown that this generation of BNIPs has consistently high cytotoxicity potency across several cancer cell lines with IC_{50} values ranging from 0.3 to 3 μM.

In comparison to other anti-cancer drugs, all three BNIPs have presented much lower IC_{50} values. Other compounds that have been tested on SW480 and SW620 cell lines have shown to be more effective in SW480 than in SW620 cells. SW620 cells represent a metastatic cell line which is known to show chemoresistance against drugs such as 5-fluouracil used widely in colorectal cancer treatment (Tentes *et al*., 2010). For examples, gold standard agents against colorectal cancer have exhibited the following IC_{50} values (μM) (SW480; SW620) 5-

fluorouracil (541.20; 497.80), oxaliplatin (43.31; 104.70), geldanamycin (45.59; 59.00) or novobiocin (139.20; 155.10) (Slater *et al*, 2018). This study has established that chemosensitivity varied upon the cell line and the drug tested. Presenting lower IC_{50} values with an average of 2 μM, the BNIPs represent strong candidates for the treatment of CRC.

Having established the robust cytotoxicity provoked by the use of BNIPs against both SW480 and SW620, these results also provide essential data for the comparison of the efficacy of the encapsulated-drug compared to the free-drug treatment *in vitro*.

3.4.1.2 The effects of SLN-encapsulated BNIPPiProp on cell cytotoxicity on colorectal cancer cells

The results reported in figure 15 (A), present the effects of SLN-encapsulated BNIPPiProp on the colorectal cells' cytotoxicity levels compared to the drug delivery system (SLN) alone. For each treatment at a specific concentration, the level of nanoparticles required to reach the targeted drug concentration has been calculated based on the percentage of drug loading (Chapter 2). For each SLN control (empty nanoparticles), the same concentration has been used.

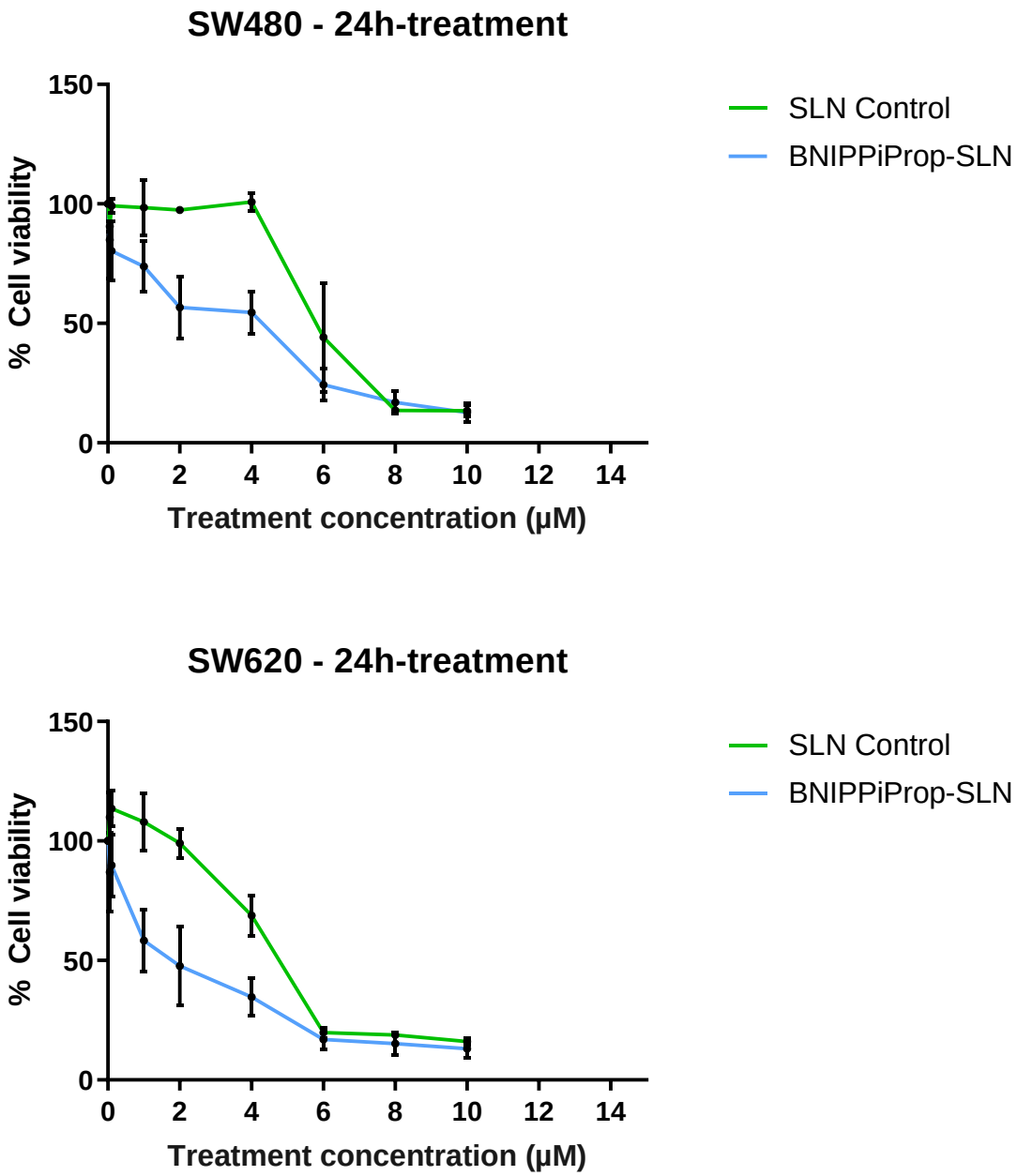

Figure 15. MTT Assay: evaluation of the percentage of cell viability of BNIPPiProp-encapsulated in solid lipid nanoparticles against SW620 (A) and SW480 (B) after a 24 hr-treatment. The data are expressed as percentage of the solvent control (DMSO/H_2O) and are presented as mean ± SEM of 3 in dependent experiments (n=3). The concentrations are the theoretical drug concentration calculated based on the percentage of drug loading in SLNs.

Table 4. IC_{50} values determined with the MTT assay from the 24-hr treatment using BNIPPiProp encapsulated in SLN against SW620 and SW480 cell lines with the empty SLN used as a control.

IC_{50} -Concentration (μM)	SLN Control	BNIPPiProp-SLN
SW480	6	4.5
SW620	5	2

The results presented in figure 15 (B) show that the empty nanoparticles had a high level of toxicity with IC_{50} values of 6 and 5 μM against SW480 and SW620 respectively after 24 hrs. However, with nanoparticles encapsulating BNIPPiProp, the IC_{50} obtained was lower against each cell line with a value of 1.5 μM against SW480 and 3 μM against SW620 (table 4). Since high toxicity levels from the drug delivery system itself were observed in both cell lines, the cytotoxicity results from the encapsulated BNIP were not comparable as toxicity might have come from either the drug or/and the delivery system itself.

This formulation without drug loaded was tested in a previous project *(personal communication)* where the control SLNs did not show any toxicity against MDA-MB-231 breast cancer cells. The solid lipid nanoparticles tested against colorectal cancer cells could present toxicity due to the high nanoparticle density in the well that could have led to a poor access to essential nutrients for the cells. This data, showing different cytotoxicity profiles using the nanocarrier alone, suggests that the decrease of cell viability was cell-specific as it was observed for colorectal cancer cells only in this case.

Solid lipid nanoparticles are composed of lipids and surfactants and it has been shown that the nature of lipids has no effect on viability as they are safe physiological compounds (Wissing *et al*., 2004). However, surfactants can cause cytotoxicity (Müller *et al.*, 1997). The non-anionic surfactant Tween 80 used in this formulation is known to be the least toxic surfactant among the most widely used and all the selected components were FDA approved (Prieto and Calvo, 2013). Further investigations are required to understand the origin of the cytotoxicity of the nanoparticles. The more detailed nanotoxicology profile should

include the cellular uptake of the formulations and the study of the cell processing routes employed (Severino *et al.*, 2012).

When BNIPPiProp was encapsulated in solid lipid nanoparticles, the IC_{50} values were 6 and 5 μM for SW480 and SW620 cells respectively. Therefore, achieving a high drug encapsulation would reduce the required number of nanoparticles per treatment and consequently, working with significantly decreased concentrations of particles to reach an IC_{50} could solve the toxicity issue.

Here, the potential of BNIPDaCHM, BNIPPiEth and BNIPPiProp as potent anti-cancer drugs against SW480 and SW620 colorectal cancer cells has been established in relation to their cytotoxicity. After 24 hours treatment, all three drugs have demonstrated strong cytotoxicity with IC_{50} values ranging from 1.3 to 2.6 μM. However, with the use of SLNs encapsulating BNIPPiProp, no conclusion on its relative cytotoxicity can be established due to the unforeseen cytotoxicity of the control SLN. Optimisation of the formulation will be required to obtain a non-toxic drug delivery system.

Due to this difficulty, the mechanism of action of the BNIP derivatives was then studied in order to have a better understanding of the biological events occurring after drug treatment. Obtaining this knowledge is key in the design of more efficient nanodrug delivery systems tailored to the delivery of BNIP derivatives based on this mechanism of action.

3.4.2. Investigating the mechanism of cell death with image cytometry

Chemotherapy is by definition the use of chemicals to destroy cancer cells. BNIPs are part of this type of compounds as previously demonstrated with the cytotoxicity study. However, there are different classes of chemotherapy agents which can be separated upon their mechanism of action such as alkylating agents, anti-metabolites or enzyme inhibitors (Huang *et al.*, 2017). For the last 50 years, a main target for anti-cancer treatment has been nucleic acids as the modification of the DNA mechanisms (replication, repair or transcription) can lead to programmed cell death (Brana *et al.*, 2001). Apoptosis is recognised as the principle chemotherapy-induced mode of cell death. However, accumulating evidence proposes the induction of other modes of cell death such as autophagy (Brown *et al.*, 2005). BNIP derivatives have demonstrated the ability to bind to DNA *via* bis-intercalation using their naphthalimido group (Barron *et al*., 2010) and to cause DNA damage in other cell lines (MDA-MB-231 and MCF-10A cells). Therefore, this project has chosen the assessment of apoptotic cell death as a first step to better comprehend the mechanism of action of BNIP derivatives against CRC.

To investigate cell death by the activation of apoptotic pathway, an image cytometry method was chosen to perform a pilot study. Image cytometry, also called slide-based cytometry, is a microscopy-based technique which uses 3 imaging channels to quantify fluorescence intensities. Coupled to a cell counting software, the cell sample is counted, and a data set is generated similar to a flow cytometry plot where cells populations can be distinguished depending on their fluorescence signal. Here the Cellometer from Nexcelom® was used to study the mode of cell death in SW620 after treatment with BNIP derivatives. This pilot study aims to develop the use of image cytometry in the detection of apoptosis, to obtain a rapid method to screen drug candidates in relation to cell death and to obtain first evidences of the induction of apoptosis by BNIP derivatives in CRC.

3.4.2.1. Optimisation of the image cytometer for the *in vitro* model

Image cytometry is the oldest form of cytometry using optical microscopy to image a population of cells entrapped on a slide (Shapiro, 2004). The progress of this technology has used fluorescent filters thus allowing the application of fluorescent dyes to the study of biological mechanisms. The use of image cytometry was preferred compared to flow cytometry as this technique is less time consuming with a slide analysis performed in seconds on the benchtop. It also provided fluorescent images of the results allowing the visualisation of the positive/ negative cells making the method ideal for a pilot study.

To optimise the system for SW480 and SW620 cells, the morphology of the cells was studied first with different fields to ensure that the cells were recognized as such rather than as artefacts (figure 16).

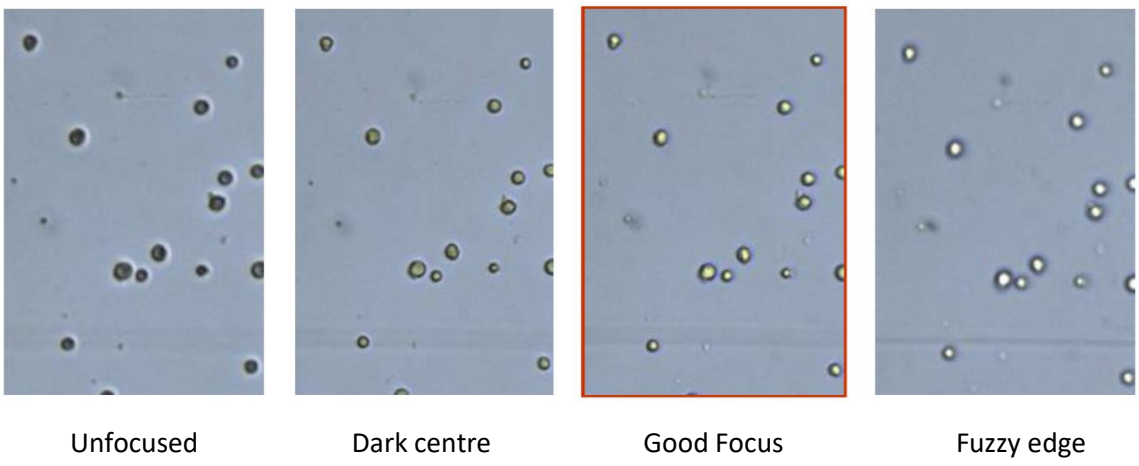

Figure 16. Illustration of the difference of focus obtained with the cellometer microscope in bright-field (10X magnification).

Once the system was set up to recognise the cells' morphology, different cell densities were loaded in the counting chamber to determine the optimum cell number to obtain the highest number of cells without saturating the counting software.

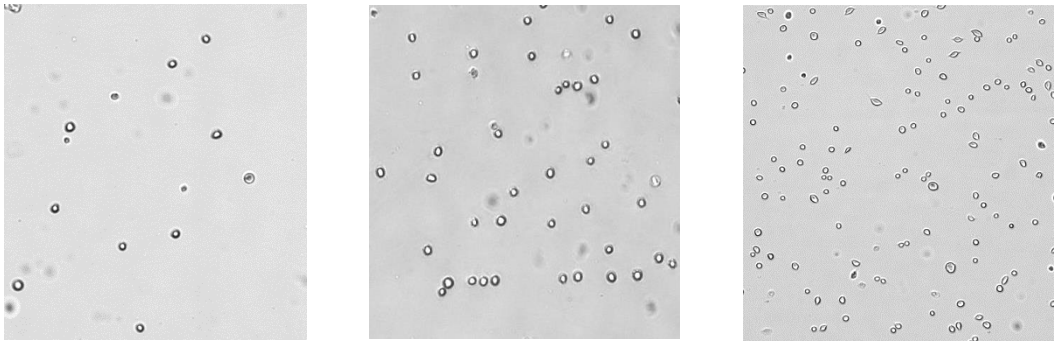

0.5 x 10^6 cells/mL 1 x 10^6 cells/mL 2 x 10^6 cells/mL

Figure 17. Illustration of the cell counting chamber using different cell density (SW620) with the Cellometer microscope in bright-field mode (10X magnification).

Based on a 60-70% on-screen confluence level recommended by the manufacturer, the optimum cell density for SW620 was set at 2 million cells/mL for all subsequent experiments (figure 17). This initial test should be performed for each newly used cell line at the start of every study.

With the optimum cell concentration determined, the cell number was then assessed on the image cytometer and compared to the haemocytometer manual counting method (figure 18). The data showed no statistical difference and a very good reproducibility between the two cell counting methods.

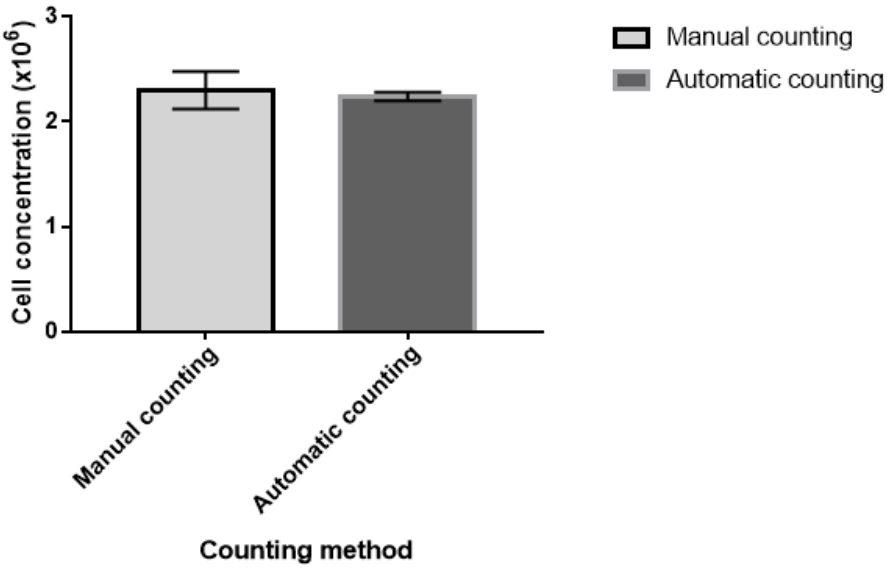

Figure 18. Comparison of the automatic counting (cellometer) and manual counting (haemocytometer) methods. The experiment has been performed in triplicate (n=3) from a SW620 cell suspension. Results are expressed as mean ± SD.

The results obtained were very similar using the two methods, thus validating the use of the automated counting system with no additional cell counting adjustments for its use in section 4.2. The automation of the cell counting process could also be generalised to routine cell maintenance to enumerate cell populations reducing the time required and the potential human error (Gupta *et al.*, 2019).

Following the validation of the key system components relative to optical cell detection, the apoptotic cell death induction of BNIPs was assessed on SW480 and SW620.

3.4.2.2. The effects on BNIPs on apoptosis in SW480 and SW620 cell lines

3.4.2.2.1. Annexin V/Propidium Iodide

To measure apoptosis, Annexin V (A5) and propidium iodide (PI) detection has been chosen as they were detectable simultaneously using the fluorescence filters of the cellometer. Annexin V is part of the Annexin group of proteins which are intracellular, and bind specifically to phosphatidylserine (PS) in the presence of calcium. PS is a common phospholipid found within the cellular membrane and exposed at the intracellular level. However, during apoptosis, PS is translocated and has an extracellular detectable exposure (Vermes *et al.*, 1995).

A5 can then be used to detect PS present on the cell surface. The use of A5 on its own is not sufficient as there would be no differentiation between necrotic or late apoptotic cells which all exhibit PS. PI is then used, as early apoptotic cells will exclude PI therefore being only A5 positive. SW620 cells were incubated for 2 hrs with IC_{25} to IC_{75} BNIPPiProp concentrations to study the A5/PI detection on the cell imaging system.

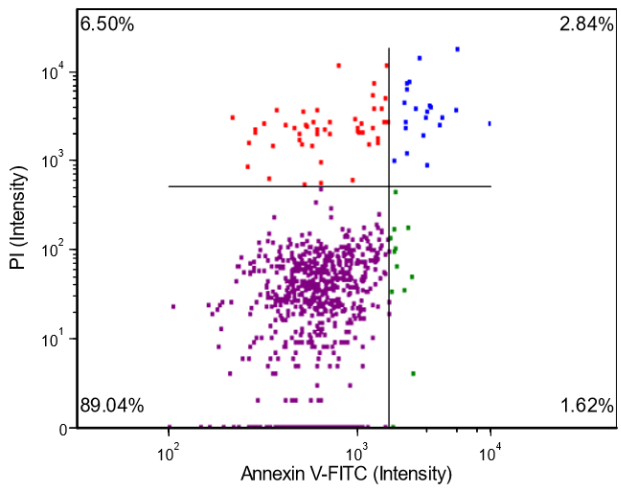

Cell Population	% of Gated Cells	Concentration
Total	100	1.05 x 10^6 cells/mL
Live	89.04	0.93 x 10^6 cells/mL
Apoptotic	1.62	0.02 x 10^6 cells/mL
Necrotic	2.84	0.03 x 10^6 cells/mL
Debris	6.50	0.07 x 10^6 cells/mL

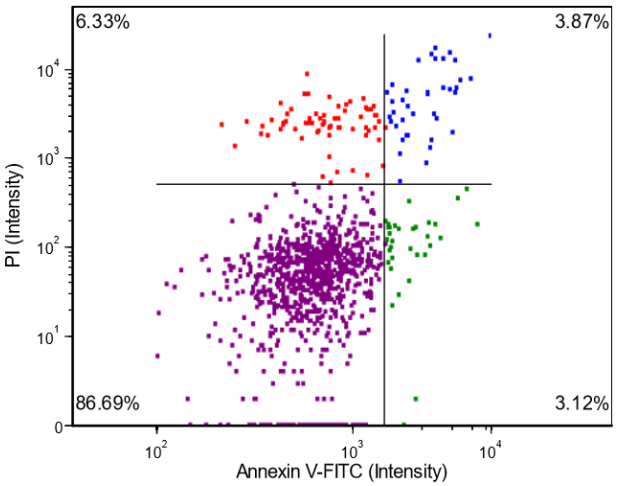

Cell Population	% of Gated Cells	Concentration
Total	100	1.51 x 10^6 cells/mL
Live	86.69	1.31 x 10^6 cells/mL
Apoptotic	3.12	0.05 x 10^6 cells/mL
Necrotic	3.87	0.06 x 10^6 cells/mL
Debris	6.33	0.10 x 10^6 cells/mL

Figure 19. FCS software reports of the detection of Annexin-V and PI after a 2 hr-treatment with BNIPPiProp against SW620.

The FCS software reports (figure 19) showed the cytometry plots with the black cross representing the gating. The gating was set manually using control experiments with no drug treatment and it was kept the same for the rest of the study. The software provided the results as a percentage of gated cells having counted the total number of cells on the slide prior fluorescent analysis. Cells with fluorescent intensities below the gating level for both Annexin V and PI were considered live cells. Cells positive to PI only were considered debris and cells positive to annexin V only were considered apoptotic. Finally, the cells were considered necrotic if positive to both fluorescent probes. This testing has allowed the optimisation of the fluorescence parameters on the system with exposure settings set at 2,000 ms.

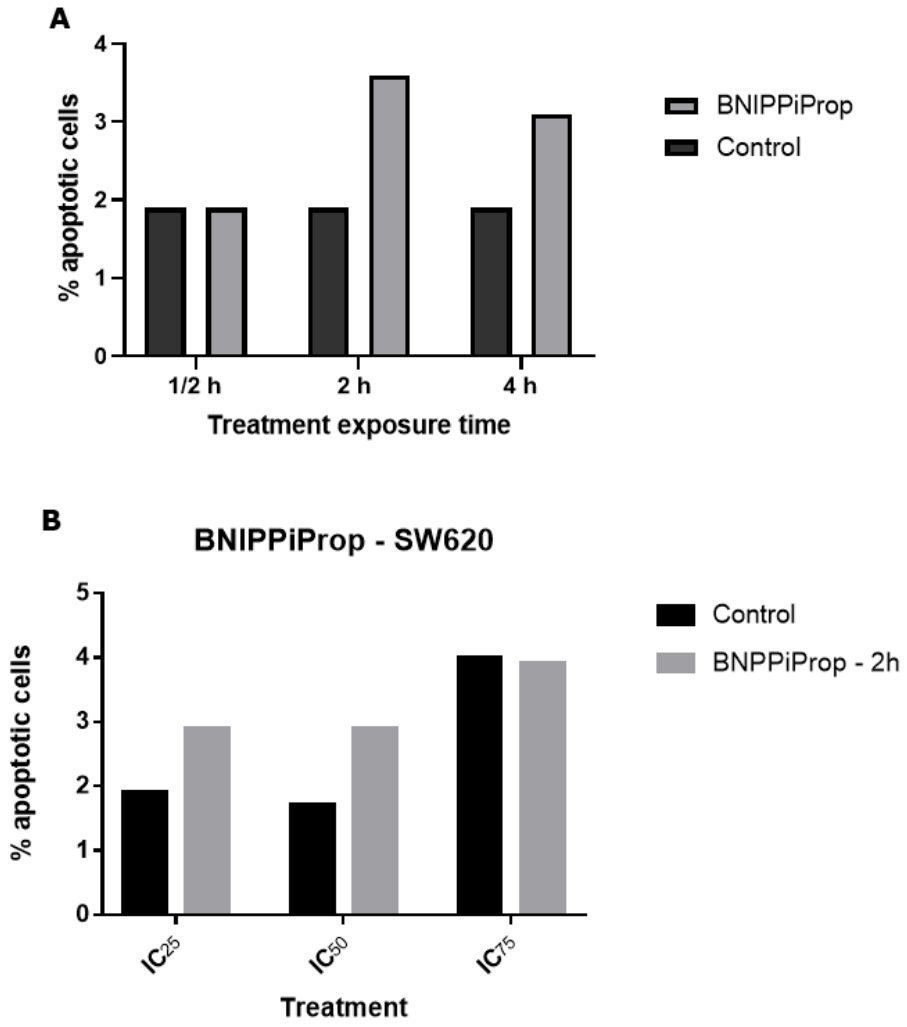

Figure 20. Annexin V/PI detection: determination of the level of early apoptotic cells after treatment with BNIPPiProp using different exposure times (A) and different concentrations after 2 hrs (B). The percentage of apoptotic cell death is compared to untreated cells (control). The experiment has been performed in duplicate for each test.

The initial optimisation of the system and of the software allowed the development of an *in vitro* assay using the image cytometer. Figure 20 (A) showed the results of Annexin V and PI detection using BNIPPiProp at IC_{25} concentration at different exposure times against SW620. Although the 30 mins time point showed no increase in apoptotic cells, the 2-hr time point showed the best result with a 3.5% increase. Using that time point, different concentrations

(IC_{25}, IC_{50} and IC_{75} were then tested (figure 20 (B)). The highest increase in apoptotic cells was observed using IC_{50} with a 1% increase compared to untreated cells.

Detection of early apoptosis using annexin-V relies on the flip of phosphatidyl serine which would mainly occur during the first 4 hrs of incubation with a cytotoxic agent (Zhang *et al.*, 1997). To validate the use of this assay on the cellometer, the same experiment could be repeated with the use of flow cytometry and using the other two compounds.

This testing has allowed the optimisation of the fluorescence parameters on the system with exposure settings set at 2,000 ms. This preliminary test is promising for the use of image cytometry to detect the effect of BNIPs on apoptosis, and more compounds on both cell lines should be tested. However, the use of other methods of apoptosis detection such as the detection of the caspase cascade activation, the detection of cytochrome c release or the cleavage of anti-apoptotic Bcl-2 proteins would be required to support this preliminary data.

3.4.2.2.2. Detection of Caspase 3/7 activity

As with Annexin V/PI, Caspase 3/7 activity allows the detection of apoptotic cell death. Annexin-V shows the translocation of phosphatidylserine to the outer membrane which is an event that occurs during early apoptosis. However, caspase activity assesses the cleavage of members of the cysteine aspartic acid-specific protease (caspase) family which play a crucial effector role in the mediation of apoptosis. Caspase 3 and 7 are the activated form of procaspases 3 and 7 which are inactive cysteine proteases. After activation during apoptosis, a signalling cascade cleaves the procaspases, activating them and leading to the irreversible programmed cell death (Martinez *et al*., 2010). Based on the small increase of apoptotic cells detected with annexin V/PI, this method was used to confirm the first indications previously obtained.

The CaspGLOW™ Fluorescein Active Caspase-3 or Caspase 7 Staining Kit is a rapid method for the detection of Caspase 3 or 7 in living cells. The test uses FITC-conjugated active-caspases 3/7 ligands (DEVD-FMKs) which can penetrate living cells and bind to these active caspases. The FITC-binding allows the

detection of the complex, formed with fluorescence detection using image cytometry. The resulting data is plotted as a histogram displaying the percentage of increase of caspase positive cells compared to untreated cells used as a control.

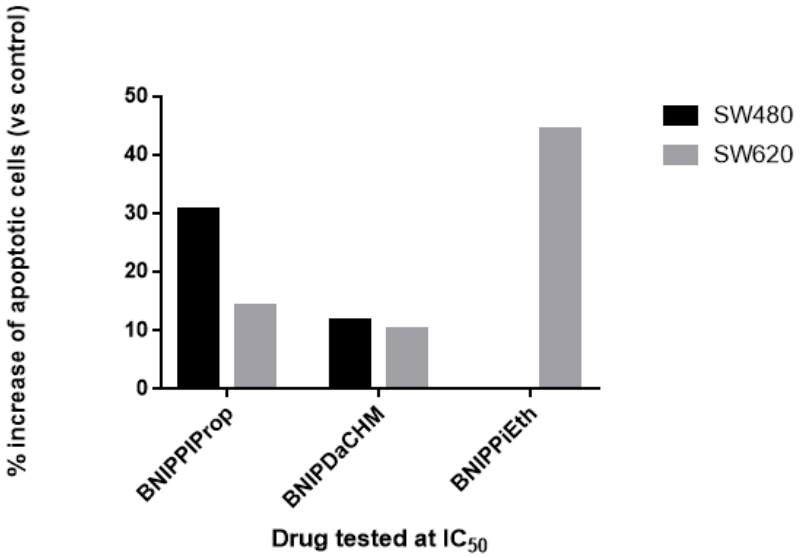

Figure 21. Caspase 3/7 detection: percentage of apoptotic cells after 24 hr-treatment with BNIPPiProp, BNIPDaCHM and BNIPPiEth against SW480 and SW620 (excluding BNIPPiEth against SW480). The percentage of apoptotic cells is normalized to the untreated cells control; n=2.

In figure 21, BNIPs modified the level of expression of caspase 3/7 after 24 hr incubation at IC_{50} concentrations. Compared to untreated cells, an increase in the percentage of apoptotic cells was observed for the 3 drugs in this study ranging from a 11 to 46% increase. BNIPPiEth increased caspase 3/7 expression the most in SW620 cells (by 46% against SW620). These results confirm that apoptosis appears to be triggered after BNIP treatment against CRC cell lines. The experiments would require to be repeated as it was a proof of concept that Caspase 3/7 level could be detected using this image cytometry system.

BNIPPiEth has not been evaluated against SW480 due to a human error during analysis and the lack of material to repeat this experiment. Further optimisation regarding the dye incubation times and the cell concentration is required to

obtain better signals and more robust data. The recent application of the microplate reader – image cytometer is a promising option to achieve this objective since this new system allows high throughput tests using 96-well plates. Moreover, the fluorescent filters of the image cytometer allow the detection of acridine orange and propidium iodide which would make possible to also assess the cell viability.

Image cytometry using the Cellometer (Nexcelom) appeared to be a promising and rapid way to screen different drug candidates on different cell lines in order to produce pilot study results and thus helping with the design of efficient future research projects. In this study, the use of the image cytometer was limited to the setup of the system and the exploration of its potential applications. However, apoptosis detection was successful using both Annexin V/PI and Caspase 3/7 activity detections. Nevertheless, more robust data is needed to draw further scientific conclusions. Section 4.3.3. will provide a more robust apoptosis analysis *via* the detection of the caspase-3 protein.

3.4.3. Effects of BNIPs on the cellular mechanisms of colorectal cancer cells leading to cell death

Based on the preliminary results obtained using the new image cytometry system, the investigation of BNIPs mechanism of action has been further explored.

Most of the chemotherapies leads to apoptosis due to their direct toxicity. For example, anti-cancer drugs can induce an increase in ROS and/or damage DNA leading to programmed cell death. More recently, many new drug candidates have been developed to target the activation of the apoptotic pathway itself such as Bcl-2 inhibitors (Bao *et al.*, 2017).

Regarding the cytotoxicity of BNIP derivatives, determining its mode of cell death is key to understanding the end point affected by the drug. Nonetheless, gaining a full understanding of the biological events happening between the cellular uptake of the drug and the resulting cell death will help the advancement of a BNIP-based chemotherapy.

There is strong evidence that chemotherapeutic agents can trigger the intrinsic pathway of programmed cell death by targeting the cytoskeleton, the synthesis of growth factors, the induction of DNA damage or the generation of oxidative stress (Claire *et al.*, 2018). Previous studies have shown that BNIP derivatives have binding affinities to DNA leading to its damage in various cell lines but not yet in SW480 and SW620 (Brana *et al.*, 1993; Brana *et al.*, 2001; Barron *et al.*, 2010). Therefore, DNA damage was assessed using COMET assay alongside the associated generation of ROS. Moreover, the expression of 35 apoptosis-related proteins was carried out using the proteome profiler human apoptosis array and the detection of caspase-3 was also performed to corroborate the mode of cell death detected using image cytometry.

3.4.3.1. Effects of BNIP derivatives on DNA damage in SW480 and SW620 cells assessed by COMET assay

DNA damage can be induced by internal factors such as ROS or by external factors such as radiation or chemical agents (Turgeon *et al.*, 2018). The main consequence of DNA damage is the modification of DNA structure *via* breaks in the nucleic acid chain or at the level of the phosphate backbone leading to alterations in the DNA metabolism (Chatterjee and Walker, 2018). These structural defects disrupting the normal cell metabolism can lead to cell death. In healthy cells, damaged DNA can be repaired using inherent mechanisms such as homologous recombination or nucleotide excision repair (Errol *et al.*, 2006). Nevertheless, if the level of damage inflicted is too high, the repair mechanisms are not effective and DNA damage can lead to apoptosis (Wang, 2019).

The COMET assay is a single gel electrophoresis assay (SCGE) for the evaluation and quantification of DNA damage. First developed by Ostling *et al.* (1984), the COMET assay consisted of the analysis of single cells embedded on agarose-coated slide (Ostling *et al*., 1984). The cells were lysed while being trapped into the gel and, after electrophoresis and fluorescent staining using a DNA specific dye, the damaged DNA was separated from the intact DNA forming the "head" of a comet shape from the "tail" corresponding to the damaged DNA which has migrated through the gel (figure 22).

The analysis under fluorescent microscopy allows the identification of the level of damage as the extent of DNA forming the tail corresponds to the amount of DNA damage (Fairbairn *et al.*, 1995).

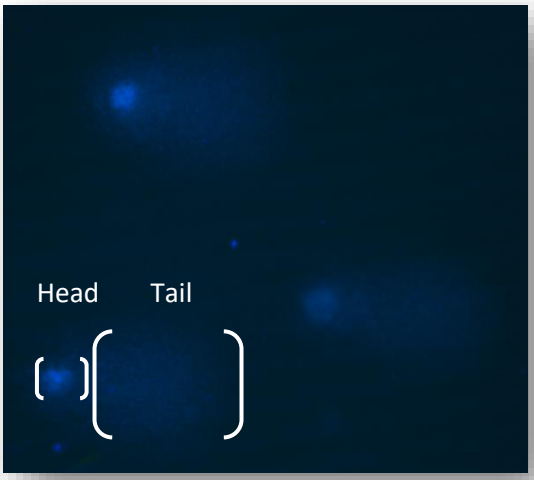

Figure 22. Fluorescent microscopy image of a COMET obtained after SW620 treatment with 200 µM H_2O_2 for 30 minutes.

3.4.3.1.1. Optimization of the positive control concentration using hydrogen peroxide

To induce consistent DNA damage and have a positive control for this experiment, hydrogen peroxide (H_2O_2) was used as it induces DSBs in cells (Benhusein *et al*, 2010). Many studies have used it as a positive control however, H_2O_2 concentration needs to be determined first for every experimental setup.

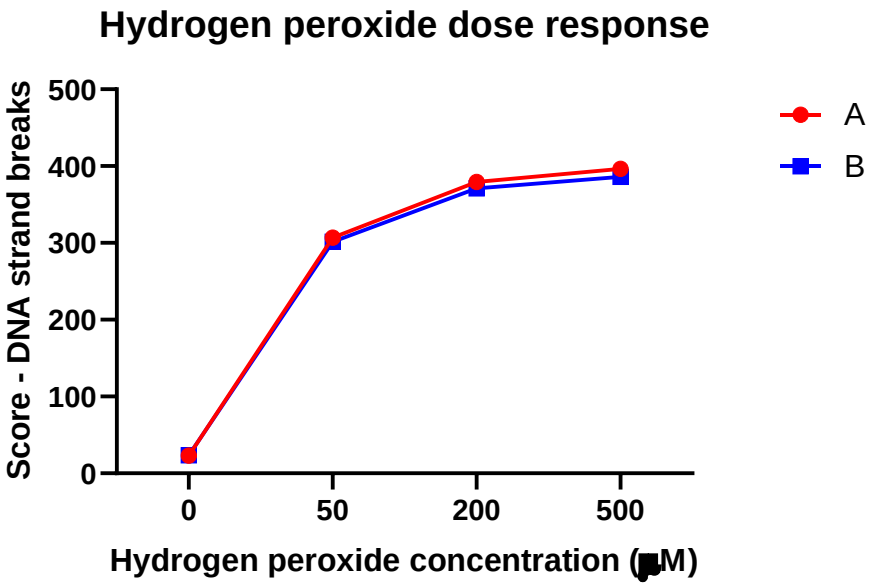

Figure 23. DNA strand breaks in SW620 induced by hydrogen peroxide determined by COMET assay. Data obtained after treatment using hydrogen peroxide (0 – 500 μM) for 30 mins on ice. The experiment has been performed in duplicate (A and B); n=2.

H_2O_2 induced DNA damage at all of the concentrations that were tested from 50 to 500 μM (figure 23). The experiment was repeated twice using two gels per experiment (n=2). For subsequent experiments, in both SW480 and SW620 cell lines, 200 μM H_2O_2 was used as positive control as it induced significant damage while 500 μM was considered unnecessary since, at 200 μM H_2O_2 concentration, the maximum damage of score 400 was already approached.

3.4.3.1.2. The effects of BNIPs on DNA damage on colorectal cancer cells

Both SW480 and SW620 cells were treated using BNIPDaCHM, BNIPPiProp and BNIPPiEth at IC_{25} for 24 hours to evaluate their effect on DNA damage.

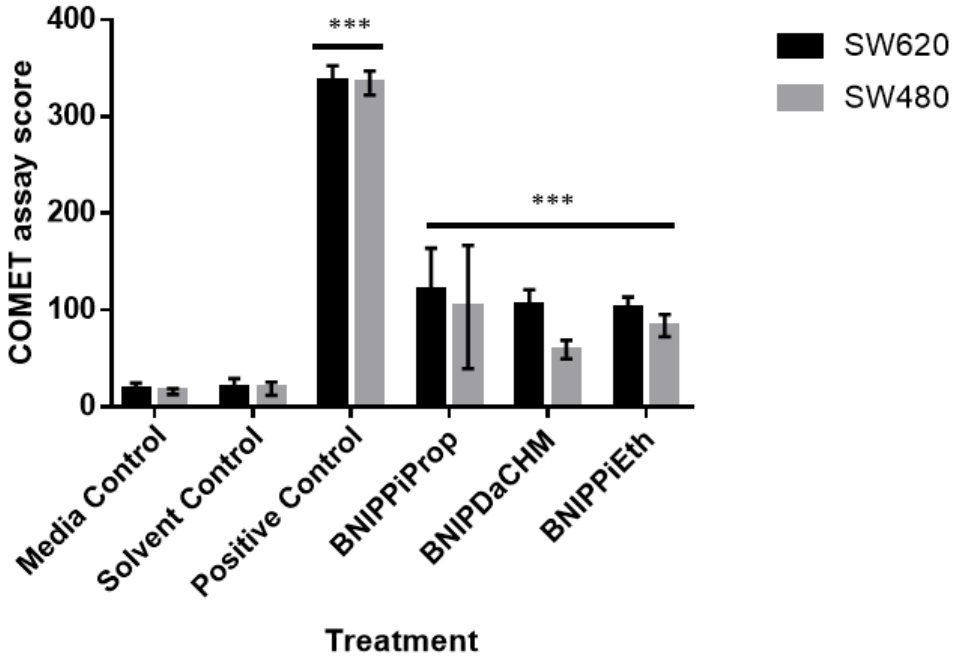

Figure 24. COMET Assay: DNA double strand breaks in SW40 and SW620 cells after a 24 hr-treatment using BNIP derivatives at their IC_{25}. Hydrogen peroxide-induced DNA damage (200µM) has been used as positive control. Data are mean ± SD of 2 replicates from 3 independent experiments (n=3).

First, figure 24 shows that the assessment of DNA damage was validated by having an average score below 20 for the negative control and with a significant increase of DNA damage for the positive controls ($p<0.001$) with similar scores for both cell lines. BNIPPiProp, BNIPDaCHM and BNIPPiEth showed significant increase in DNA damage ($p<0.001$) in both cell lines with scores ranging from 59 to 121. The two cell lines tested, exhibited similar responses to the treatment. These results are concurring the results of Kopsida *et al.* (2018): the latter reported the induction of DNA damage by these 3 drugs against MDA-MB-231

and SKBR-3 breast cancer cells. Additionally, Barron *et al.* (2015) reported similar results for BNIPDaCHM in MDA-MB-231 cells. As highlighted in those studies, the proliferation rate of a cell line may affect its DNA stability, with the cells which have the highest replication rate, being more sensitive to DNA damage. Interestingly, this difference can be observed here with the results shown by the SW620 cell line. The latter exhibited an increased score in DNA damage of 20 to 40 compared to the SW480 cell line results for all of the three drugs (figure 18). Yeh *et al.* (2008) has shown the SW620 cell line to have a higher proliferation rate than SW480 due to its metastatic properties which could explain the increase in DNA damage observed here. However, the difference in scores was not statistically significant between the two cell lines. In relation to the drugs tested, significant differences in DNA damage scores were detected among the two breast cancer cell lines studied by Kopsida *et al.* (2018), demonstrating that different cells can behave differently and that further BNIP concentrations could be tested to see similar effects. In these CRC cells, similar effects of DNA damage were also observed with anticancer drugs, Oxaliplatin or Trifluorothymidine (Temmink et al., 2007).

With BNIPs significantly inducing DNA strand breaks in SW480 and SW620 cells, it was then decided to continue the investigation with the potential mechanistic link between DNA damage and the generation of oxidative stress by reactive oxygen species.

3.4.3.2. Determination of ROS levels after BNIP treatment

ROS is a term that includes molecules, ions and free radicals derived from molecular oxygen which are highly reactive due to the single unpaired electron located on their most external electronic shell. At high levels, ROS can lead to cellular damage including DNA damage (Lori *et al*., 2008). Many anti-cancer drugs, such as physalin, have demonstrated the induction of apoptosis in cancer cells *via* the promotion of ROS signalling pathways (Kang *et al.*, 2016). Therefore, the level of ROS generation of an anti-cancer drug is key to assessing its potential clinical translation (Gibellini *et al*., 2010).

ROS production, as a result of BNIP treatment, was assessed by fluorescence with CM-H_2DCFDA dye. Both SW480 and SW620 cell lines were treated with the BNIPs derivatives at IC_{25} and IC_{50}.

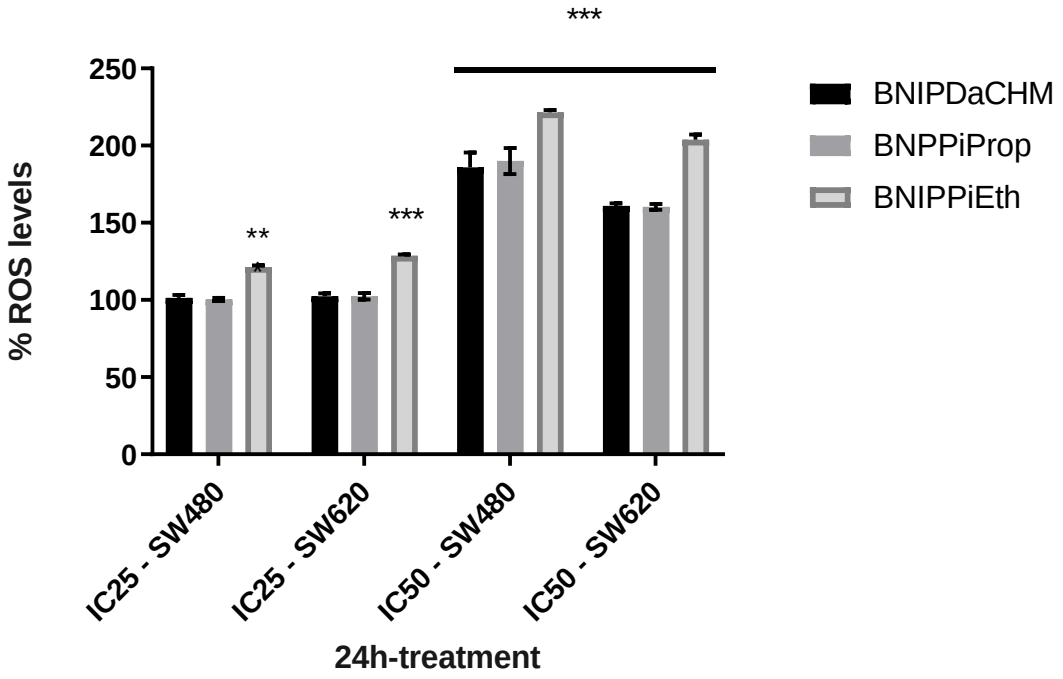

Figure 25. Relative percentage ROS levels in SW40 and SW620 cells after 24 hr-treatment with BNIP derivatives at their IC_{25} and IC_{50}. The results are expressed as a ratio treatment/control (untreated cells) with control being 100% ROS level. Data are mean ± SD of from 3 independent experiments (n=3).

After 24 hr-treatment, BNIPPiProp, BNIPDaCHM and BNIPPiEth all showed an increase in ROS production. However, only BNIPPiEth at IC_{25} significantly increased ROS levels in SW480 ($p<0.01$) and SW620 ($p<0.001$) cells (figure 25) whereas the other two drugs had no effect at that concentration. At IC_{50}, all three drugs showed a significant increase in ROS production in both cell lines ($p<0.001$). For each cell line, BNIPPiEth (IC_{50}) showed a greater induction of ROS levels (with the greatest increase for SW480 cells), however this was not statistically significant.

The more stable the chemical structure is, the more difficult it is for the compound to undertake oxidation (Davasagaya *et al*., 2004). With the highest response obtained with BNIPPiEth, this difference can be explained by its chemical structure: it is the compound with the shorter linker chain (figure 3. section 1.2.2.). This particularity may result in the chemical instability leading to an increased ROS generation.

This study has demonstrated the generation of ROS by BNIPDaCHM, BNIPPiEth and BNIPPiProp at their IC_{50} values (1.3 – 2.6 µM) after a 24-hour treatment against both SW480 and SW620 cells. Gold standard drugs such as Tamoxifen or Doxorubicin showed similar mode of action linking DNA damage to ROS generation which support the clinical relevance of BNIPs against CRC. Since ROS are increased by BNIPs, it is important to understand the link between ROS generation and the mode of cell death.

3.4.3.3. Effects of BNIP derivatives on apoptotic cell death in SW480 and SW620 cells assessed by Caspase-3 detection

One of the first initiating events of apoptosis is the activation of the caspases which makes the detection of these proteins a key method in the mode of cell death investigation. As a mediator of apoptosis, caspase-3 has been the target of choice and this enzyme is responsible for the cleavage and activation of other caspases (6, 7 and 9). Thus, the detection of caspase-3 is directly linked to the programmed cell death pathway and is an important marker of apoptosis (figure 7. section 1.4.2.).

The chosen method for Caspase-3 detection was the Caspase-3/CPP32 colorimetric Assay Kit. This method is based on the detection of p-nitroaniline or pNA. pNA is a chromophore which is conjugated to a specific sequence, an amino acid motif called DEVD. As an intracellular cysteine protease and once activated, Caspase-3 will specifically cleave the DEVD sequence which allows pNA to be detected using spectrophotometry detection at 405 nm. The level of the Caspase-3 activity is then directly proportional to the quantity of pNA released.

Here, caspase 3 activity in SW480 and SW620 cells has been investigated after a 24 hr-treatment with BNIP derivatives at IC_{25}.

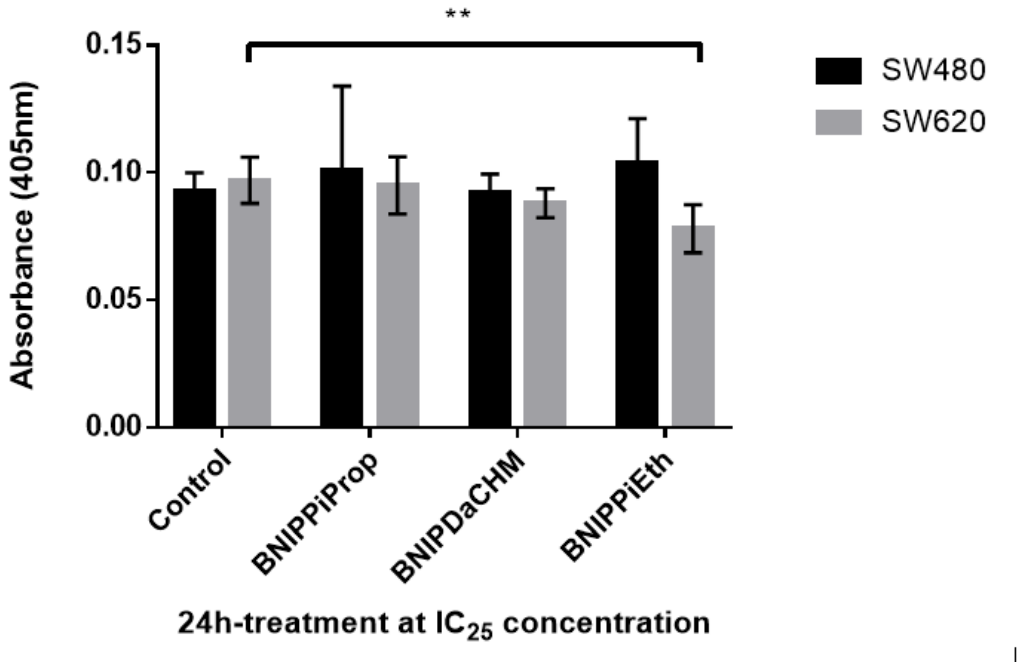

Figure 26. Detection of caspse-3 level in SW480 and SW620 cells after a 24 hr-treatment using BNIP derivatives at their IC_{25}. Data are mean ± SD of 6 replicates from 3 independent experiments (n=3).

The results in figure 26 showed that, when compared to control, there was no significant increase in the detection of caspase-3 after treatment with any of the three drugs at their respective IC_{25} concentrations (0.75 - 2.1 µM). Of note, the results obtained were consistent between the two cell lines. However, treatment with BNIPPiEth exhibited a significant decrease ($p<0.01$) in caspase-3 compared to the control only in SW620 cells, implying a potential chemoresistance of SW620 for BNIPPiEth.

Taking together all of the preliminary data obtained using image cytometry, apoptosis appeared to be a potential mode of cell death induced by BNIP derivatives. The results exhibited in figure 26 showed that apoptosis was not

observed after a 24 hr-treatment using the BNIP derivatives against SW480 and SW620.

The use of the 24 hr-time point at the IC_{25} concentration of the BNIP derivatives implied that cell death was occurring, having previously observed a decrease of cell viability with MTT assay. However, the detection of apoptosis using caspase-3 relies on the detection of this particular protein. The commercial kit used in this experiment will only detect the active form of caspase-3 in the cell lysate and not the inactive procaspase-3. Therefore, the evaluation of caspase-3 activity would be useful to confirm the absence of apoptosis. The chosen 24 hr time point might be too long for an effective apoptosis detection using this test; a range of time points should be investigated to confirm these findings.

3.4.3.4. Effects of BNIP derivatives on protein expression in SW480 and SW620 cells assessed by human apoptosis array

Protein array technology was used to further explore molecular mechanisms associated with apoptosis and which could be affected by cells treatment with BNIP derivatives.

The proteome profiler human apoptosis kit allows the simultaneous detection of 35 apoptosis-related proteins in the cell lysate. This membrane-based sandwich immunoassay (figure 27) was used on both SW480 and SW620 lysate after a 24 hr-treatment with BNIPDaCHM, BNIPPiProp and BNIPPiEth at IC_{25}.

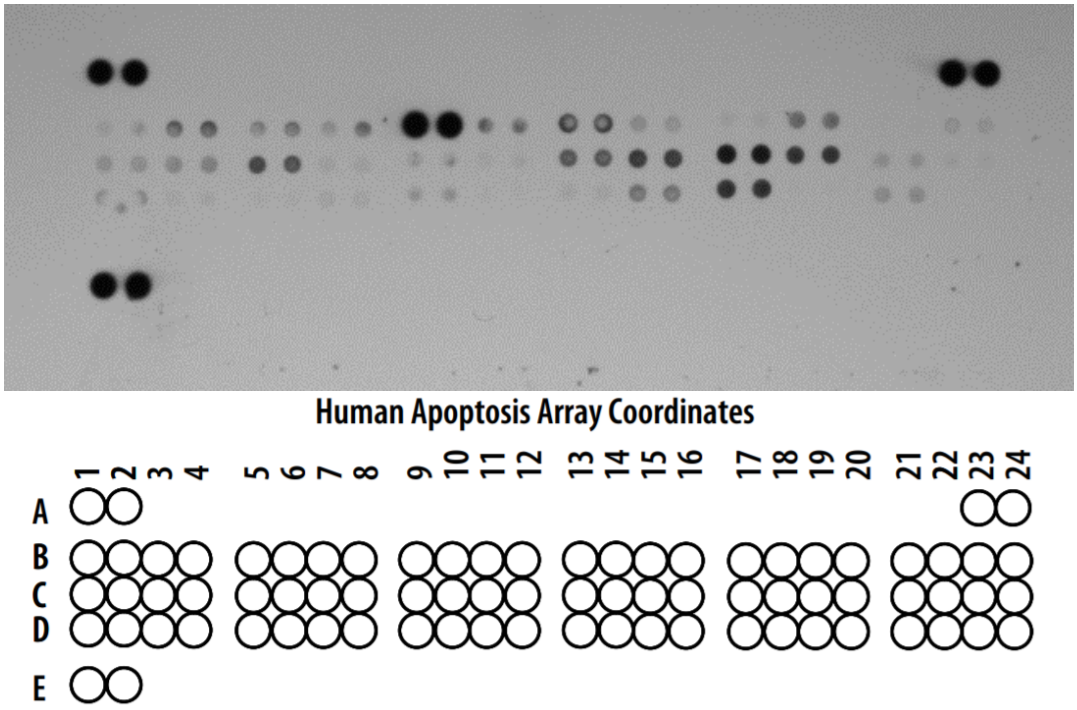

Figure 27. Picture of an X-ray film after exposure to a treated array membrane (BNIPPiEth) with the associated spot coordinates, with each spot corresponding to a single protein (see Table 5).

Table 5. List of proteins detected by the human apoptosis array with their associated membrane coordinates (extracted from the supplier site, rndsystems.com).

Coordinate	Target/Control	Coodinate	Target/Control
A1, A2	Reference Spots	C13, C14	HO-2/HMOX2
A23, A24	Reference Spots	C15, C16	HSP27
B1, B2	Bad	C17, C18	HSP60
B3, B4	Bax	C19, C20	HSP70
B5, B6	Bcl-2	C21, C22	HTRA2/Omi
B7, B8	Bcl-x	C23, C24	Livin
B9, B10	Pro-Caspase-3	D1, D2	PON2
B11, B12	Cleaved Caspase-3	D3, D4	p21/CIP1/CDKN1A
B13, B14	Catalase	D5, D6	p27/Kip1
B15, B16	cIAP-1	D7, D8	Phospho-p53 (S15)
B17, B18	cIAP-2	D9, D10	Phospho-p53 (S46)
B19, B20	Claspin	D11, D12	Phospho-p53 (S392)
B21, B22	Clusterin	D13, D14	Phospho-Rad17 (S635)
B23, B24	Cytochrome c	D15, D16	SMAC/Diablo
C1, C2	TRAIL R1/DR4	D17, D18	Survivin
C3, C4	TRAIL R2/DR5	D19, D20	TNF RI/TNFRSF1A
C5, C6	FADD	D21, D22	XIAP
C7, C8	Fas/TNFRSF6/CD95	D23, D24	PBS (Negative Control)
C9, C10	HIF-1α	E1, E2	Reference Spots
C11, C12	HO-1/HMOX1/HSP32		

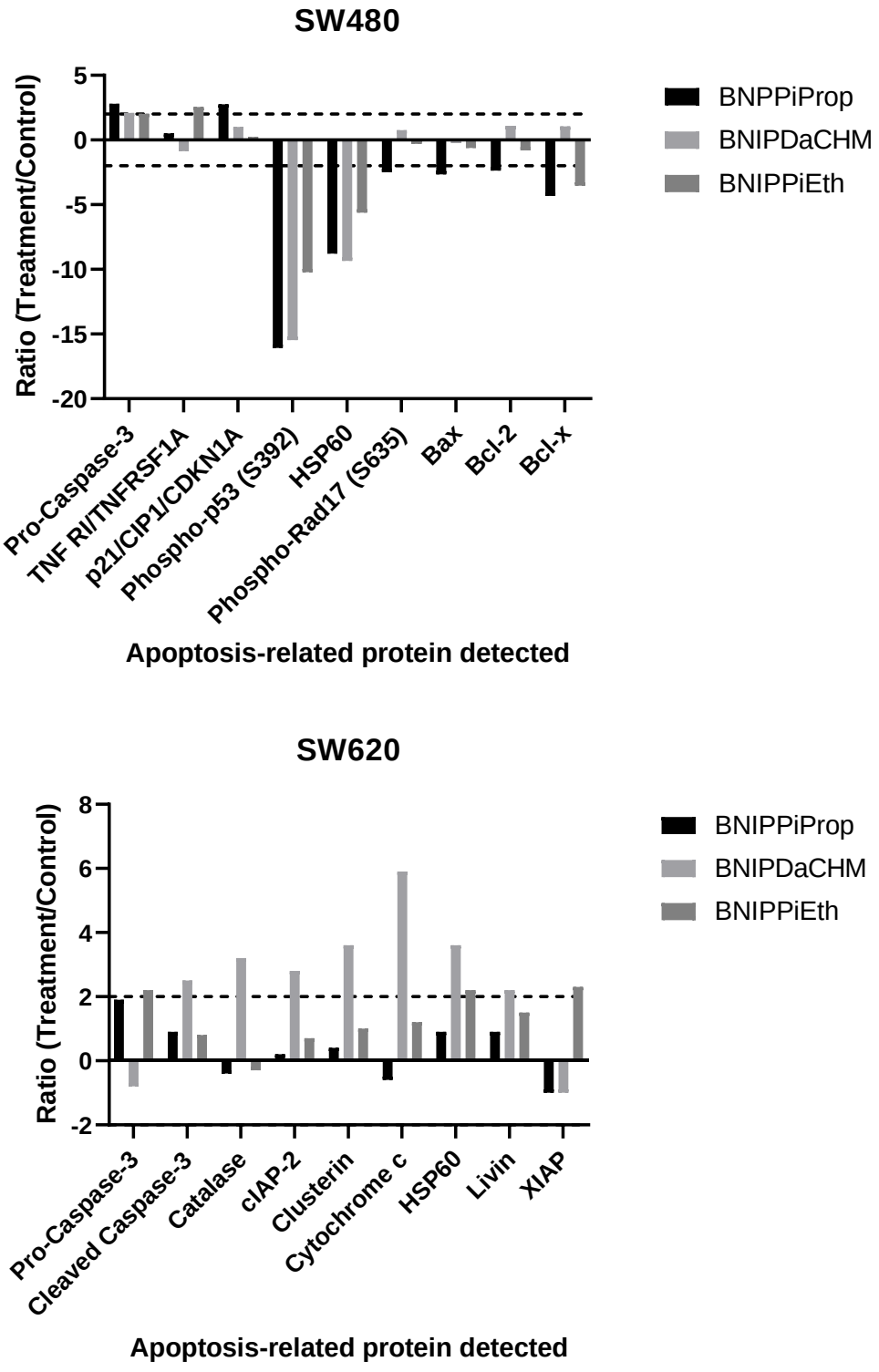

Figure 28. Relative expression of proteins expressed by SW480 and SW620 cells treated with BNIPPiProp, BNIPDaCHM and BNIPPiEth at IC_{25} concentrations for 24 hrs. Results expressed as ratio treatment to control for proteins with ratio >2 or <2 Experiments performed in duplicate.

With the SW480 cell line, 3 proteins were upregulated (figure 28) presenting a ratio to control of 2.0 or more. Pro-caspase-3 were found to be upregulated after treatment with the 3 drugs. TNFRI/TNFRSF1A were upregulated only using BNIPPiEth and P21/CIP1/CDK1N1A only after treatment with BNIPPiProp. Six proteins were found to be downregulated (figure 28) showing a ratio treatment/ control below -2. All six proteins were downregulated by BNIPPiProp. Phospho-p53 and HSP60 were highly downregulated with ratio between -5 and -15 and they were the only two proteins downregulated by all the drugs. Finally, Bcl-x was downregulated by both BNIPPiProp and BNIPPiEth.

On the other hand, with the SW620 cell line, 9 proteins were found to be up regulated (Pro-Caspase-3, Cleaved-Caspase-3, Catalase, cIAP-2, Clusterin, Cytochrome c, HSP60, Livin and XIAP). The treatment using BNIPDaCHM induced more greater changes with 7 proteins upregulated. Moreover, these upregulations are unique to the treatment of BNIPDaCHM (exception of HSP60 also upregulated). XIAP was only up regulated by BNIPPiEth and pro-caspase-3 was upregulated by BNIPPiProp and BNIPPiEth but down regulated by BNIPDaCHM. Interestingly, between the two cell lines, pro-caspase-3 is the only protein that has been found to be upregulated in both cases. Moreover, HSP60, which is downregulated in SW480, is upregulated in SW620.

The vast majority of the protein detected were not affected by the BNIPs (ratio treatment/control between -2 and 2) with no change in their expression level compared to the untreated control.

Starting with SW480, the only two proteins that were upregulated were TNFR1 and p21. TNF R1 or tumour necrosis factor receptor 1 is a tumour membrane receptor which mediates apoptosis. Once bonded with TNF-alpha, TNFR1 recruits the death domain protein TRADD at the intracellular level which results in the activation of the caspase cascade (Baud and Karin, 2001). Only BNIPPiEth has presented an upregulation of TNF R1 in SW480. Even if related to apoptosis mediation, the detection of this protein alone is not directly linked to an increase in apoptosis but potentially to an increase in the expression of the membrane receptor to enhance the apoptotic response.

The p21 protein, known as cyclin-dependent kinase inhibitor p21, is a proliferation inhibitor causing cell cycle arrest and is involved in the prevention of tumour development. For example, human cancer cell lines treated with alkylating agents saw their cycle arrested by the action of p21. The cleavage of p21 then led to apoptotic death (Zhang *et al.*, 1999). Barron *et al.* (2010) showed that BNIPDaCHM induced DNA damage and repaired instability in triple negative breast cancer cells *via* p21 expression.

Pro-caspase-3 is the non-cleaved or inactivated form of caspase-3. Once activated, the resulting proteolytic cascade leads to the amplification of the apoptotic signalling pathway. The upregulation of pro-caspase-3 was found in both cell lines.

Phospho-p53 (S392) corresponds to the p53 transcription factor phosphorylated at serine 15. S392 corresponds to Serine 392 which is the phosphor-acceptor site located in the C-terminal regulatory domain (Hupp *et al*., 1995). This specific phosphorylation enhances the DNA-binding properties of p53. This enzyme is known as a tumour suppressor reacting to diverse stress signals to deliver antiproliferative responses. More precisely, one of its main function is the activation of programmed cell death in a transcription-dependant manner (Fridman and Lowe, 2003). The inhibition of p53 action causes tumour promotion and chemoresistance. Here, the protein has been highly downregulated in SW480 but not in SW620. Additionally, previous research has already linked the activation of p53 to the treatment with BNIP derivatives in cancer cell lines (Li et *al.*, 2012; Liang *et al*., 2011).

Bax, Bcl-2 and Bcl-x are three mitochondrial proteins. They mediate apoptosis *via* the regulation of the liberation of cytochrome c from mitochondria which lead to the activation caspase and ultimately to programmed cell death (Korsmeyer, 1995). The 3 proteins were found to be downregulated by BNIPPiProp alone in SW480. Jiang *and Milner* (2003) has shown that the downregulation of this family of proteins resulted in the induction of apoptosis in glioblastoma cells. Moreover, BNIPPiProp was found to down regulate cytochrome c in SW480 alone confirming the mediation of apoptosis. Interestingly, the HSP60 protein is downregulated in SW480 but upregulated in SW620. The heat-shock protein 60 (HSP60) is a mitochondrial protein which is used as a danger signal for stressed or damaged

cells and prevents protein aggregation that can often occur during stress (Wiechmann *et al.*, 2017). Based on these results for SW480, the down-regulations of a majority of pro-apoptotic factor can indicate that apoptosis is not the node of cell death observed using BNIPPiProp, BNIPDaCHM and BNIPPiProp corroborating the previous data obtained with caspase-3 detection. However, the up-regulation of pro-caspase-3 may suggest the presence of another regulated mode of cell death such as autophagy.

In SW620, 7 proteins were upregulated by BNIPDaCHM only including Cleaved-Caspase-3, Catalase, cIAP-2, Clusterin, Cytochrome c, HSP60 and Livin. The upregulated proteins are found to be factors inhibiting apoptosis. The cellular inhibitor of apoptosis 2 (cIAP2/HIAP1) is a strong inhibitor of apoptosis. Moreover, catalase is a H_2O_2 specific scavenger which is known to reduce apoptotic levels after the use of drugs such as etoposide, camptothecin or doxorubicin (Sancho *et al*., 2003). Additionally, Livin is also an inhibitor of apoptosis inhibiting caspase activity (Kasof and Gomes, 2001), and Clusterin, when overexpressed, protects the cell from apoptosis induced by chemotherapy (Koltai, 2014). The upregulation of all of these factors leads to the conclusion that BNIPDaCHM induced an inhibition of apoptosis in SW620. However, the upregulation of cytochrome c and of the caspase-3 proteins showed that there was a simultaneous promotion of apoptotic cell death. This implies that SW620 might be exhibiting a specific drug resistance to BNIPDaCHM. Luo *et al.* (2016) has previously shown that there is greater ability of drug resistance in metastatic cells SW620 than in primary SW480 supporting this data.

Therefore, the results obtained with the proteome profiler array, showed the presence of heterogeneity on drug resistance between SW620 and SW480 cell line. Moreover, the differences in the mechanism of action of the 3 drugs can be clearly observed. Together, these findings provide a first indication of the complexity of the BNIP mechanism of action relating to cell death by exhibiting a different pattern depending on the type of cell line, experimental conditions and the drug tested. Interestingly, studies have studied apoptotic signalling pathways and demonstrated the existence of crosstalk between the different mode of cell with for example autophagy and this have been discussed further in the next chapter.

Chapter 4

General discussion and conclusion

4.1. General discussion

The use of solid lipid nanoparticles for the encapsulation of BNIPPiProp was limited by the drug delivery system cytotoxicity in SW480 and SW620 CRC cell lines.

In chapter 2, the encapsulation of BNIPPiProp into solid lipid nanoparticles has been performed. This technology developed in 1991 by Müller is promising by being at the interface of liposomes and polymeric nanoparticles (Corrias and Lai, 2011). They have been extensively studied for a wide range of biomedical applications ranging from drug and gene delivery to diagnostic tools (Yang *et al.,* 2016). The SLNs were successfully manufactured offering physico-chemical properties matching the standards of chemotherapy drug delivery systems with an average size of 150 nm, associated with a PDI of 0.2, and a negative zeta-potential below -20 for the selected batch Ae. However, the low encapsulation efficiency (<1%) obtained for BNIPPiProp encapsulation coupled with the high cytotoxicity observed with the empty nanovectors against both SW480 and SW620 colon cancer cell lines, questions this formulation's suitability and needs further investigation.

The cytotoxicity of the empty nanocarrier can be potentially linked to the presence of surfactants as stearic acid has be reported to be non-cytotoxic (Thakkar *et al*., 2016). The original using this combination of surfactants did not assess its cytotoxicity (Aditya *et al*., 2014). Regarding manufacture, the hot homogenisation method has been reliable with a good batch-to-batch reproducibility. Moreover, this method did not require sophisticated equipment while avoiding the use of organic solvents. This represents a unique opportunity to design a scalable drug delivery system production at a reasonable cost (Marengo *et al*., 2000). First, the determination of the origin of the toxicity should be investigated and it is usually performed by replacing components of the nanoparticles such as the surfactants. Although, batch Ae was selected as the candidate for the *in vitro* study, different formulations were manufactured with the use of PEG stearate creating different lipid/surfactants combinations. Therefore, the other empty formulations should firstly be tested against both cell lines to observe potential changes in the cytotoxicity profile.

On the other hand, to improve the loading efficiency of BNIPs inside SLNs which was still limited (<1%), changes in the drug/lipid ratio could also lead to an increased drug loading. Offering a mix of lipid to the solid core of the nanoparticle could lead to the creation of more imperfections allowing more drug to be encapsulated. If the presented solutions remain unsuccessful, the use of NLCs could also be investigated as its liquid lipid core could be more suited for the encapsulation of BNIPs.

Further characterisation of the SLNs would also be beneficial to obtain a better understanding of the impact of formulation changes. The evaluation of the stability, the release profile and also the use of differential scanning calorimetry would provide more information to compare the different batches and to assess how the incorporation of the drug impacts the nanoparticles (Campos *et al*., 2020). For example, determining if the encapsulated drug is in an amorphous or crystalline state within the particle core would give an indication of its degree of solubility in lipids leading to key formulation adjustments.

Although early in its development, it is also important to discuss the translation of the *in vitro* study of BNIP drug delivery systems to an animal model. While the EPR effect is an essential mechanism for the delivery of chemotherapy, 2D *in vitro* assessment of its benefits can be difficult due to the inner limitations of cell culture systems. More physiologically relevant models have been developed including the use of 3D cell culture platforms using for example the growth of cancer cells on 3D hydrogel scaffolds which could be more relevant for further studies (Shi *et al.*, 2016).

A previous study by Costa Lima *et al*. (2012) reported an attempt to encapsulate BNIP derivatives inside pegylated PLA nanoparticles with an associated *in vitro* study against *Leishmania infantum* protozoa. The PLA nanoparticles exhibited an encapsulation efficiency of more than 80%. The low encapsulation efficiency (<1%) obtained for BNIPPiProp encapsulation coupled with the high cytotoxicity observed for the empty nanovectors against SW620 and SW480 has been a drawback in the development of a drug delivery system for BNIP derivatives.

However, obtaining a better understanding of the drug's cellular mechanism of action represented the next step to refine the design of SLNs to produce a tailored drug delivery system targeting CRC. The development of targeted nanoparticles

specific to CRC therapy can be achieve by the grafting of antibodies peptides or aptamers to functionalized the surface of the nanoparticles (Cisterna *et al.*, 2016). For example, poly(D,L-lactic-co-glycolic acid)-block-polyethylene glycol nanoparticles encapsulating cisplatin were formulated and a integrin-receptor specific cyclic pentapeptide were added to the drug carrier surface to bind to this CRC overexpressed receptor (Graf *et al.*, 2012).

The design nanoparticle drug delivery systems for the delivery of BNIPs is still at an early stage but this study presented the opportunities associated with the use of lipid based-carriers. Subsequent discoveries of the BNIP mode of action reported in this project are important information which could lead to the formulation of more tailored nanomaterials for the delivery of BNIPPiProp, BNIPDaCHM and BNIPPiEth to treat CRC.

BNIPPiProp, BNIPDaCHM and BNIPPiEth demonstrated strong cytotoxicity against SW480 and SW620 CRC cell lines.

Without being encapsulated, BNIPPiProp, BNIPDaCHM and BNIPPiEth all showed strong cytotoxicity against both cell lines with IC_{50} values ranging from 1.3 to 2.6 µM. As previously stated, these IC_{50} values are much lower than the ones obtained using the most common chemotherapy agents against CRC. Moreover, BNIPPiProp, BNIPDaCHM and BNIPPiEth also appeared more cytotoxic than previous version of BNIP derivatives. For example, amonafide presented an IC_{50} of 4.67 µM and BNIPOSpm, >50 µM, against HT-29 CRC cell line. This comparison shows the success of the formulation of the latest generation of BNIPs with the design of the linker chain leading to an increased cytotoxicity against CRC *in vitro*.

The MTT assay is considered as the gold standard for cell viability assessment since the 1980s (Mosmann, 1883). However, the scientific community has reported several challenges associated to its use. MTT relies on the metabolic activity of living cells to produce formazan, however endogenous and exogenous compounds can also be the initiator of this change (Hansen *et al.*, 1989; Zhang *et al*., 1990). The choice of a cell viability assay needs to be rationalised based

on the sensitivity of the test allowing the detection of the cell viability variation with a good reproducibility under controlled experimental conditions (Tonder *et al.*, 2015). Alternative assays can be chosen with for example the use of the Resazurin reduction assay (McMillian *et al.,* 2002) or the sulforhodamine B assay (Rubinstein *et al*., 1990). A comparative study performed by Tonder *et al.* (2015), demonstrated that the MTT assay presented the highest variability due to interferences with compounds tested compared to the two other methods. However, in the case of this project, MTT assay remained the most time- and cost-effective choice for the determination of BNIPs cytotoxicity and it also provided a unique and reliable way to compare the IC_{50} values determined from this study to previous generations of BNIPs tested in the past. The extension of the BNIP exposure time (>24 hrs) would provide interesting data to assess a change in the cytotoxic profile of the BNIPs, allowing the determination of IC_{50} values for different time points for future experiments. The incorporation of commercially available colorectal cancer anti-cancer drugs in the cytotoxicity testing would also be a great addition to obtain a direct comparison of the cytotoxicity of BNIPs against the current chemotherapy gold standards. This well-studied control could then be kept throughout the *in vitro* study to show an internal control for the drugs' mechanism of action investigation.

With the 3 drugs showing the same cytotoxicity pattern on both cell lines, the use of BNIPPiProp, BNIPDaCHM and BNIPPiEth appeared to be clinically relevant for the treatment of CRC and could potentially lower the chemotherapy side effects by requiring a much lower dose.

BNIPPiProp, BNIPPiEth and BNIPDaCHM generated a >50% increase of ROS levels and provoked DNA double strand breaks in SW480 and SW620.

The generation of ROS after treatment with anticancer drugs caused the accumulation of ROS within the cells which preceded oxidative stress and eventually cell death *via* apoptosis or terminal differentiation (Watson *et al.*, 2011). Moreover, ROS are considered as mediators of DNA damage contributing to the genotoxicity of chemotherapeutic drugs such as cisplatin or doxorubicin (Conklin, 2004). More generally, anthracyclines, alkylating agents and platinum

complexes are ROS generators which interfere with cellular events such as cell cycle progression and apoptosis (Mizutani *et al.*, 2005). For example, the synergistic effect of oxaliplatin with piperlongumine has been proven to be ROS-mediated against human HCT-116 and LoVo cells (Chen *et al.,* 2019). Additionally, the study of Cheng *et al.* (2015) showed that the combined use of oxaliplatin and piperlongumine increased ROS levels and also triggered endoplasmic reticulum stress which led to the activation of the ER stress-specific apoptotic cascade protein CHOP leading to apoptosis (Cheng *et al*., 2019).

Here, the reported generation of ROS associated with the induction is a major finding that contributes to the elucidation on the mechanism of action of BNIPs. BNIPPiProp, BNIPDaCHM and BNIPPiEth all induced more than a 50% increase of ROS levels against both SW620 and SW480 after a 24 hr-treatment at IC_{50} concentrations. In this study, the CM-H_2DCFDA dye was used which became fluorescent after oxidation, allowing us to assess the ROS levels in vitro. The use of a positive control such as H_2O_2, PMA (4beta-phorbol, 12-myristate, 13-acetate) and tert-butyl hydroperoxide (TBHP) could also be employed in future experiments.

As CRC cells generates higher basal ROS levels than regular cells, the important increase of ROS produced after BNIP-treatment can be responsible for cancer cell death (Lin *et al*., 2018). ROS generation can be initiated in two major ways: the mitochondrial ROS generation or the inhibition of the antioxidant protective system (Yang *et al*., 2018). Drugs such as arsenic trioxide (Shi *et al.,* 2004) or Doxorubicin (Marullo *et al*., 2013) targeted the mitochondria to induce ROS generation whereas Imexon (Dragovich *et al*., 2007) or Mangafodipir (Alexandre *et al*., 2006) regenerated the reduced form of antioxidants. Therefore, determining more precisely the cellular mechanism behind the BNIP-induced ROS generation can be interesting to explore in greater detail the mechanism of action of these drugs compared to other anti-cancer drugs. The generation of ROS can also participate to the reduction of multi-drug resistance with the example of piperlongumine which increase the expression of p53 in SW620 due to the induction of oxidative stressed. Combined with doxorubicin, the therapy demonstrated a greater anti-cancer potential increasing the drug sensitivity *via* the production of ROS (Basak *et al*., 2016). Consequently, the BNIP-induced generation of ROS levels is particularly promising for the treatment of late stage

CRC even if no significant differences were observed between SW480 and SW620 here.

In addition to the generation of ROS, COMET assay revealed that BNIPPiProp, BNIPPiEth and BNIPDaCHM were found to significantly augment DNA DSBs in both SW480 and SW620 using IC_{50} concentrations. These findings showed that the BNIP treatment led to genomic instability in both cell lines. However, no significant differences were observed between them as it could have been expected due to the higher proliferation rate of SW620 often associated with more DNA damage induced. As with ROS generation, DNA damage can be observed during chemotherapy-induced cell death (Borges *et al.*, 2009). These two events can be found independently or associated, with one caused by the other one. For example, the use of Actinomycin D creates single and double strand breaks with an associated increase of ROS levels (Wang *et al*., 2007). Furthermore, ionizing radiation can cause both DSBs and hydroxyl radical formation (Hall et al., 1973). Interestingly, previous studies on BNIPDaCHM, the parental compound of BNIPPiProp and BNIPPiEth, proved the induction of DSBs and the inhibition of DNA repair in triple negative breast cancer cells (Barron *et al.,* 2015). Here, the significant increase of ROS and DSBs in both cell lines using BNIPDaCHM, BNIPPiProp and BNIPPiEth is a key component to explain the cytotoxicity of these compounds.

Barron *et al.* (2015) also showed that BNIPDaCHM was capable to inhibit DNA repair in triple breast cancer cell lines. Two mechanisms for the repair of double DNA strand breaks can occur, namely the homologous recombination and the non-homologous end-joining (Rasool *et al*., 2007). These mechanisms play a fundamental role as they can be the source of chemotherapy resistance (Murugesan *et al.*, 2017). Demonstrating a significant change of DNA repair levels between the two cell lines after treatment using the BNIPPiProp, BNIPDaCHM and BNIPPiEth would need to be further explored as it would offer a viable option to treat chemo-resistant cancer.

With no significant differences observed between the 3 drugs in terms of cytotoxicity, ROS generation or DNA damage induction, no conclusion can be made regarding their relative potency making them all strong candidates in the treatment of CRC. The use of more time points in the study of their mechanism

of action could provide interesting data regarding the potential impact of the molecular structural differences of the 3 drugs which might not be perceived after 24 hours. Additionally, the study of the cellular drug uptake would allow the determination of a more precise time frame for biochemical assays.

With the determination of low IC_{50} values using MTT assay, the evaluation of the mode of cell death appeared critical as many drug discovery strategies focus on the molecular targets of the drugs associated with cell death or the disruption of cell cycle. Although other regulated mode of cell death such as autophagy or necroptosis are known to be linked to the action of anti-cancer drug (Portt *et al*., 2011), the detection of ROS generation and DNA damage induction by BNIPPiProp, BNIPDaCHM and BNIPPiEth firstly led to the investigation of apoptosis as proposed mode of cell death.

The use of BNIPPiProp, BNIPPiEth and BNIPDaCHM revealed the existence of a drug- and cell line- dependant complex regulated mode of cell death in CRC SW480 and SW620 cell lines.

First, a pilot study using image cytometry was performed to obtain first evidences indicating the induction of apoptosis by BNIP derivatives. In recent years, the use of image cytometry has been developed due to the technical improvement of these systems meeting clinical accuracy requirements (Lohman *et al.*, 2018). For example, the use of image cytometry included the detection of circulating tumour cell detection in hepatocellular carcinoma (Liu et *al.*, 2016).

The results obtained with the caspase-3 detection showed no differences between the caspase 3 level of untreated cells and treated cells by the BNIPPiProp, BNIPPiEth and BNIPDaCHM at IC_{25} concentration for 24 hours. This assessment did not corroborate the first evidence obtained using image cytometry. Further experiments should be performed to evaluate if this absence of apoptosis detection can be due to an inaccurate time-point of analysis. Moreover, the expression of caspase-3 can be specific to tumour type and the activity level of this protein could change during upon the cancer stage (Fujikawa *et al.*, 2000;

Grigoriev *et al.*, 2002). Therefore, emerging therapies are looking at targeting caspase-3 to induce apoptosis in cancer cells (Hu *et al.*, 2020).

Subsequently, this result was challenged by the human apoptotic array analysis which provided a deeper insight into the mode of cell undertaken by SW480 and SW620 after BNIP treatment.

Using the human apoptosis array, a more global picture of the impact of BNIPs on the complex apoptotic pathway was obtained. As this experiment was only perform in duplicate, the major trends were discussed. Among the 35 apoptotic-related proteins detected, pro-caspase-3 was the only protein which was found to be upregulated in both SW480 and SW620. Although pro-caspase-3 is the inactive form of caspase-3, this result is particularly promising as the leveraging of pro-caspase-3 overexpression is currently a molecular target for selective anticancer therapy (Boudreau *et al.*, 2019). As most of the current cytotoxic compounds trigger apoptosis by affecting molecules upstream of pro-caspase-3, the direct upregulation of caspase-3 induced by BNIPs can represent a strategy to overcome apoptotic evasion and chemoresistance (Baig *et al.*, 2016). For the moment, this strategy requires the synergistic use of a combination of anti-cancer drugs such as temozolomide with procaspase activating compound 1 capable of activating the overexpressed pro-caspase-3. The resulting treatment allowed the activation of the overexpressed protein to induce a stronger apoptosis response and this could be explored using the BNIPs (Joshi *et al*., 2017). Consequently, the ubiquitous detection of pro-caspase-3 upregulation can be an indicator of the stimulation of the apoptotic pathway in both cell lines using the 3 compounds. Nevertheless, the validation of the overexpression of pro-caspase-3 should also be validate using ELISA prior to further studies.

More specifically in SW480, both phospho-p53 and HSP60 were found greatly down-regulated (from -5 to -15) indicating the absence of apoptosis as previously showed with caspase-3 detection.

The second important trend showed by the array analysis was the upregulation of several apoptosis-inhibiting factors by BNIPDaCHM specifically against SW620. BNIPDaCHM appeared to have a greater impact on the regulation of the apoptosis-related proteins analysed which suggested that BNIPDaCHM had more impact on the cell death machinery of metastatic CRC.

Interestingly, the simultaneous regulation of pro- and anti- apoptosis factors also indicated that a complex cell death pathway regulation is taking place which could involve crosstalk between the apoptotic and autophagic modes of cell death. Additionally, an increasing number of studies showed the existence of alternative caspase-independent forms of programmed cell death which could potentially be occurring here. Therefore, the results presented related to the investigation of apoptosis as BNIP-induced mode cell death revealed the existence of a complex regulation potentially involving several pathways. These findings suggest that the mode of cell death induced by BNIPPiProp, BNIPPiEth and BNIPDaCHM remains undetermined and more specific studies exploring autophagy or necroptosis pathways are necessary.

4.2. Conclusion

In this study, a solid lipid nanoparticle drug delivery system has been formulated to overcome the current limitations of BNIP derivatives for their delivery in CRC cells. Stearic acid-solid lipid nanoparticles were manufactured and the encapsulation of BNIPPiProp was performed (>1% drug loading). The development of the BNIP nanotherapeutics was hindered by the cytotoxicity of the empty nanocarrier against SW480 and SW620 cell lines. The cytotoxicity study revealed that the native 3 drugs BNIPPiProp, BNIPDaCHM and BNIPPiEth were strongly cytotoxic against both CRC cell lines after 24 hours (IC_{50} 0.75 - 2.60 µM). From there, the mechanism of action of BNIP derivatives was further elucidated. After a 24 hr-treatment, all 3 drugs showed an increase in ROS levels (>50%) and a significant creation of DNA double strand breaks assessed via COMET assay. The mode of cell death was also investigated. For the first time, image cytometry was used to screen the 3 compounds for apoptotic cell death. A more robust apoptotic cell death detection was then performed using a caspase-3 detection kit, however, no significant changes after treatment were noticed. Nevertheless, the proteome profiler array showed the upregulation and down regulation of a total of 16 different apoptotic-related proteins. BNIP derivatives appeared to regulate apoptotic factors in a cell line- and drug-dependant manner and suggests the existence of crosstalk between cell death pathways. Taken together, these findings showed the clinical relevance of BNIPPiProp, BNIPPiEth and BNIPDaCHM in the treatment of CRC. This study has improved the understanding of the BNIP mechanism of action against CRC which will help to design novel anti-cancer drugs and associated tailored drug delivery systems for the development of the next generation of CRC treatment.

References

This bibliography was produced using the reference manager software Mendeley (Mendeley Ltd, Elsevier, USA) using the Harvard style of referencing automatically performed from the software's library.

Acharya, S., & Sahoo, S. K. (2011). PLGA nanoparticles containing various anticancer agents and tumour delivery by EPR effect. In *Advanced Drug Delivery Reviews* (Vol. 63, Issue 3, pp. 170–183). Adv Drug Deliv Rev. https://doi.org/10.1016/j.addr.2010.10.008

Aditya, N. P., Macedo, A. S., Doktorovova, S., Souto, E. B., Kim, S., Chang, P. S., & Ko, S. (2014). Development and evaluation of lipid nanocarriers for quercetin delivery: A comparative study of solid lipid nanoparticles (SLN), nanostructured lipid carriers (NLC), and lipid nanoemulsions (LNE). *LWT - Food Science and Technology*, *59*(1), 115–121. https://doi.org/10.1016/j.lwt.2014.04.058

Alami, N., Paterson, J., Belanger, S., Juste, S., Grieshaber, C. K., & Leyland-Jones, B. (2007). Comparative analysis of xanafide cytotoxicity in breast cancer cell lines. *British Journal of Cancer*, *97*(1), 58–64. https://doi.org/10.1038/sj.bjc.6603829

Aleksandrowicz, R., Taciak, B., & Krol, M. (2017). Drug delivery systems improving chemical and physical properties of anticancer drugs currently investigated for treatment of solid tumors. In *Journal of Physiology and Pharmacology* (Vol. 68, Issue 2, pp. 165–174). Polish Physiological Society. https://europepmc.org/article/med/28614765

Alexandre, J., Batteux, F., Nicco, C., Chéreau, C., Laurent, A., Guillevin, L., Weill, B., & Goldwasser, F. (2006). Accumulation of hydrogen peroxide is an early and crucial step for paclitaxel-induced cancer cell death both in vitro and in vivo. *International Journal of Cancer*, *119*(1), 41–48. https://doi.org/10.1002/ijc.21685

Alexandre, J., Nicco, C., Chéreau, C., Laurent, A., Weill, B., Goldwasser, F., & Batteux, F. (2006). Improvement of the therapeutic index of anticancer drugs by the superoxide dismutase mimic mangafodipir. *Journal of the*

National Cancer Institute, *98*(4), 236–244. https://doi.org/10.1093/jnci/djj049

Amado, R. G., Wolf, M., Peeters, M., Van Cutsem, E., Siena, S., Freeman, D. J., Juan, T., Sikorski, R., Suggs, S., Radinsky, R., Patterson, S. D., & Chang, D. D. (2008). Wild-type KRAS is required for panitumumab efficacy in patients with metastatic colorectal cancer. *Journal of Clinical Oncology*, *26*(10), 1626–1634. https://doi.org/10.1200/JCO.2007.14.7116

Ashktorab, H., & Brim, H. (2014). DNA Methylation and Colorectal Cancer. In *Current Colorectal Cancer Reports* (Vol. 10, Issue 4, pp. 425–430). Current Medicine Group LLC 1. https://doi.org/10.1007/s11888-014-0245-2

Aydinlik, S., Erkisa, M., Cevatemre, B., Sarimahmut, M., Dere, E., Ari, F., & Ulukaya, E. (2017). Enhanced cytotoxic activity of doxorubicin through the inhibition of autophagy in triple negative breast cancer cell line. *Biochimica et Biophysica Acta - General Subjects*, *1861*(2), 49–57. https://doi.org/10.1016/j.bbagen.2016.11.013

Baban, D. F., & Seymour, L. W. (1998). Control of tumour vascular permeability. In *Advanced Drug Delivery Reviews* (Vol. 34, Issue 1, pp. 109–119). Elsevier Sci B.V. https://doi.org/10.1016/S0169-409X(98)00003-9

Bae, K. H., Chung, H. J., & Park, T. G. (2011). Nanomaterials for cancer therapy and imaging. In *Molecules and Cells* (Vol. 31, Issue 4, pp. 295–302). Mol Cells. https://doi.org/10.1007/s10059-011-0051-5

Baig, S., Seevasant, I., Mohamad, J., Mukheem, A., Huri, H. Z., & Kamarul, T. (2016). Potential of apoptotic pathway-targeted cancer therapeutic research: Where do we stand. In *Cell Death and Disease* (Vol. 7, Issue 1, p. e2058). Nature Publishing Group. https://doi.org/10.1038/cddis.2015.275

Bangham, A. D. (1993). Liposomes: the Babraham connection. *Chemistry and Physics of Lipids*, *64*(1–3), 275–285. https://doi.org/10.1016/0009-3084(93)90071-A

Bardaweel, S. K., Gul, M., Alzweiri, M., Ishaqat, A., Alsalamat, H. A., & Bashatwah, R. M. (2018). Reactive oxygen species: The dual role in physiological and pathological conditions of the human body. In *Eurasian Journal of Medicine* (Vol. 50, Issue 3, pp. 193–201). AVES İbrahim KARA. https://doi.org/10.5152/eurasianjmed.2018.17397

Barenholz, Y. (2012). Doxil® - The first FDA-approved nano-drug: Lessons learned. In *Journal of Controlled Release* (Vol. 160, Issue 2, pp. 117–134). Elsevier. https://doi.org/10.1016/j.jconrel.2012.03.020

Barret, M., Boustiere, C., Canard, J. M., Arpurt, J. P., Bernardini, D., Bulois, P., Chaussade, S., Heresbach, D., Joly, I., Lapuelle, J., Laugier, R., Lesur, G., Pienkowski, P., Ponchon, T., Pujol, B., Richard-Molard, B., Robaszkiewicz, M., Systchenko, R., Abbas, F., … Cellier, C. (2013). Factors Associated with Adenoma Detection Rate and Diagnosis of Polyps and Colorectal Cancer during Colonoscopy in France: Results of a Prospective, Nationwide Survey. *PLoS ONE*, *8*(7). https://doi.org/10.1371/journal.pone.0068947

Barron, G. A., Bermano, G., Gordon, A., & Kong Thoo Lin, P. (2010). Synthesis, cytotoxicity and DNA-binding of novel bisnaphthalimidopropyl derivatives in breast cancer MDA-MB-231 cells. *European Journal of Medicinal Chemistry*, *45*(4), 1430–1437. https://doi.org/10.1016/j.ejmech.2009.12.047

Barron, G. A., Goua, M., Kuraoka, I., Bermano, G., Iwai, S., & Kong Thoo Lin, P. (2015). Bisnaphthalimidopropyl diaminodicyclohexylmethane induces DNA damage and repair instability in triple negative breast cancer cells via p21 expression. *Chemico-Biological Interactions*, *242*, 307–315. https://doi.org/10.1016/j.cbi.2015.10.017

Baud, V., & Karin, M. (2001). Signal transduction by tumor necrosis factor and its relatives. In *Trends in Cell Biology* (Vol. 11, Issue 9, pp. 372–377). Trends Cell Biol. https://doi.org/10.1016/S0962-8924(01)02064-5

Begum, A., Jones, M., Lim, G., … T. M.-… of P. and, & 2008, undefined. (n.d.). Curcumin structure-function, bioavailability, and efficacy in models of neuroinflammation and Alzheimer's disease. *ASPET*. Retrieved September 25, 2020, from http://jpet.aspetjournals.org/content/326/1/196.short?casa_token=sUZwu

3ceG5cAAAAA:1TAzx7szg2k77wbJ2hggjTu42a70LAyFXJAIt1KXdq0Pervr3ZY
IShD3IHQLVwLgeiGcYioy_g

Benhusein, G. M., Mutch, E., Aburawi, S., & Williams, F. M. (2010). Genotoxic effect induced by hydrogen peroxide in human hepatoma cells using comet assay. *Libyan Journal of Medicine*, *5*(1), 1–6. https://doi.org/10.3402/ljm.v5i0.4637

Bernstein, C., R., A., Nfonsam, V., & Bernstei, H. (2013). DNA Damage, DNA Repair and Cancer. In *New Research Directions in DNA Repair*. InTech. https://doi.org/10.5772/53919

Bhatt, R., De Vries, P., Tulinsky, J., Bellamy, G., Baker, B., Singer, J. W., & Klein, P. (2003). Synthesis and in vivo antitumor activity of poly(L-glutamic acid) conjugates of 20(S)-camptothecin. *Journal of Medicinal Chemistry*, *46*(1), 190–193. https://doi.org/10.1021/jm020022r

Blanco, E., Shen, H., & Ferrari, M. (2015). Principles of nanoparticle design for overcoming biological barriers to drug delivery. In *Nature Biotechnology* (Vol. 33, Issue 9, pp. 941–951). Nature Publishing Group. https://doi.org/10.1038/nbt.3330

Bobo, D., Robinson, K. J., Islam, J., Thurecht, K. J., & Corrie, S. R. (2016). Nanoparticle-Based Medicines: A Review of FDA-Approved Materials and Clinical Trials to Date. In *Pharmaceutical Research* (Vol. 33, Issue 10, pp. 2373–2387). Springer New York LLC. https://doi.org/10.1007/s11095-016-1958-5

Borges, H. L., Linden, R., & Wang, J. Y. J. (2008). DNA damage-induced cell death: Lessons from the central nervous system. *Cell Research*, *18*(1), 17–26. https://doi.org/10.1038/cr.2007.110

Boudreau, M. W., Peh, J., & Hergenrother, P. J. (2019). Procaspase-3 Overexpression in Cancer: A Paradoxical Observation with Therapeutic Potential. In *ACS Chemical Biology* (Vol. 14, Issue 11, pp. 2335–2348). American Chemical Society. https://doi.org/10.1021/acschembio.9b00338

Bragado, P., Armesilla, A., Silva, A., & Porras, A. (2007). Apoptosis by cisplatin requires p53 mediated p38α MAPK activation through ROS generation. *Apoptosis*, *12*(9), 1733–1742. https://doi.org/10.1007/s10495-007-0082-8

Brana, M. F., Castellano, J. M., Moran, M., Perez de Vega, M. J., Romerdahl, C. R., Qian, X. D., Bousquet, P., Emling, F., Schlick, E., & Keilhauer, G. (1993). Bis-naphthalimides: A new class of antitumor agents. *Anti-Cancer Drug Design*, *8*(4), 257–268. https://europepmc.org/article/med/8240655

Braña, M. F., & Ramos, A. (2001). Naphthalimides as anti-cancer agents: synthesis and biological activity. In *Current medicinal chemistry. Anti-cancer agents* (Vol. 1, Issue 3, pp. 237–255). Curr Med Chem Anticancer Agents. https://doi.org/10.2174/1568011013354624

Braña, Miguel F., Cacho, M., Ramos, A., Domínguez, M. T., Pozuelo, J. M., Abradelo, C., Rey-Stolle, M. F., Yuste, M., Carrasco, C., & Bailly, C. (2003). Synthesis, biological evaluation and DNA binding properties of novel mono and bisnaphthalimides. *Organic and Biomolecular Chemistry*, *1*(4), 648–654. https://doi.org/10.1039/b209042b

Braña, Miguel F., Gradillas, A., Ovalles, A. G., López, B., Acero, N., Llinares, F., & Mingarro, D. M. (2006). Synthesis and biological activity of N,N-dialkylaminoalkyl-substituted bisindolyl and diphenyl pyrazolone derivatives. *Bioorganic & Medicinal Chemistry*, *14*(1), 9–16. https://doi.org/10.1016/j.bmc.2005.09.059

Brody, H. (2015). Colorectal cancer. In *Nature* (Vol. 521, Issue 7551, p. S1). Nature Publishing Group. https://doi.org/10.1038/521S1a

Brown, J. M., & Attardi, L. D. (2005). The role of apoptosis in cancer development and treatment response. *Nature Reviews Cancer*, *5*(3), 231–237. https://doi.org/10.1038/nrc1560

Campos, J. R., Severino, P., Santini, A., Silva, A. M., Shegokar, R., Souto, S. B., & Souto, E. B. (2020). Solid lipid nanoparticles (SLN). In *Nanopharmaceuticals* (pp. 1–15). Elsevier. https://doi.org/10.1016/b978-0-12-817778-5.00001-4

Cancer Genome Atlas Network, T. (2012). Comprehensive molecular characterization of human colon and rectal cancer. *Nature*, *487*(7407), 330–337. https://doi.org/10.1038/nature11252

Castaneda, S. A., & Strasser, J. (2017). Updates in the Treatment of Breast Cancer with Radiotherapy. In *Surgical Oncology Clinics of North America* (Vol. 26, Issue 3, pp. 371–382). W.B. Saunders. https://doi.org/10.1016/j.soc.2017.01.013

Chatterjee, N., & Walker, G. C. (2017). Mechanisms of DNA damage, repair, and mutagenesis. In *Environmental and Molecular Mutagenesis* (Vol. 58, Issue 5, pp. 235–263). John Wiley and Sons Inc. https://doi.org/10.1002/em.22087

Chen, A. Y., Yu, C., Gatto, B., & Liu, L. F. (1993). DNA minor groove-binding ligands: A different class of mammalian DNA topoisomerase I inhibitors. *Proceedings of the National Academy of Sciences of the United States of America*, *90*(17), 8131–8135. https://doi.org/10.1073/pnas.90.17.8131

Chen, Y., Liu, J. M., Xiong, X. X., Qiu, X. Y., Pan, F., Liu, D., Lan, S. J., Jin, S., Yu, S. Bin, & Chen, X. Q. (2015). Piperlongumine selectively kills hepatocellular carcinoma cells and preferentially inhibits their invasion via ROS-ER-MAPKs-CHOP. *Oncotarget*, *6*(8), 6406–6421. https://doi.org/10.18632/oncotarget.3444

Cheng, Z., Al Zaki, A., Hui, J. Z., Muzykantov, V. R., & Tsourkas, A. (2012). Multifunctional nanoparticles: Cost versus benefit of adding targeting and imaging capabilities. In *Science* (Vol. 338, Issue 6109, pp. 903–910). American Association for the Advancement of Science. https://doi.org/10.1126/science.1226338

Chertok, B., Moffat, B. A., David, A. E., Yu, F., Bergemann, C., Ross, B. D., & Yang, V. C. (2008). Iron oxide nanoparticles as a drug delivery vehicle for MRI monitored magnetic targeting of brain tumors. *Biomaterials*, *29*(4), 487–496. https://doi.org/10.1016/j.biomaterials.2007.08.050

Cheung-Ong, K., Giaever, G., & Nislow, C. (2013). DNA-damaging agents in cancer chemotherapy: Serendipity and chemical biology. In *Chemistry and Biology* (Vol. 20, Issue 5, pp. 648–659). Elsevier.

https://doi.org/10.1016/j.chembiol.2013.04.007

Cho, K., Wang, X., Nie, S., Chen, Z., & Shin, D. M. (2008). Therapeutic nanoparticles for drug delivery in cancer. In *Clinical Cancer Research* (Vol. 14, Issue 5, pp. 1310–1316). Clin Cancer Res. https://doi.org/10.1158/1078-0432.CCR-07-1441

Choi, C. H. J., Alabi, C. A., Webster, P., & Davis, M. E. (2010). Mechanism of active targeting in solid tumors with transferrin-containing gold nanoparticles. *Proceedings of the National Academy of Sciences of the United States of America*, *107*(3), 1235–1240. https://doi.org/10.1073/pnas.0914140107

Cisterna, B. A., Kamaly, N., Choi, W. Il, Tavakkoli, A., Farokhzad, O. C., & Vilos, C. (2016). Targeted nanoparticles for colorectal cancer. In *Nanomedicine* (Vol. 11, Issue 18, pp. 2443–2456). Future Medicine Ltd. https://doi.org/10.2217/nnm-2016-0194

Colorectal cancer facts. (2005). *The Journal of the Kentucky Medical Association*, *103*(3), 118.

Conklin, K. A. (2004). Chemotherapy-associated oxidative stress: Impact on chemotherapeutic effectiveness. In *Integrative Cancer Therapies* (Vol. 3, Issue 4, pp. 294–300). Integr Cancer Ther. https://doi.org/10.1177/1534735404270335

Cooke, M. S., Evans, M. D., Dizdaroglu, M., & Lunec, J. (2003). Oxidative DNA damage: mechanisms, mutation, and disease. *The FASEB Journal*, *17*(10), 1195–1214. https://doi.org/10.1096/fj.02-0752rev

Corrias, F., & Lai, F. (2011). New Methods for Lipid Nanoparticles Preparation. *Recent Patents on Drug Delivery & Formulation*, *5*(3), 201–213. https://doi.org/10.2174/187221111797200597

Costa Lima, S., Rodrigues, V., Garrido, J., Borges, F., Kong Thoo Lin, P., & Cordeiro Da Silva, A. (2012). *In vitro* evaluation of bisnaphthalimidopropyl derivatives loaded into pegylated nanoparticles against Leishmania infantum protozoa. *International Journal of Antimicrobial Agents*, *39*(5), 424–430. https://doi.org/10.1016/j.ijantimicag.2012.01.003

Coussens, L. M., & Werb, Z. (2002). Inflammation and cancer. In *Nature* (Vol. 420, Issue 6917, pp. 860–867). Nature. https://doi.org/10.1038/nature01322

Cunningham, D., Atkin, W., Lenz, H. J., Lynch, H. T., Minsky, B., Nordlinger, B., & Starling, N. (2010). Colorectal cancer. In *The Lancet* (Vol. 375, Issue 9719, pp. 1030–1047). Elsevier. https://doi.org/10.1016/S0140-6736(10)60353-4

Curtin, N. J. (2012). DNA repair dysregulation from cancer driver to therapeutic target. *Nature Reviews Cancer*, *12*(12), 801–817. https://doi.org/10.1038/nrc3399

D'Arcy, M. S. (2019). Cell death: a review of the major forms of apoptosis, necrosis and autophagy. In *Cell Biology International* (Vol. 43, Issue 6, pp. 582–592). Wiley-Blackwell Publishing Ltd. https://doi.org/10.1002/cbin.11137

Dahlgren, C., & Karlsson, A. (1999). Respiratory burst in human neutrophils. *Journal of Immunological Methods*, *232*(1–2), 3–14. https://doi.org/10.1016/S0022-1759(99)00146-5

Danaei, M., Dehghankhold, M., Ataei, S., Hasanzadeh Davarani, F., Javanmard, R., Dokhani, A., Khorasani, S., & Mozafari, M. R. (2018). Impact of particle size and polydispersity index on the clinical applications of lipidic nanocarrier systems. In *Pharmaceutics* (Vol. 10, Issue 2). MDPI AG. https://doi.org/10.3390/pharmaceutics10020057

Das, S., & Chaudhury, A. (2011). Recent advances in lipid nanoparticle formulations with solid matrix for oral drug delivery. In *AAPS PharmSciTech* (Vol. 12, Issue 1, pp. 62–76). Springer. https://doi.org/10.1208/s12249-010-9563-0

de Mello, R. A., Marques, A. M., & Araújo, A. (2013). Epidermal growth factor receptor and metastatic colorectal cancer: Insights into target therapies. In *World Journal of Gastroenterology* (Vol. 19, Issue 38, pp. 6315–6318). Baishideng Publishing Group Inc. https://doi.org/10.3748/wjg.v19.i38.6315

Díaz-Rubio, E., Tabernero, J., Gómez-España, A., Massutí, B., Sastre, J., Chaves, M., Abad, A., Carrato, A., Queralt, B., Reina, J. J., Maurel, J., González-Flores, E., Aparicio, J., Rivera, F., Losa, F., & Aranda, E. (2007). Phase III study of capecitabine plus oxaliplatin compared with continuous-infusion fluorouracil plus oxaliplatin as first-line therapy in metastatic colorectal cancer: Final report of the Spanish Cooperative Group for the treatment of digestive tumors trial. *Journal of Clinical Oncology*, *25*(27), 4224–4230. https://doi.org/10.1200/JCO.2006.09.8467

Dragovich, T., Gordon, M., Mendelson, D., Wong, L., Modiano, M., Chow, H. H. S., Samulitis, B., O'Day, S., Grenier, K., Hersh, E., & Dorr, R. (2007). Phase I trial of imexon in patients with advanced malignancy. *Journal of Clinical Oncology*, *25*(13), 1779–1784. https://doi.org/10.1200/JCO.2006.08.9672

Elmore, S. (2007). Apoptosis: A Review of Programmed Cell Death. In *Toxicologic Pathology* (Vol. 35, Issue 4, pp. 495–516). NIH Public Access. https://doi.org/10.1080/01926230701320337

Errol, C. F., Graham, C. W., Wolfram, S., Richard, D. W., Roger, A. S., & Tom, E. (2006). DNA Repair and Mutagenesis, Second Edition. In *DNA Repair and Mutagenesis, Second Edition*. American Society of Microbiology. https://doi.org/10.1128/9781555816704

Fairbairn, D. W., Olive, P. L., & O'Neill, K. L. (1995). The comet assay: a comprehensive review. *Mutation Research/Reviews in Genetic Toxicology*, *339*(1), 37–59. https://doi.org/10.1016/0165-1110(94)00013-3

Falchook, G. S., & Kurzrock, R. (2015). VEGF and dual-EGFR inhibition in colorectal cancer. In *Cell Cycle* (Vol. 14, Issue 8, pp. 1129–1130). Taylor and Francis Inc. https://doi.org/10.1080/15384101.2015.1022071

Fang, Y. P., Wu, P. C., Huang, Y. Bin, Tzeng, C. C., Chen, Y. L., Hung, Y. H., Tsai, M. J., & Tsai, Y. H. (2012). Modification of polyethylene glycol onto solid lipid nanoparticles encapsulating a novel chemotherapeutic agent (PK-L4) to enhance solubility for injection delivery. *International Journal of Nanomedicine*, *7*, 4995–5005. https://doi.org/10.2147/IJN.S34301

Farboud, E. S., Nasrollahi, S. A., & Tabbakhi, Z. (2011). Novel formulation and evaluation of a Q10-loaded solid lipid nanoparticle cream: in vitro and in vivo studies. *International Journal of Nanomedicine*, *6*, 611–617. https://doi.org/10.2147/ijn.s16815

Fearon, E. R. (2011). Molecular genetics of colorectal cancer. *Annual Review of Pathology: Mechanisms of Disease*, *6*, 479–507. https://doi.org/10.1146/annurev-pathol-011110-130235

Ferrari, M. (2010). Frontiers in cancer nanomedicine: Directing mass transport through biological barriers. *Trends in Biotechnology*, *28*(4), 181–188. https://doi.org/10.1016/j.tibtech.2009.12.007

Fridman, J. S., & Lowe, S. W. (2003). Control of apoptosis by p53. In *Oncogene* (Vol. 22, Issue 56 REV. ISS. 8, pp. 9030–9040). Nature Publishing Group. https://doi.org/10.1038/sj.onc.1207116

Fulda, S., & Debatin, K. M. (2006). Extrinsic versus intrinsic apoptosis pathways in anticancer chemotherapy. In *Oncogene* (Vol. 25, Issue 34, pp. 4798–4811). Nature Publishing Group. https://doi.org/10.1038/sj.onc.1209608

Gibellini, L., Pinti, M., Nasi, M., de Biasi, S., Roat, E., Bertoncelli, L., & Cossarizza, A. (2010). Interfering with ROS metabolism in cancer cells: The potential role of quercetin. In *Cancers* (Vol. 2, Issue 2, pp. 1288–1311). Cancers (Basel). https://doi.org/10.3390/cancers2021288

Goldar, S., Khaniani, M. S., Derakhshan, S. M., & Baradaran, B. (2015). Molecular mechanisms of apoptosis and roles in cancer development and treatment. In *Asian Pacific Journal of Cancer Prevention* (Vol. 16, Issue 6, pp. 2129–2144). Asian Pacific Organization for Cancer Prevention. https://doi.org/10.7314/APJCP.2015.16.6.2129

Golombek, S. K., May, J. N., Theek, B., Appold, L., Drude, N., Kiessling, F., & Lammers, T. (2018). Tumor targeting via EPR: Strategies to enhance patient responses. In *Advanced Drug Delivery Reviews* (Vol. 130, pp. 17–38). Elsevier B.V. https://doi.org/10.1016/j.addr.2018.07.007

Gonzalez-Mira, E., Egea, M., … M. G.-C. and S. B., & 2010, undefined. (n.d.). Design and ocular tolerance of flurbiprofen loaded ultrasound-engineered NLC. *Elsevier*. Retrieved September 26, 2020, from https://www.sciencedirect.com/science/article/pii/S0927776510004091?casa_token=_miJMhl8rw8AAAAA:pi86EVdI5zJ5SJFyg40THgeyBuPWyiGaPQLqzNhBaP_gPdtZ3p879PlfqF5TAnyUDt1Tay2y

Grady, W. M., & Carethers, J. M. (2008). Genomic and Epigenetic Instability in Colorectal Cancer Pathogenesis. In *Gastroenterology* (Vol. 135, Issue 4, pp. 1079–1099). W.B. Saunders. https://doi.org/10.1053/j.gastro.2008.07.076

Graf, N., Bielenberg, D. R., Kolishetti, N., Muus, C., Banyard, J., Farokhzad, O. C., & Lippard, S. J. (2012). αvβ 3 integrin-targeted PLGA-PEG nanoparticles for enhanced anti-tumor efficacy of a Pt(IV) prodrug. *ACS Nano*, *6*(5), 4530–4539. https://doi.org/10.1021/nn301148e

Grigoriev, M. Y., Pozharissky, K. M., Hanson, K. P., Imyanitov, E. N., & Zhivotovsky, B. (n.d.). Cell Cycle Expression of Caspase-3 and-7 Does Not Correlate with the Extent of Apoptosis in Primary Breast Carcinomas. *Cell Cycle*, *1*(5), 337–342. https://doi.org/10.4161/cc.1.5.152

Guo, Yu, Xiong, B. H., Zhang, T., Cheng, Y., & Ma, L. (2016). XELOX vs. FOLFOX in metastatic colorectal cancer: An updated meta-analysis. *Cancer Investigation*, *34*(2), 94–104. https://doi.org/10.3109/07357907.2015.1104689

Guo, Yuqing, & Hui, S. W. (1997). Poly(ethylene glycol)-conjugated surfactants promote or inhibit aggregation of phospholipids. *Biochimica et Biophysica Acta - Biomembranes*, *1323*(2), 185–194. https://doi.org/10.1016/S0005-2736(96)00190-3

Gupta, A., Harrison, P. J., Wieslander, H., Pielawski, N., Kartasalo, K., Partel, G., Solorzano, L., Suveer, A., Klemm, A. H., Spjuth, O., Sintorn, I., & Wählby, C. (2019). Deep Learning in Image Cytometry: A Review. *Cytometry Part A*, *95*(4), 366–380. https://doi.org/10.1002/cyto.a.23701

Haggar, F., & Boushey, R. (2009). Colorectal Cancer Epidemiology: Incidence, Mortality, Survival, and Risk Factors. *Clinics in Colon and Rectal Surgery*, *22*(04), 191–197. https://doi.org/10.1055/s-0029-1242458

Hall, E. J. (1973). Radiobiology of heavy particle radiation therapy: cellular studies. *Radiology*, *108*(1), 119–129. https://doi.org/10.1148/108.1.119

Hansen, M. B., Nielsen, S. E., & Berg, K. (1989). Re-examination and further development of a precise and rapid dye method for measuring cell growth/cell kill. *Journal of Immunological Methods*, *119*(2), 203–210. https://doi.org/10.1016/0022-1759(89)90397-9

Hassan, M., Watari, H., Abualmaaty, A., Ohba, Y., & Sakuragi, N. (2014). Apoptosis and molecular targeting therapy in cancer. In *BioMed Research International* (Vol. 2014). Hindawi Publishing Corporation. https://doi.org/10.1155/2014/150845

Havrilesky, L. J., Reiner, M., Morrow, P. K., Watson, H., & Crawford, J. (2015). A review of relative dose intensity and survival in patients with metastatic solid tumors. In *Critical Reviews in Oncology/Hematology* (Vol. 93, Issue 3, pp. 203–210). Elsevier Ireland Ltd. https://doi.org/10.1016/j.critrevonc.2014.10.006

Heidelberger, C., Chaudhuri, N. K., Danneberg, P., Mooren, D., Griesbach, L., Duschinsky, R., Schnitzer, R. J., Pleven, E., & Scheiner, J. (1957). Fluorinated pyrimidines, a new class of tumour-inhibitory compounds. *Nature*, *179*(4561), 663–666. https://doi.org/10.1038/179663a0

Hoeijmakers, J. H. J. (2009). DNA damage, aging, and cancer. In *New England Journal of Medicine* (Vol. 361, Issue 15, pp. 1475–1485). Massachussetts Medical Society. https://doi.org/10.1056/NEJMra0804615

Hohenberger, W., Weber, K., Matzel, K., Papadopoulos, T., & Merkel, S. (2009). Standardized surgery for colonic cancer: Complete mesocolic excision and central ligation - Technical notes and outcome. *Colorectal Disease*, *11*(4), 354–364. https://doi.org/10.1111/j.1463-1318.2008.01735.x

Hoskins C, Ouaissi M, Lima SC, Cheng WP, Loureirio I, Mas E, Lombardo D, Cordeiro-da-Silva A, Ouaissi A, Kong Thoo Lin P. (2010). In vitro and in vivo anticancer activity of a novel nano-sized formulation based on self-assembling polymers against pancreatic cancer. Pharmaceutical Research, 27(12), 2694–2703. https://doi.org/10.1007/s11095-010-0268-6

Hu, L., Chen, M., Chen, X., Zhao, C., Fang, Z., Wang, H., & Dai, H. (2020). Chemotherapy-induced pyroptosis is mediated by BAK/BAX-caspase-3-GSDME pathway and inhibited by 2-bromopalmitate. *Cell Death and Disease*, *11*(4), 1–17. https://doi.org/10.1038/s41419-020-2476-2

Hu, X., Wang, Y., & Peng, B. (2014). Chitosan-Capped Mesoporous Silica Nanoparticles as pH-Responsive Nanocarriers for Controlled Drug Release. *Chemistry - An Asian Journal*, *9*(1), 319–327. https://doi.org/10.1002/asia.201301105

Huang, C. Y., Ju, D. T., Chang, C. F., Muralidhar Reddy, P., & Velmurugan, B. K. (2017). A review on the effects of current chemotherapy drugs and natural agents in treating non-small cell lung cancer. In *BioMedicine (France)* (Vol. 7, Issue 4, pp. 12–23). EDP Sciences. https://doi.org/10.1051/bmdcn/2017070423

Huang, Y., & Sadée, W. (2006). Membrane transporters and channels in chemoresistance and -sensitivity of tumor cells. In *Cancer Letters* (Vol. 239, Issue 2, pp. 168–182). Cancer Lett. https://doi.org/10.1016/j.canlet.2005.07.032

Hupp, T. R., Sparks, A., & Lane, D. P. (1995). Small peptides activate the latent sequence-specific DNA binding function of p53. *Cell*, *83*(2), 237–245. https://doi.org/10.1016/0092-8674(95)90165-5

Ionov, Y., Peinado, M. A., Malkhosyan, S., Shibata, D., & Perucho, M. (1993). Ubiquitous somatic mutations in simple repeated sequences reveal a new mechanism for colonic carcinogenesis. *Nature*, *363*(6429), 558–561. https://doi.org/10.1038/363558a0

Jiang, M., & Milner, J. (2003). Bcl-2 constitutively suppresses p53-dependent apoptosis in colorectal cancer cells. *Genes and Development*, *17*(7), 832–837. https://doi.org/10.1101/gad.252603

Jiang, Z., Zheng, X., & Rich, K. M. (2003). Down-regulation of Bcl-2 and Bcl-xL expression with bispecific antisense treatment in glioblastoma cell lines induce cell death. *Journal of Neurochemistry*, *84*(2), 273–281. https://doi.org/10.1046/j.1471-4159.2003.01522.x

Jonker, D. J., O'Callaghan, C. J., Karapetis, C. S., Zalcberg, J. R., Tu, D., Au, H.-J., Berry, S. R., Krahn, M., Price, T., Simes, R. J., Tebbutt, N. C., van Hazel, G., Wierzbicki, R., Langer, C., & Moore, M. J. (2007). Cetuximab for the Treatment of Colorectal Cancer. *New England Journal of Medicine*, *357*(20), 2040–2048. https://doi.org/10.1056/NEJMoa071834

Joshi, A. D., Botham, R. C., Schlein, L. J., Roth, H. S., Mangraviti, A., Borodovsky, A., Tyler, B., Joslyn, S., Looper, J. S., Podell, M., Fan, T. M., Hergenrother, P. J., & Riggins, G. J. (2017). Synergistic and targeted therapy with a procaspase-3 activator and temozolomide extends survival in glioma rodent models and is feasible for the treatment of canine malignant glioma patients. *Oncotarget*, *8*(46), 80124–80138. https://doi.org/10.18632/oncotarget.19085

Julien, O., & Wells, J. A. (2017). Caspases and their substrates. In *Cell Death and Differentiation* (Vol. 24, Issue 8, pp. 1380–1389). Nature Publishing Group. https://doi.org/10.1038/cdd.2017.44

Kamal, A., Bolla, N. R., Srikanth, P. S., & Srivastava, A. K. (2013). Naphthalimide derivatives with therapeutic characteristics: a patent review. *Expert Opinion on Therapeutic Patents*, *23*(3), 299–317. https://doi.org/10.1517/13543776.2013.746313

Kang, N., Jian, J., Cao, S., Zhang, Q., Mao, Y., Huang, Y., Peng, Y., Qiu, F., & Gao, X. (2016). Physalin A induces G2/M phase cell cycle arrest in human non-small cell lung cancer cells: involvement of the p38 MAPK/ROS pathway. *Molecular and Cellular Biochemistry*, *415*(1–2), 145–155. https://doi.org/10.1007/s11010-016-2686-1

Karp's Cell and Molecular Biology: Concepts and Experiments, 8th Edition | Wiley. (n.d.). Retrieved September 26, 2020, from https://www.wiley.com/en-us/Karp%27s+Cell+and+Molecular+Biology%3A+Concepts+and+Experime

nts%2C+8th+Edition-p-9781118886144

Kasof, G. M., & Gomes, B. C. (2001). Livin, a Novel Inhibitor of Apoptosis Protein Family Member. *Journal of Biological Chemistry*, *276*(5), 3238–3246. https://doi.org/10.1074/jbc.M003670200

Kathe, N., Henriksen, B., & Chauhan, H. (2014). Physicochemical characterization techniques for solid lipid nanoparticles: Principles and limitations. *Drug Development and Industrial Pharmacy*, *40*(12), 1565–1575. https://doi.org/10.3109/03639045.2014.909840

Kim, S. J., Kim, H. S., & Seo, Y. R. (2019). Understanding of ROS-Inducing Strategy in Anticancer Therapy. In *Oxidative Medicine and Cellular Longevity* (Vol. 2019). Hindawi Limited. https://doi.org/10.1155/2019/5381692

Kim, T. Y., Kim, D. W., Chung, J. Y., Shin, S. G., Kim, S. C., Heo, D. S., Kim, N. K., & Bang, Y. J. (2004). Phase I and pharmacokinetic study of Genexol-PM, a Cremophor-free, polymeric micelle-formulated paclitaxel, in patients with advanced malignancies. *Clinical Cancer Research*, *10*(11), 3708–3716. https://doi.org/10.1158/1078-0432.CCR-03-0655

Kinzler, K. W., & Vogelstein, B. (1996). Lessons from hereditary colorectal cancer. In *Cell* (Vol. 87, Issue 2, pp. 159–170). Cell Press. https://doi.org/10.1016/S0092-8674(00)81333-1

Kopsida, M., Barron, G. A., Bermano, G., Kong Thoo Lin, P., & Goua, M. (2016). Novel bisnaphthalimidopropyl (BNIPs) derivatives as anticancer compounds targeting DNA in human breast cancer cells. *Organic and Biomolecular Chemistry*, *14*(41), 9780–9789. https://doi.org/10.1039/c6ob01850e

Korsmeyer, S. J. (1995). Regulators of cell death. In *Trends in Genetics* (Vol. 11, Issue 3, pp. 101–105). Elsevier Current Trends. https://doi.org/10.1016/S0168-9525(00)89010-1

Landfester, K. (2001). Polyreactions in miniemulsions. In *Macromolecular Rapid Communications* (Vol. 22, Issue 12, pp. 896–936). John Wiley & Sons, Ltd. https://doi.org/10.1002/1521-3927(20010801)22:12<896::AID-MARC896>3.0.CO;2-R

Laurent, S., Forge, D., Port, M., Roch, A., Robic, C., Vander Elst, L., & Muller, R. N. (2008). Magnetic iron oxide nanoparticles: Synthesis, stabilization, vectorization, physicochemical characterizations and biological applications. *Chemical Reviews*, *108*(6), 2064–2110. https://doi.org/10.1021/cr068445e

Leaf, A. N., Neuberg, D., Schwartz, E. L., Wadler, S., Ritch, P. S., Dutcher, J. P., & Adams, G. L. (1997). An ECOG phase II study of amonafide in unresectable or recurrent carcinoma of the head and neck (PB390). *Investigational New Drugs*, *15*(2), 165–172. https://doi.org/10.1023/A:1005823703909

Lee, M.-K., Lim, S.-J., & Kim, C.-K. (2007). Preparation, characterization and in vitro cytotoxicity of paclitaxel-loaded sterically stabilized solid lipid nanoparticles. *Biomaterials*, *28*(12), 2137–2146. https://doi.org/10.1016/j.biomaterials.2007.01.014

Leonardi, A., Bucolo, C., Romano, G. L., Platania, C. B. M., Drago, F., Puglisi, G., & Pignatello, R. (2014). Influence of different surfactants on the technological properties and in vivo ocular tolerability of lipid nanoparticles. *International Journal of Pharmaceutics*, *470*(1–2), 133–140. https://doi.org/10.1016/j.ijpharm.2014.04.061

Li, C., Cao, X. W., Zhao, J., & Wang, F. J. (2020). Effective Therapeutic Drug Delivery by GALA3, an Endosomal Escape Peptide with Reduced Hydrophobicity. *Journal of Membrane Biology*, *253*(2), 139–152. https://doi.org/10.1007/s00232-020-00109-2

Li, Y., Shao, J., Shen, K., Xu, Y., Liu, J., & Qian, X. (2012). E2F1-dependent pathways are involved in amonafide analogue 7-d-induced DNA damage, G2/M arrest, and apoptosis in p53-deficient K562 cells. *Journal of Cellular Biochemistry*, *113*(10), 3165–3177. https://doi.org/10.1002/jcb.24194

Liang, X., Wu, A., Xu, Y., Xu, K., Liu, J., & Qian, X. (2011). B1, a novel naphthalimide-based DNA intercalator, induces cell cycle arrest and apoptosis in HeLa cells via p53 activation. *Investigational New Drugs*, *29*(4), 646–658. https://doi.org/10.1007/s10637-010-9403-9

Liemburg-Apers, D. C., Willems, P. H. G. M., Koopman, W. J. H., & Grefte, S. (2015). Interactions between mitochondrial reactive oxygen species and

cellular glucose metabolism. In *Archives of Toxicology* (Vol. 89, Issue 8, pp. 1209–1226). Springer Verlag. https://doi.org/10.1007/s00204-015-1520-y

Lim, S.-J., & Kim, C.-K. (2002). Formulation parameters determining the physicochemical characteristics of solid lipid nanoparticles loaded with all-trans retinoic acid. *International Journal of Pharmaceutics*, *243*(1–2), 135–146. https://doi.org/10.1016/S0378-5173(02)00269-7

Lin, P. K. T., & Pavlov, V. A. (2000). The synthesis and in vitro cytotoxic studies of novel bis-naphthalimidopropyl polyamine derivatives. *Bioorganic & Medicinal Chemistry Letters*, *10*(14), 1609–1612. https://doi.org/10.1016/S0960-894X(00)00293-6

Lin, S., Li, Y., Zamyatnin, A. A., Werner, J., & Bazhin, A. V. (2018). Reactive oxygen species and colorectal cancer. *Journal of Cellular Physiology*, *233*(7), 5119–5132. https://doi.org/10.1002/jcp.26356

Lindahl, T., & Barnes, D. E. (2000). Repair of endogenous DNA damage. *Cold Spring Harbor Symposia on Quantitative Biology*, *65*, 127–133. https://doi.org/10.1101/sqb.2000.65.127

Liou, G. Y., & Storz, P. (2010). Reactive oxygen species in cancer. In *Free Radical Research* (Vol. 44, Issue 5, pp. 479–496). NIH Public Access. https://doi.org/10.3109/10715761003667554

Liu, Z., Guo, W., Zhang, D., Pang, Y., Shi, J., Wan, S., Cheng, K., Wang, J., & Cheng, S. (2016). Circulating tumor cell detection in hepatocellular carcinoma based on karyoplasmic ratios using imaging flow cytometry. *Scientific Reports*, *6*. https://doi.org/10.1038/srep39808

Lohman, A. C., Van Rijn, I., Lindhardt, C. L., Vonthein, R., Rades, D., & Holländer, N. H. (2018). Preliminary results from a prospective study comparing white blood cell and neutrophil counts from a laboratory to those measured with a new device in patients with breast cancer. *In Vivo*, *32*(5), 1283–1288. https://doi.org/10.21873/invivo.11378

Lopez, J., & Tait, S. W. G. (2015). Mitochondrial apoptosis: Killing cancer using

the enemy within. In *British Journal of Cancer* (Vol. 112, Issue 6, pp. 957–962). Nature Publishing Group. https://doi.org/10.1038/bjc.2015.85

MÃ¼ller, R. (2000). Solid lipid nanoparticles (SLN) for controlled drug delivery â€“ a review of the state of the art. *European Journal of Pharmaceutics and Biopharmaceutics*, *50*(1), 161–177. https://doi.org/10.1016/S0939-6411(00)00087-4

Maeda, H., Wu, J., Sawa, T., Matsumura, Y., & Hori, K. (2000). Tumor vascular permeability and the EPR effect in macromolecular therapeutics: a review. *Journal of Controlled Release*, *65*(1–2), 271–284. https://doi.org/10.1016/S0168-3659(99)00248-5

Malik, N., Evagorou, E. G., & Duncan, R. (1999). Dendrimer-platinate: A novel approach to cancer chemotherapy. *Anti-Cancer Drugs*, *10*(8), 767–776. https://doi.org/10.1097/00001813-199909000-00010

Marengo, E., Cavalli, R., Caputo, O., Rodriguez, L., & Gasco, M. R. (2000). Scale-up of the preparation process of solid lipid nanospheres. Part I. *International Journal of Pharmaceutics*, *205*(1–2), 3–13. https://doi.org/10.1016/S0378-5173(00)00471-3

Markowitz, S. D., & Bertagnolli, M. M. (2009). Molecular Basis of Colorectal Cancer. *New England Journal of Medicine*, *361*(25), 2449–2460. https://doi.org/10.1056/NEJMra0804588

Martinez, M. M., Reif, R. D., & Pappas, D. (2010). Detection of apoptosis: A review of conventional and novel techniques. In *Analytical Methods* (Vol. 2, Issue 8, pp. 996–1004). Royal Society of Chemistry. https://doi.org/10.1039/c0ay00247j

Marullo, R., Werner, E., Degtyareva, N., Moore, B., Altavilla, G., Ramalingam, S. S., & Doetsch, P. W. (2013). Cisplatin induces a mitochondrial-ros response that contributes to cytotoxicity depending on mitochondrial redox status and bioenergetic functions. *PLoS ONE*, *8*(11). https://doi.org/10.1371/journal.pone.0081162

Matsumura, Y., & Maeda, H. (1986). A New Concept for Macromolecular

Therapeutics in Cancer Chemotherapy: Mechanism of Tumoritropic Accumulation of Proteins and the Antitumor Agent Smancs. *Cancer Research*, *46*(12 Part 1).

McMillian, M. K., Li, L., Parker, J. B., Patel, L., Zhong, Z., Gunnett, J. W., Powers, W. J., & Johnson, M. D. (2002). An improved resazurin-based cytotoxicity assay for hepatic cells. *Cell Biology and Toxicology*, *18*(3), 157–173. https://doi.org/10.1023/A:1015559603643

Mehnert, W., & Mäder, K. (2001). *Solid Lipid Nanoparticles: Production, Characterization and Applications. Ad-vanced Drug Delivery Reviews, 47, 165-196*.

Melcher, R., Steinlein, C., Feichtinger, W., Müller, C. R., Menzel, T., Lührs, H., Scheppach, W., & Schmid, M. (2000). Spectral karyotyping of the human colon cancer cell lines SW480 and SW620. *Cytogenetics and Cell Genetics*, *88*(1–2), 145–152. https://doi.org/10.1159/000015508

Mishra, V., Bansal, K. K., Verma, A., Yadav, N., Thakur, S., Sudhakar, K., & Rosenholm, J. M. (2018). Solid lipid nanoparticles: Emerging colloidal nano drug delivery systems. In *Pharmaceutics* (Vol. 10, Issue 4). MDPI AG. https://doi.org/10.3390/pharmaceutics10040191

Mizutani, H., Tada-Oikawa, S., Hiraku, Y., Kojima, M., & Kawanishi, S. (2005). Mechanism of apoptosis induced by doxorubicin through the generation of hydrogen peroxide. *Life Sciences*, *76*(13), 1439–1453. https://doi.org/10.1016/j.lfs.2004.05.040

Moghimi, S. M., Hunter, A. C., & Murray, J. C. (2005). Nanomedicine: current status and future prospects. *The FASEB Journal*, *19*(3), 311–330. https://doi.org/10.1096/fj.04-2747rev

Moiel, D. (2011). Early Detection of Colon Cancer—The Kaiser Permanente Northwest 30-Year History: How Do We Measure Success? Is It the Test, the Number of Tests, the Stage, or the Percentage of Screen-Detected Patients. *The Permanente Journal*, *15*(4), 30. https://doi.org/10.7812/tpp/11-128

Monti, M., & Motta, S. (2007). Clinical management of cutaneous toxicity of

anti-EGFR agents. *International Journal of Biological Markers*, *22*(1 SUPPL. 4). https://doi.org/10.5301/jbm.2008.2035

Mosmann, T. (1983). Rapid colorimetric assay for cellular growth and survival: Application to proliferation and cytotoxicity assays. *Journal of Immunological Methods*, *65*(1–2), 55–63. https://doi.org/10.1016/0022-1759(83)90303-4

Mourdikoudis, S., Pallares, R. M., & Thanh, N. T. K. (2018). Characterization techniques for nanoparticles: Comparison and complementarity upon studying nanoparticle properties. In *Nanoscale* (Vol. 10, Issue 27, pp. 12871–12934). Royal Society of Chemistry. https://doi.org/10.1039/c8nr02278j

Mukherjee, S., Ray, S., & Thakur, R. S. (2009). Solid lipid nanoparticles: A modern formulation approach in drug delivery system. In *Indian Journal of Pharmaceutical Sciences* (Vol. 71, Issue 4, pp. 349–358). Wolters Kluwer -- Medknow Publications. https://doi.org/10.4103/0250-474X.57282

Müller, R. H., Radtke, M., & Wissing, S. A. (2002). Solid lipid nanoparticles (SLN) and nanostructured lipid carriers (NLC) in cosmetic and dermatological preparations. *Advanced Drug Delivery Reviews*, *54*(SUPPL.). https://doi.org/10.1016/S0169-409X(02)00118-7

Müller, Rainer H., Rühl, D., Runge, S., Schulze-Forster, K., & Mehnert, W. (1997). Cytotoxicity of solid lipid nanoparticles as a function of the lipid matrix and the surfactant. *Pharmaceutical Research*, *14*(4), 458–462. https://doi.org/10.1023/A:1012043315093

Muzny, D. M., Bainbridge, M. N., Chang, K., Dinh, H. H., Drummond, J. A., Fowler, G., Kovar, C. L., Lewis, L. R., Morgan, M. B., Newsham, I. F., Reid, J. G., Santibanez, J., Shinbrot, E., Trevino, L. R., Wu, Y. Q., Wang, M., Gunaratne, P., Donehower, L. A., Creighton, C. J., … Thomson., E. (2012). Comprehensive molecular characterization of human colon and rectal cancer. *Nature*, *487*(7407), 330–337. https://doi.org/10.1038/nature11252

Napper, D. (1983). *Polymeric stabilization of colloidal dispersions*.

Naseri, N., Valizadeh, H., & Zakeri-Milani, P. (2015). Solid lipid nanoparticles and nanostructured lipid carriers: Structure preparation and application. In *Advanced Pharmaceutical Bulletin* (Vol. 5, Issue 3, pp. 305–313). Tabriz University of Medical Sciences. https://doi.org/10.15171/apb.2015.043

Oltersdorf, T., Elmore, S. W., Shoemaker, A. R., Armstrong, R. C., Augeri, D. J., Belli, B. A., Bruncko, M., Deckwerth, T. L., Dinges, J., Hajduk, P. J., Joseph, M. K., Kitada, S., Korsmeyer, S. J., Kunzer, A. R., Letai, A., Li, C., Mitten, M. J., Nettesheim, D. G., Ng, S. C., … Rosenberg, S. H. (2005). An inhibitor of Bcl-2 family proteins induces regression of solid tumours. *Nature*, *435*(7042), 677–681. https://doi.org/10.1038/nature03579

Ostling, O., & Johanson, K. J. (1984). Microelectrophoretic study of radiation-induced DNA damages in individual mammalian cells. *Biochemical and Biophysical Research Communications*, *123*(1), 291–298. https://doi.org/10.1016/0006-291X(84)90411-X

Pfeffer, C. M., & Singh, A. T. K. (2018). Apoptosis: A target for anticancer therapy. In *International Journal of Molecular Sciences* (Vol. 19, Issue 2). MDPI AG. https://doi.org/10.3390/ijms19020448

Pino, M. S., & Chung, D. C. (2010). The Chromosomal Instability Pathway in Colon Cancer. *Gastroenterology*, *138*(6), 2059–2072. https://doi.org/10.1053/j.gastro.2009.12.065

Poon, I. K. H., Lucas, C. D., Rossi, A. G., & Ravichandran, K. S. (2014). Apoptotic cell clearance: Basic biology and therapeutic potential. In *Nature Reviews Immunology* (Vol. 14, Issue 3, pp. 166–180). Nat Rev Immunol. https://doi.org/10.1038/nri3607

Pope-Harman, A., Cheng, M. M. C., Robertson, F., Sakamoto, J., & Ferrari, M. (2007). Biomedical Nanotechnology for Cancer. In *Medical Clinics of North America* (Vol. 91, Issue 5, pp. 899–927). Med Clin North Am. https://doi.org/10.1016/j.mcna.2007.05.008

Portt, L., Norman, G., Clapp, C., Greenwood, M., & Greenwood, M. T. (2011). Anti-apoptosis and cell survival: A review. In *Biochimica et Biophysica Acta - Molecular Cell Research* (Vol. 1813, Issue 1, pp. 238–259). https://doi.org/10.1016/j.bbamcr.2010.10.010

Prieto, C., & Calvo, L. (2013). Performance of the Biocompatible Surfactant Tween 80, for the Formation of Microemulsions Suitable for New Pharmaceutical Processing. *Journal of Applied Chemistry*, *2013*, 1–10. https://doi.org/10.1155/2013/930356

Puar, Y. R., Shanmugam, M. K., Fan, L., Arfuso, F., Sethi, G., & Tergaonkar, V. (2018). Evidence for the involvement of the master transcription factor NF-κB in cancer initiation and progression. In *Biomedicines* (Vol. 6, Issue 3). MDPI AG. https://doi.org/10.3390/biomedicines6030082

Ralton, L., Bestwick, C., & Thoo Lin, P. K. (2007). Polyamine Analogues and Derivatives as Potential Anticancer Agents. *Current Bioactive Compounds*, *3*(3), 179–191. https://doi.org/10.2174/157340707781695497

Rastogi, R. P., Richa, Kumar, A., Tyagi, M. B., & Sinha, R. P. (2010). Molecular mechanisms of ultraviolet radiation-induced DNA damage and repair. In *Journal of Nucleic Acids* (Vol. 2010, p. 32). Hindawi Limited. https://doi.org/10.4061/2010/592980

Rubinstein, L. V., Shoemaker, R. H., Paull, K. D., Simon, R. M., Tosini, S., Skehan, P., Scudiero, D. A., Monks, A., & Boyd, M. R. (1990). Comparison of in vitro anticancer-drug-screening data generated with a tetrazolium assay versus a protein assay against a diverse panel of human tumor cell lines. *Journal of the National Cancer Institute*, *82*(13), 1113–1117. https://doi.org/10.1093/jnci/82.13.1113

Sabbatini, P., Aghajanian, C., Dizon, D., Anderson, S., Dupont, J., Brown, J. V., Peters, W. A., Jacobs, A., Mehdi, A., Rivkin, S., Eisenfeld, A. J., & Spriggs, D. (2004). Phase II study of CT-2103 in patients with recurrent epithelial ovarian, fallopian tube, or primary peritoneal carcinoma. *Journal of Clinical Oncology*, *22*(22), 4523–4531. https://doi.org/10.1200/JCO.2004.12.043

Saikolappan, S., Kumar, B., Shishodia, G., Koul, S., & Koul, H. K. (2019). Reactive oxygen species and cancer: A complex interaction. In *Cancer Letters* (Vol. 452, pp. 132–143). Elsevier Ireland Ltd. https://doi.org/10.1016/j.canlet.2019.03.020

Sakthivel, K. M., & Hariharan, S. (2017). Regulatory players of DNA damage repair mechanisms: Role in Cancer Chemoresistance. In *Biomedicine and Pharmacotherapy* (Vol. 93, pp. 1238–1245). Elsevier Masson SAS. https://doi.org/10.1016/j.biopha.2017.07.035

Sancho, P., Troyano, A., Fernández, C., De Blas, E., & Aller, P. (2003). Differential effects of catalase on apoptosis induction in human promonocytic cells. Relationships with heat-shock protein expression. *Molecular Pharmacology*, *63*(3), 581–589. https://doi.org/10.1124/mol.63.3.581

Sato, S., & Itamochi, H. (2015). DNA Repair and Chemotherapy. In *Advances in DNA Repair*. InTech. https://doi.org/10.5772/59513

Schwarz, C., Mehnert, W., Lucks, J., release, R. M.-J. of controlled, & 1994, undefined. (n.d.). Solid lipid nanoparticles (SLN) for controlled drug delivery. I. Production, characterization and sterilization. *Elsevier*. Retrieved September 26, 2020, from https://www.sciencedirect.com/science/article/pii/0168365994900477

SEER Cancer Statistics Review 1975-2005 - Previous Version - SEER Cancer Statistics. (n.d.). Retrieved September 26, 2020, from https://seer.cancer.gov/archive/csr/1975_2005/

Segundo, M. A., Abreu, V. L. R. G., Osório, M. V., Nogueira, S., Lin, P. K. T., Cordeiro-da-Silva, A., & Lima, S. A. C. (2016). Development and validation of HPLC method with fluorometric detection for quantification of bisnaphthalimidopropyldiaminooctane in animal tissues following administration in polymeric nanoparticles. *Journal of Pharmaceutical and Biomedical Analysis*, *120*, 290–296. https://doi.org/10.1016/j.jpba.2015.12.033

Severino, P, Pinho, S., … E. S.-C. and S. B., & 2011, undefined. (n.d.). Polymorphism, crystallinity and hydrophilic–lipophilic balance of stearic acid and stearic acid–capric/caprylic triglyceride matrices for production of stable. *Elsevier*. Retrieved September 26, 2020, from https://www.sciencedirect.com/science/article/pii/S0927776511001743?casa_token=f1B81HCiLZcAAAAA:U9x3too7eXlXmHaUXgsPdp_MzQxpDLbWLHU0UfDJVPvk7NXwsiaXwmm0xCecwf5zTkODTrkG

Severino, Patrícia, Andreani, T., Macedo, A. S., Fangueiro, J. F., Santana, M. H. A., Silva, A. M., & Souto, E. B. (2012). Current State-of-Art and New Trends on Lipid Nanoparticles (SLN and NLC) for Oral Drug Delivery. *Journal of Drug Delivery*, *2012*, 1–10. https://doi.org/10.1155/2012/750891

Shapiro, H. M. (2004). The evolution of cytometers. *Cytometry*, *58A*(1), 13–20. https://doi.org/10.1002/cyto.a.10111

Shi, H., Shi, X., & Liu, K. J. (2004). Oxidative mechanism of arsenic toxicity and carcinogenesis. In *Molecular and Cellular Biochemistry* (Vol. 255, Issues 1–2, pp. 67–78). Mol Cell Biochem. https://doi.org/10.1023/B:MCBI.0000007262.26044.e8

Shi, W., Weng, D., & Niu, W. (2016). Nanoparticle drug delivery systems and three-dimensional cell cultures in cancer treatments and research. *Cancer Translational Medicine*, *2*(5), 154. https://doi.org/10.4103/2395-3977.192933

Simon, K. (2016). Colorectal cancer development and advances in screening. In *Clinical Interventions in Aging* (Vol. 11, pp. 967–976). Dove Medical Press Ltd. https://doi.org/10.2147/CIA.S109285

Slater, C., De La Mare, J. A., & Edkins, A. L. (2018). In vitro analysis of putative cancer stem cell populations and chemosensitivity in the SW480 and SW620 colon cancer metastasis model. *Oncology Letters*, *15*(6), 8516–8526. https://doi.org/10.3892/ol.2018.8431

Stewart, B., & Kleihues, P. (2003). *World cancer report*. https://www.env.go.jp/air/asbestos/commi_hhmd/03/ext01.pdf

Stewart, W. W. (1978). Functional connections between cells as revealed by dye-coupling with a highly fluorescent naphthalimide tracer. *Cell*, *14*(3), 741–759. https://doi.org/10.1016/0092-8674(78)90256-8

Study on the distribution of lung targeted-tetrandrine sustained-release albumin microcapsules in vivo--《Chinese Journal of Hospital Pharmacy》2001年05期. (n.d.). Retrieved September 28, 2020, from http://en.cnki.com.cn/Article_en/CJFDTotal-ZGYZ200105000.htm

Subramaniam, B., Siddik, Z. H., & Nagoor, N. H. (2020). Optimization of nanostructured lipid carriers: understanding the types, designs, and parameters in the process of formulations. In *Journal of Nanoparticle Research* (Vol. 22, Issue 6, p. 141). Springer. https://doi.org/10.1007/s11051-020-04848-0

Szatrowski, T. P., & Nathan, C. F. (1991). Production of Large Amounts of Hydrogen Peroxide by Human Tumor Cells. *Cancer Research*, *51*(3).

Talegaonkar, S., & Bhattacharyya, A. (2019). Potential of Lipid Nanoparticles (SLNs and NLCs) in Enhancing Oral Bioavailability of Drugs with Poor Intestinal Permeability. In *AAPS PharmSciTech* (Vol. 20, Issue 3, pp. 1–15). Springer New York LLC. https://doi.org/10.1208/s12249-019-1337-8

Tanaka, N., Kanatani, S., Tomer, R., Sahlgren, C., Kronqvist, P., Kaczynska, D., Louhivuori, L., Kis, L., Lindh, C., Mitura, P., Stepulak, A., Corvigno, S., Hartman, J., Micke, P., Mezheyeuski, A., Strell, C., Carlson, J. W., Fernández Moro, C., Dahlstrand, H., … Uhlén, P. (2017). Whole-tissue biopsy phenotyping of three-dimensional tumours reveals patterns of cancer heterogeneity. *Nature Biomedical Engineering*, *1*(10), 796–806. https://doi.org/10.1038/s41551-017-0139-0

Tang, L., Yang, X., Dobrucki, L. W., Chaudhury, I., Yin, Q., Yao, C., Lezmi, S., Helferich, W. G., Fan, T. M., & Cheng, J. (2012). Aptamer-functionalized, ultra-small, monodisperse silica nanoconjugates for targeted dual-modal imaging of lymph nodes with metastatic tumors. *Angewandte Chemie - International Edition*, *51*(51), 12721–12726.

https://doi.org/10.1002/anie.201205271

Testa, U., Pelosi, E., & Castelli, G. (2018). Colorectal Cancer: Genetic Abnormalities, Tumor Progression, Tumor Heterogeneity, Clonal Evolution and Tumor-Initiating Cells. *Medical Sciences*, *6*(2), 31. https://doi.org/10.3390/medsci6020031

Thakkar, A., Chenreddy, S., Thio, A., Khamas, W., Wang, J., & Prabhu, S. (2016). Preclinical systemic toxicity evaluation of chitosan-solid lipid nanoparticle-encapsulated aspirin and curcumin in combination with free sulforaphane in BALalB/c mice. *International Journal of Nanomedicine*, *11*, 3265–3276. https://doi.org/10.2147/IJN.S106736

Torchilin, V. P. (2005). Recent advances with liposomes as pharmaceutical carriers. In *Nature Reviews Drug Discovery* (Vol. 4, Issue 2, pp. 145–160). Nat Rev Drug Discov. https://doi.org/10.1038/nrd1632

Trachootham, D., Alexandre, J., discovery, P. H.-N. reviews D., & 2009, undefined. (n.d.). Targeting cancer cells by ROS-mediated mechanisms: a radical therapeutic approach? *Nature.Com*. Retrieved September 28, 2020, from https://www.nature.com/articles/nrd2803

Turgeon, M. O., Perry, N. J. S., & Poulogiannis, G. (2018). DNA damage, repair, and cancer metabolism. In *Frontiers in Oncology* (Vol. 8, Issue FEB, p. 15). Frontiers Media S.A. https://doi.org/10.3389/fonc.2018.00015

Uster, P., Working, P., pharmaceutics, J. V.-I. journal of, & 1998, undefined. (n.d.). Pegylated liposomal doxorubicin (DOXIL®, CAELYX®) distribution in tumour models observed with confocal laser scanning microscopy. *Elsevier*. Retrieved September 25, 2020, from https://www.sciencedirect.com/science/article/pii/S0378517397004158?casa_token=VtNntb2wWnYAAAAA:n8Tdj0iGLhzXNXc0B9Byb3JcPjx4Uf47dPg-F-3z0Fwert1NydhhPU0BS97uXF2KRb0ltSUu

van Cutsem, E. J. D., Oliveira, J., & Kataja, V. V. (2005). ESMO minimum clinical recommendations for diagnosis, treatment and follow-up of advanced colorectal cancer. *Annals of Oncology*, *16*(SUPPL. 1). https://doi.org/10.1093/annonc/mdi803

van Tonder, A., Joubert, A. M., & Cromarty, A. (2015). Limitations of the 3-(4,5-dimethylthiazol-2-yl)-2,5-diphenyl-2H-tetrazolium bromide (MTT) assay when compared to three commonly used cell enumeration assays. *BMC Research Notes*, *8*(1), 47. https://doi.org/10.1186/s13104-015-1000-8

Venditto, V. J., & Szoka, F. C. (2013). Cancer nanomedicines: So many papers and so few drugs! In *Advanced Drug Delivery Reviews* (Vol. 65, Issue 1, pp. 80–88). NIH Public Access. https://doi.org/10.1016/j.addr.2012.09.038

Vermes, I., Haanen, C., Steffens-Nakken, H., & Reutelingsperger, C. (n.d.). A novel assay for apoptosis Flow cytometric detection of phosphatidylserine early apoptotic cells using fluorescein labelled expression on Annexin V. In *JOURNAL OF MMMO~OGICAL ELSEVTER Journal of Immunological Methods* (Vol. 184).

Wang, J. Y. J. (2019). Cell death response to dna damage. *Yale Journal of Biology and Medicine*, *92*(4), 771–779. /pmc/articles/PMC6913835/?report=abstract

Wang, J., & Yi, J. (2008). Background: Two Paradoxical ROS-Manipulation Strategies in Cancer Treatment. *Cancer Biology & Therapy*, *7*(12), 1875–1884. https://doi.org/10.4161/cbt.7.12.7067

Wang, K., Wang, Y., Yan, X., Chen, H., Ma, G., Zhang, P., Li, J., Li, X., & Zhang, J. (2012). DNA binding and anticancer activity of naphthalimides with 4-hydroxyl-alkylamine side chains at different lengths. *Bioorganic and Medicinal Chemistry Letters*, *22*(2), 937–941. https://doi.org/10.1016/j.bmcl.2011.12.018

Wang, M. J., Liu, S., Liu, Y., & Zheng, D. (2007). Actinomycin D enhances TRAIL-induced caspase-dependent and -independent apoptosis in SH-SY5Y neuroblastoma cells. *Neuroscience Research*, *59*(1), 40–46. https://doi.org/10.1016/j.neures.2007.05.010

Watson, A. S., Mortensen, M., & Simon, A. K. (2011). Autophagy in the pathogenesis of myelodysplastic syndrome and acute myeloid leukemia. *Cell Cycle*, *10*(11), 1719–1725. https://doi.org/10.4161/cc.10.11.15673

Wempe, M. F., Wright, C., Little, J. L., Lightner, J. W., Large, S. E., Caflisch, G. B., Buchanan, C. M., Rice, P. J., Wacher, V. J., Ruble, K. M., & Edgar, K. J. (2009). Inhibiting efflux with novel non-ionic surfactants: Rational design based on vitamin E TPGS. *International Journal of Pharmaceutics*, *370*(1–2), 93–102. https://doi.org/10.1016/j.ijpharm.2008.11.021

Wiechmann, K., Müller, H., König, S., Wielsch, N., Svatoš, A., Jauch, J., & Werz, O. (2017). Mitochondrial Chaperonin HSP60 Is the Apoptosis-Related Target for Myrtucommulone. *Cell Chemical Biology*, *24*(5), 614-623.e6. https://doi.org/10.1016/j.chembiol.2017.04.008

Wilczewska, A. Z., Niemirowicz, K., Markiewicz, K. H., & Car, H. (2012). Nanoparticles as drug delivery systems. In *Pharmacological Reports* (Vol. 64, Issue 5, pp. 1020–1037). Elsevier B.V. https://doi.org/10.1016/S1734-1140(12)70901-5

Wisse, E., Braet, F., Luo, D., De Zanger, R., Jans, D., Crabbé, E., & Vermoesen, A. (1996). Structure and function of sinusoidal lining cells in the liver. *Toxicologic Pathology*, *24*(1), 100–111. https://doi.org/10.1177/019262339602400114

Wissing, S. A., Kayser, O., & Müller, R. H. (2004). Solid lipid nanoparticles for parenteral drug delivery. *Advanced Drug Delivery Reviews*, *56*(9), 1257–1272. https://doi.org/10.1016/j.addr.2003.12.002

Wong, H. L., Rauth, A. M., Bendayan, R., Manias, J. L., Ramaswamy, M., Liu, Z., Erhan, S. Z., & Wu, X. Y. (2006). A New Polymer–Lipid Hybrid Nanoparticle System Increases Cytotoxicity of Doxorubicin Against Multidrug-Resistant Human Breast Cancer Cells. *Pharmaceutical Research*, *23*(7), 1574–1585. https://doi.org/10.1007/s11095-006-0282-x

Xu, Z., Qian, X., & Cui, J. (2005). Colorimetric and ratiometric fluorescent chemosensor with a large red-shift in emission: Cu(II)-only sensing by deprotonation of secondary amines as receptor conjugated to naphthalimide fluorophore. *Organic Letters*, *7*(14), 3029–3032. https://doi.org/10.1021/ol051131d

Yang, H., Villani, R. M., Wang, H., Simpson, M. J., Roberts, M. S., Tang, M., & Liang, X. (2018). The role of cellular reactive oxygen species in cancer chemotherapy. In *Journal of Experimental and Clinical Cancer Research* (Vol. 37, Issue 1). BioMed Central Ltd. https://doi.org/10.1186/s13046-018-0909-x

Yang, H. W., Hua, M. Y., Liu, H. L., Huang, C. Y., Tsai, R. Y., Lu, Y. J., Chen, J. Y., Tang, H. J., Hsien, H. Y., Chang, Y. S., Yen, T. C., Chen, P. Y., & Wei, K. C. (2011). Self-protecting core-shell magnetic nanoparticles for targeted, traceable, long half-life delivery of BCNU to gliomas. *Biomaterials*, *32*(27), 6523–6532. https://doi.org/10.1016/j.biomaterials.2011.05.047

Yang, S. C., & Zhu, J. B. (2002). Preparation and Characterization of Camptothecin Solid Lipid Nanoparticles. *Drug Development and Industrial Pharmacy*, *28*(3), 265–274. https://doi.org/10.1081/DDC-120002842

Yang, S., Zhu, J., Lu, Y., Liang, B., & Yang, C. (1999). Body distribution of camptothecin solid lipid nanoparticles after oral administration. *Pharmaceutical Research*, *16*(5), 751–757. https://doi.org/10.1023/A:1018888927852

Yassin, A. E. B., Khalid Anwer, M. D., Mowafy, H. A., El-Bagory, I. M., Bayomi, M. A., & Alsarra, I. A. (2010). Optimization of 5-fluorouracil solid-lipid nanoparticles: A preliminary study to treat colon cancer. *International Journal of Medical Sciences*, *7*(6), 398–408. https://doi.org/10.7150/ijms.7.398

Yeldag, G., Rice, A., & Hernández, A. del R. (2018). Chemoresistance and the self-maintaining tumor microenvironment. In *Cancers* (Vol. 10, Issue 12). MDPI AG. https://doi.org/10.3390/cancers10120471

Yildiz, I., Taskaynatan, H., Varol, U., Salman, T., Oflazoglu, U., Yildiz, Y., Kucukzeybek, Y., Alacacioglu, A., & Tarhan, M. O. (2018). The role of FOLFOXIRI in chemorefractory metastatic colorectal cancer patients. *Journal of Oncological Sciences*, *4*(1), 60–61. https://doi.org/10.1016/j.jons.2018.03.001

Yoo, J., Park, C., Yi, G., Lee, D., & Koo, H. (2019). Active targeting strategies using biological ligands for nanoparticle drug delivery systems. *Cancers*, *11*(5). https://doi.org/10.3390/cancers11050640

Zaman, S., Wang, R., & Gandhi, V. (2014). Targeting the apoptosis pathway in hematologic malignancies. In *Leukemia and Lymphoma* (Vol. 55, Issue 9, pp. 1980–1992). Informa Healthcare. https://doi.org/10.3109/10428194.2013.855307

Zhang, G., Gurtu, V., Kain, S. R., & Yan, G. (1997). Early detection of apoptosis using a fluorescent conjugate of annexin V. *BioTechniques*, *23*(3), 525–531. https://doi.org/10.2144/97233pf01

Zhang, J., Wang, X., Vikash, V., Ye, Q., Wu, D., Liu, Y., & Dong, W. (2016). ROS and ROS-Mediated Cellular Signaling. In *Oxidative Medicine and Cellular Longevity* (Vol. 2016). Hindawi Limited. https://doi.org/10.1155/2016/4350965

Zhang, S. Z., Lipsky, M. M., Trump, B. F., & Hsu, I. C. (1990). Neutral red (NR) assay for cell viability and xenobiotic-induced cytotoxicity in primary cultures of human and rat hepatocytes. *Cell Biology and Toxicology*, *6*(2), 219–234. https://doi.org/10.1007/BF00249595

Zhang, Y., Fujita, N., & Tsuruo, T. (1999). Caspase-mediated cleavage of p21(Waf1/Cip1) converts cancer cells from growth arrest to undergoing apoptosis. *Oncogene*, *18*(5), 1131–1138. https://doi.org/10.1038/sj.onc.1202426